Thesis work for the Degree of Licentiate of Technology
Sundsvall 2012

Modelling and Optimization of Sky Surveillance Visual Sensor Network

Naeem Ahmad

Supervisors: Professor Mattias O'Nils
Dr. Najeem Lawal
Professor Bengt Oelmann

Electronics Design Division, in the
Department of Information Technology and Media
Mid Sweden University, SE-851 70 Sundsvall, Sweden

ISSN **1652-8948**
Mid Sweden University Licentiate Thesis **86**

ISBN **978-91-87103-25-4**

Akademisk avhandling som med tillstånd av Mittuniversitetet i Sundsvall framläggs till offentlig granskning för avläggande av licentiatexamen i elektronik onsdagen den 22 augusti 2012, klockan 10:15 i sal O111, Mittuniversitetet Sundsvall. Seminariet kommer att hållas på engelska.

Modelling and Optimization of Sky Surveillance Visual Sensor Network

Naeem Ahmad

Electronics Design Division, in the
Department of Information Technology and Media
Mid Sweden University, SE-851 70 Sundsvall
Sweden

Telephone: +46 (0)60 148561

Printed by Kopieringen Mittuniversitetet, Sundsvall, Sweden, 2012

ABSTRACT

A Visual Sensor Network (VSN) is a distributed system of a large number of camera sensor nodes. The main components of a camera sensor node are image sensor, embedded processor, wireless transceiver and energy supply. The major difference between a VSN and an ordinary sensor network is that a VSN generates two dimensional data in the form of an image, which can be exploited in many useful applications. Some of the potential application examples of VSNs include environment monitoring, surveillance, structural monitoring, traffic monitoring, and industrial automation. However, the VSNs also raise new challenges. They generate large amount of data which require higher processing powers, large bandwidth requirements and more energy resources but the main constraint is that the VSN nodes are limited in these resources.

This research focuses on the development of a VSN model to track the large birds such as Golden Eagle in the sky. The model explores a number of camera sensors along with optics such as lens of suitable focal length which ensures a minimum required resolution of a bird, flying at the highest altitude. The combination of a camera sensor and a lens formulate a monitoring node. The camera node model is used to optimize the placement of the nodes for full coverage of a given area above a required lower altitude. The model also presents the solution to minimize the cost (number of sensor nodes) to fully cover a given area between the two required extremes, higher and lower altitudes, in terms of camera sensor, lens focal length, camera node placement and actual number of nodes for sky surveillance.

The area covered by a VSN can be increased by increasing the higher monitoring altitude and/or decreasing the lower monitoring altitude. However, it also increases the cost of the VSN. The desirable objective is to increase the covered area but decrease the cost. This objective is achieved by using optimization techniques to design a heterogeneous VSN. The core idea is to divide a given monitoring range of altitudes into a number of sub-ranges of altitudes. The sub-ranges of monitoring altitudes are covered by individual sub VSNs, the VSN_1 covers the lower sub-range of altitudes, the VSN_2 covers the next higher sub-range of altitudes and so on, such that a minimum cost is used to monitor a given area.

To verify the concepts, developed to design the VSN model, and the optimization techniques to decrease the VSN cost, the measurements are performed with actual cameras and optics. The laptop machines are used with the camera nodes as data storage and analysis platforms. The area coverage is measured at the desired lower altitude limits of homogeneous as well as heterogeneous VSNs and verified for 100% coverage. Similarly, the minimum resolution is measured at the desired higher altitude limits of homogeneous as well as heterogeneous VSNs to ensure that the models are able to track the bird at these highest altitudes.

ACKNOWLEDGEMENTS

All praise and thanks to ALMIGHTY ALLAH, the most beneficent and merciful. There is a long list of people to whom I would like to say thanks who are directly or indirectly related to this thesis work.

- My supervisor Professor Mattias O'Nils for his guidance, support, encouragement, patience, helping attitude and trust to pursue this opportunity. Without his persistent encouragement, supervision and valuable suggestions throughout my research, it was not possible to complete this Licentiate work.
- Dr. Najeem Lawal for his sincerity, motivation and support during this work.
- Professor Bengt Oelmann for his support to pursue research and helping attitude.
- Leif Olsson for providing valuable help to understand optimization techniques.
- Fanny Burman, Christine Grafström, Lotta Söderström, Carolina Blomberg and Anne Åhlin for all administrative matters.
- Magnus Ödling for IT support and sparing valuable time inspite of tight schedule.
- My friends Muhammad Imran and Khursheed Khursheed being my office mates for providing every possible cooperation to continue my work without any disturbance.
- My friends and colleagues Abdul Majid, Jawad Saleem, Khurram Shahzad, Abdul Waheed Malik, Mohammad Anzar Alam, Muhammad Nazar Ul Islam, Hari Babu Kotte, Radhika Ambatipudi, Mikael Bylund, Mazhar Hussain and Muhammad Amir Yousaf for their support and cooperation.
- All my colleagues in the department, Dr. Benny Thörnberg, Krister Alden, Cheng Peng, Sebastian Bader, Xiaozhou Meng, David Krapohl, and Stefan Haller for their support and cooperation.
- Government of Pakistan, my parent organization (PAEC), Higher Education Commission (HEC) Pakistan, Swedish Institute (SI) Sweden, Mid Sweden University (MIUN), and Knowledge Foundation (KK) for their financial and administrative support.

- My brothers Nadeem, Waseem, Shahid and Salman for handling all family matters and providing me opportunity to work with concentration. Special thanks to Shahid for inspiring and encouraging me in difficult situations.
- My respectable mother and father for their sincere prays. This work was not possible without their support and motivation. The real credit of my achievements goes to both of them.
- Finally, my wife Riffat Naeem for her patience and cooperation and my cute daughters Isha Naeem, Uswah Naeem and Dua Naeem. They are constant source of inspiration and happiness for me in my life. They equally suffered all the hardships and never complaint.

Naeem Ahmad

Sundsvall, August 2012

TABLE OF CONTENTS

ACRONYMS

2D	2 Dimensional
3D	3 Dimensional
AC	Alternating Current
ADC	Analog to Digital Converter
AoV	Angle of View
API	Application Programming Interface
BS	Base Station
CBS	Central Base Station
CMOS	Complementary Metal Oxide Semiconductor
CPLD	Complex Programmable Logic Device
CPU	Central Processing Unit
FIFO	First In First Out
FoV	Field of View
Fps	frames per second
GB	Giga Byte
GHz	Giga Hertz
GPIO	General Purpose Input Output
GPS	Global Positioning System
IR	Infra Red
JPEG	Joint Photographic Expert Group
KB	Kilo Byte
Kbps	Kilo bits per second
Km	Kilo meter
M	meter
MB	Mega Byte
MCU	Micro Controller Unit
MHz	Mega Hertz
Mm	Millimeter
Mp	Mega pixel
PDA	Personal Digital Assistant
PIR	Passive InfraRed

PLL	Phase Lock Loop
PSF	Parking Space Finder
PTZ	Pan Tilt Zoom
QoS	Quality of Service
QVGA	Quarter Video Graphic Array
RAM	Random Access Memory
RF	Radio Frequency
SD	Secure Digital
SDRAM	Synchronous Dynamic Random Access Memory
SRAM	Static Random Access Memory
TTL	Transistor Transistor Logic
USB	Universal Serial Bus
VGA	Video Graphic Array
VSN	Visual Sensor Network
WLAN	Wireless Local Area Network
WSN	Wireless Sensor Network
WVGA	Wide Video Graphic Array

LIST OF FIGURES

LIST OF TABLES

LIST OF PAPERS

The thesis is mainly based on following four papers:

Paper I **Model and Placement Optimization of a Sky Surveillance Visual Sensor Network**

Naeem Ahmad, Najeem Lawal, Mattias O'Nils, Bengt Oelmann, Muhammad Imran, Khursheed Khursheed.

International Conference on Broadband and Wireless Computing, Communication and Applications, IEEE Computer Society, Barcelona, Spain, Oct. 25-28, 2011.

Paper II **Cost Optimization of a Sky Surveillance Visual Sensor Network**

Naeem Ahmad, Khursheed Khursheed, Muhammad Imran, Najeem Lawal, Mattias O'Nils.

Proceedings of SPIE Vol. 8437, Real-Time Image and Video Processing 2012, Brussels, Belgium, April. 18-19, 2012.

Paper III **Model, Placement Optimization and Verification of a Sky Surveillance Visual Sensor Network**

Naeem Ahmad, Muhammad Imran, Khursheed Khursheed, Najeem Lawal, Mattias O'Nils.

Submitted to International Journal of Space-Based and Situated Computing (IJSSC), 2012, (under review).

Paper IV **Modelling and Verification of a Heterogeneous Sky Surveillance Visual Sensor Network**

Naeem Ahmad, Khursheed Khursheed, Muhammad Imran, Najeem Lawal, Mattias O'Nils.

Submitted to Supervisor for review and is planned to publish as Journal publication.

Related papers (not included in this thesis):

Paper V **Selection of Bi-level Image Compression Methods for Reduction of Communication Energy in Wireless Visual Sensor Networks**

Khursheed Khursheed, Muhammad Imran, Naeem Ahmad, Mattias O'Nils.

Proceedings of SPIE Vol. 8437, Real-Time Image and Video Processing 2012, Brussels, Belgium, April. 18-19, 2012.

Paper VI **Complexity Analysis of Vision Functions for Implementation of Wireless Smart Cameras Using System Taxonomy**

Muhammad Imran, Khursheed Khursheed, Naeem Ahmad, Abdul Waheed Malik, Mattias O'Nils, Najeem Lawal.

Proceedings of SPIE Vol. 8437, Real-Time Image and Video Processing 2012, Brussels, Belgium, April. 18-19, 2012.

Paper VII **Architecture Exploration Based on Tasks Partitioning Between Hardware, Software and Locality for a Wireless Vision Sensor Node**

Muhammad Imran, Khursheed Khursheed, Abdul Waheed Malik, Naeem Ahmad, Mattias O'Nils, Najeem Lawal, Benny Thörnberg.

International Journal of Distributed Systems and Technologies, 2011.

Paper VIII **The Effect of Packets Relaying in a Multihop WVSN on the Implementation of a Wireless VSN**

Khursheed Khursheed, Muhammad Imran, Mattias O'Nils, Najeem Lawal, Naeem Ahmad.

Submitted to ACM Journal, Transaction on Sensor Networks 2011.

Paper IX **Implementation of Vision Sensor Node for Characterization of Magnetic Particles in Fluids**

Muhammad Imran, Khursheed Khursheed, Najeem Lawal, Mattias O'Nils, Naeem Ahmad.

Submitted to IEEE Transactions on Circuits and Systems for Video Technology, 2011.

Paper X **Analysis and Characterization of Vision Systems for Taxonomy Formulation**

Muhammad Imran, Khaled Benkrid, Khursheed Khursheed, Naeem Ahmad, Mattias O'Nils, Najeem Lawal.

Submitted to IEEE Transactions on Circuits and Systems for Video Technology, 2011.

1 VISUAL SENSOR NETWORKS

This chapter provides a general overview about the Visual Sensor Networks (VSNs). It starts from vey brief introduction of the Wireless Sensor Networks (WSNs) and progresses towards the VSNs. The brief introduction of VSNs is followed by the VSN types, the homogeneous VSNs and heterogeneous VSNs. After introducing the VSN types the major data transmission techniques, including the single hop transmission, multihop transmission and multipath transmission are discussed. The chapter progresses towards the description of the challenges which are involved in the design of the VSNs. The energy consumption of a VSN is very critical factor. A brief discussion about energy consumption in the VSNs is provided later on. Finally, the main objective of the thesis is presented along with the major contributions of the research. The chapter is concluded with the description of the thesis outline.

1.1 INTRODUCTION

The wireless networks of scalar sensor nodes which collect scalar data are referred to as WSNs. The common examples of the scalar data are temperature, pressure, and humidity. The WSNs are the distributed and ad hoc networks which connect the small devices. These devices are equipped with their own sensing, computation, communication and power resources. The WSNs monitor the environment and collect the specific data about it. These sensors generate a limited amount of information. This information is insufficient for many applications even if a large number of such sensors are deployed. This discrepancy is resolved by adding camera sensors to WSNs [1].

The networks formed by the addition of camera sensors to the WSNs are referred to as the VSNs. The major difference between scalar sensor nodes and camera sensor nodes is that the scalar sensor nodes collect one dimensional data in the area around them while the camera sensor nodes collect two dimensional data in the form of images from the areas which may not be in their vicinity. The image data collected by camera sensors contains a lot of information. The VSNs offer many valuable applications. Some examples of the VSN applications include environmental monitoring, surveillance, traffic monitoring, industrial automation. However, the VSNs also involve many new challenges. The processing and transmission of the visual data requires large computational and communication resources. The VSNs are low-power networks and have severe resource constraints. Therefore, it is a challenging task to process the large amount of visual data by resource constrained VSNs [1]. The use of image sensors in WSNs is feasible if such networks preserve low power consumption profile [2].

The advances in the image sensor technology have made the availability of low-power image sensors possible. The developments in the fields of sensor networking and distributed processing have made it possible to use these image sensors in the networks. The combination of these technologies made the VSNs

possible. The VSNs consist of small visual sensor nodes, which are called camera nodes. These nodes consist of an image sensor, embedded processor and wireless transceiver [2].

The VSNs are the sensor-based distributed systems. They consist of a large number of low-power camera sensor nodes. These nodes collect the image data of a monitored area and perform the distributed and collaborative processing on this data [3], [4]. The nodes extract the useful information from the collected images by processing the image data locally. They also collaborate with other nodes in the VSN to create useful information about the captured events. The large amount of image data produced by the camera nodes and the network resource constraints demands the exploration of new means for data processing, communication and sensor management. Meeting these challenges require interdisciplinary approaches which utilize the vision processing, communication, networking and embedded processing [2].

The visual sensor nodes usually use more powerful processors as compared to wireless sensor nodes. The processors used in visual sensor nodes usually have higher processing speed which is helpful in faster data processing. Some designs may use a second processor for additional processing and control. The examples of such architectures are presented in [5], [6]. Most processors have small internal memories. Thus, additional memory is used for frame buffering and permanent data storage. Some design examples use two image sensors for stereo vision. The examples of such implementations are presented in [7], [6]. The MeshEye architecture [5] uses two low resolution cameras for stereo vision. An additional high resolution camera (VGA) is used in between these low resolution cameras. One low-resolution camera detects the object in the Field of View (FoV). The stereo vision with two low resolution cameras detects the object size and position. The VGA camera is used to capture the high resolution image of the object.

The IEEE 802.15.4 RF transceiver is commonly used in wireless sensor nodes as well as the visual sensor nodes. The achievable data rates are very low for vision based applications. There is a need for the development of the new radio standards with higher data rates. However, it will increase the energy dissipation of the node. To decrease the amount of data which is communicated among the camera nodes, the light-weight processing algorithms should be used. One such example is given in [8]. A distributed scheme for target tracking in a multicamera environment which reduces the communication is discussed in [9].

1.2 TYPES OF VSNS

The camera sensor nodes with different types, costs, optical and mechanical properties, computation capabilities, communication powers, energy requirements are available to design the VSNs. The choice of the camera nodes for VSNs depends on the application requirements and constraints. Depending on the types of the camera sensor nodes used, the VSNs can be divided into two major

categories, heterogeneous and homogeneous VSNs [1].

1.2.1 Homogeneous VSNs

This VSN uses similar type of camera sensor nodes and one or more Base Stations (BSs). The homogeneous design is suitable for large-scale VSNs for a number of reasons. First, it reduces the complexity of the network, second, it supports the scalability and third it is self-organized and no central control is required to manage it. The homogeneous VSNs are ideal for applications, such as habitat monitoring [10]. These applications are used to monitor wildlife in remote natural reserves. Hundreds of camera nodes can be deployed for such applications which collect data from the monitored site and send it to the BS. The multitier architecture can be used to design the homogeneous VSNs. In this design, the sensor nodes are organized in a number of tiers. In multitier design, the nodes will be organized in clusters. Any node in a cluster can perform the role as head cluster which will aggregate the data of the whole cluster [1].

1.2.2 Heterogeneous VSNs

This VSN uses different type of camera sensor nodes, actuators and other types of sensors. These networks assign different sensing and processing tasks to different type of sensor nodes. A task is assigned to a node on the basis of its capabilities. Thus, the heterogeneous VSNs provide better functionality than homogeneous VSNs. However, the heterogeneous VSNs are more complex than the homogeneous VSNs. The complexity of these networks is handled by using multitier design. The sensor nodes are organized in a number of tiers, with the same type of nodes on a given tier. Thus, a VSN is heterogeneous on multitier basis but homogeneous on a single tier basis. Generally, the bottom tiers contain a large number of low-cost and low-power sensor nodes. The number of nodes gradually reduced from bottom to higher tiers but their processing power is increased from bottom to higher tiers. The communication between the two tiers is made via middle tiers [1].

The example of a heterogeneous VSN is a clustered network. It consists of two tiers. The first tier contains sensor nodes. These nodes are separated into clusters. Each cluster collects the environmental data and sends it to the respective aggregation nodes, which act like the cluster heads. All the aggregations nodes form the second tier of the VSN. The aggregation nodes collect data from the sensor nodes, process it and send the processed information to the BS [1].

The SensEye is a VSN which is designed for surveillance applications. It follows multitier architecture design and contains three tiers. Each tier uses the different type of camera nodes, having capabilities suitable for the tasks to be performed. The first tier contains low-end QVGA camera sensor nodes. These nodes are used for object detection. The second tier contains VGA sensor nodes. These nodes are used for object recognition. The third tier contains PTZ (Pan Tilt Zoom) cameras. These nodes track the moving objects and also communicate with the BS. The

SensEye dictates that the low power and low latency is possible with multitier design [11] .

1.3 DATA TRANSMISSION TECHNIQUES

The reliable transmission of data is an important requirement in VSNs. The data transmission techniques used in the VSNs can be divided into three categories which include the single hope, multihop and multipath transmission [1].

1.3.1 Single hop transmission

This category includes the techniques which consider the image/video transmission over a single hop. The first example of the work in this category is presented in [12], which proposes a system for JPEG-2000 image transmission over VSNs that reduces the energy consumption. The second example is presented in [13], which proposes a mechanism for wavelet-based image transmission in the VSNs based on decomposing a source image using a discrete wavelet transform and packetizing it into packets of different priorities.

1.3.2 Multihop transmission

This category includes the techniques that consider multihop transmission where the transmission strategy is determined on hop-by-hop basis. The example of work in this category is presented in [14], which proposes a hop-by-hop reliability scheme based on generating and sending multiple copies of the same data bitstream. An adaptive image transmission scheme is discussed in [15]. This scheme optimizes the image quality over a multihop network while considering the multihop path condition such as delay constraints and the probability of delay violation.

1.3.3 Multipath transmission

This category includes the end-to-end multipath transmission techniques. In this category, many works combine the error correcting codes and path diversification to provide end-to-end reliability in the multihop networks, where multiple transmission paths are used to increase the reliability. An efficient multipath transmission mechanism splits the data stream into small packets, say L packets, adds a number of redundancy packets using forward error correction, and transmits all these packets over a number of paths from source node to the BS. The information bitstream can be reconstructed successfully at the destination if any of the L transmitted packets are received. Fast algorithms to find the number of channel packets and the transmission paths, that optimize the reliability-energy cost trade-off, are proposed in [16], [17].

1.4 CHALLENGES OF VSNS

VSNs offer new opportunities for many promising applications compared to the scalar sensor networks. However, they also raise new challenges. The camera sensors generate huge amount of data as compared to scalar sensors. Large

computational and bandwidth resources are required to process this data. The camera nodes are generally low-power and have severe resource constraints. Processing and transmitting of large data by these nodes is a challenging task. The VSNs are unique and more challenging in many ways. The major challenges which are faced in the context of VSNs are resource constraints, real time performance, time synchronization, coverage optimization, algorithmic constraints, object occlusion and data reliability. All these constraints are described below.

1.4.1 Resource Requirements

A camera node requires energy to sense, process and transmit data. Generally, the camera nodes are powered by batteries and have limited lifetime due to the battery powered operation. The camera nodes generate a large amount of image data. Energy is required to process and communicate this data. If a node transmits raw data without processing or with very little processing, then more energy is required for communication and less energy for processing. Moreover, more the larger bandwidth is required to transmit this data. If more processing is performed on the node, then it is likely to be less data for transmission. In this case more energy will be required for processing and less energy for communication. Also, the smaller bandwidth will be sufficient to transmit this data. The energy and bandwidth constraints in VSNs are severe than other types of WSN [1], [2]. The channel bandwidth utilization must be considered carefully in VSNS. A bandwidth framework is discussed in [18].

The VSNs have limited energy and bandwidth resources. Therefore, it is impractical to transmit all the collected data. The local processing of the image data reduces the amount of data that needs to be communicated through the network. The cost involved in processing the data is significantly lower than the cost involved in the communication of the data. Therefore, the size of the data should be reduced before transmission [19]. The amount of data can be reduced by describing the captured events with the least amount of data. However, the visual data is large in size and more cost can be involved to process this data. Therefore, it is challenging task to decide the type of data processing involved such as compression, fusion, filtering. Moreover, it is challenging to decide whether this processing should be performed at a tier, at BS or at all of them.

By integrating the camera nodes with other types of low power and low cost sensors, such as audio sensors, Passive InfraRed (PIR) sensors, vibration sensors, light sensors, the lifetime of the camera nodes can be significantly increased due to the minimization of the communication in the network. Such multimedia networks [11] usually employ a hierarchical architecture. The ultra-low power sensors (such as microphones, PIRs, vibration, or light sensors) continuously monitor the environment over long periods of time while the higher-power sensors, such as cameras, sleep most of the time. When the lower-power sensors detect an event they notify it to the higher-power sensors for further action.

1.4.2 Real Time Performance

The VSN applications generally require the data from camera nodes in real time. Thus, strict limits are set on the allowable delays to receive the data from camera nodes after demanded by the users. The most common reasons which affect the real time operation of camera nodes are processing time, multihop routing, communication time and error protection schemes. Most camera nodes contain embedded processors with limited processing speeds. The high speeds processors are avoided due to the limited energy sources of the nodes. The limited processing capabilities increase the time required the processing of the image data, which affects the real-time performance of a VSN. The multihop routing is the preferred data transmission method in WSNs. However, the multihop routing can increase the delay due to the data queuing and data processing at the intermediate nodes. The delay increases by increasing the number of hops on the routing path. Thus, the multihop routing also affects the real time performance of the VSNs.

Wireless channels have many limitations such as available bandwidth, modulation type, data rate. All these limitations affect the real time operation. The employed wireless standard and the current condition of the network are also responsible for data delays. For example, on detecting an event the camera nodes can suddenly inject a lot of data in the network, which can cause data congestion which increases the data delays. Thus, the time required for the transmission of the data through the network affects the real-time performance of a VSN. The reliable transmission of the data is an important requirement of VSNs. The error protection schemes are necessary to ensure the reliable transmission of data. The error protection schemes ensure the reliability of data but they affect the real time data transmission through the network [2].

1.4.3 Time Synchronization

Many processing applications involve multiple cameras. The common examples of such applications are object localization and object tracking. These applications depend on highly synchronized camera snapshots. The image data can become meaningless if the information about image capture time is not available. The synchronization of the cameras and the development of the synchronization protocols is a challenging issue in the VSNs. The time synchronization protocols developed for WSNs [20] can also be used for the synchronization in VSNs.

1.4.4 Coverage Optimization

The camera coverage algorithms ensure the minimum required coverage by managing the camera sensors and preserve coverage in case of a sensor failure. The coverage optimization of the VSNs is more complex as compared to the WSNs. This is because the data capture style of the camera sensors is different from ordinary scalar sensors and that the higher number of control parameters are involved. The coverage algorithms place the redundant sensor nodes to the sleep mode which is helpful in saving energy. It is challenging to decide that which nodes should be made active and which nodes should be made sleep. This decision

affects the network lifetime, minimum coverage assurance, connectivity and completion of the task at hand. Moreover, it is challenging to make these algorithms simple and less complex as the VSNs have processing constraints and energy limitations [1].

1.4.5 Algorithmic Constraints

Most of the vision processing algorithms are developed without the consideration of the processing limitations. Also, many vision processing algorithms are developed for the single camera systems. The challenges are involved to adapt these existing vision processing algorithms to the resource constrained distributed networks of low-resolution cameras. The camera nodes in VSNs have limited processing capabilities and thus support light weight processing algorithms. However, the algorithms required to support the distributed processing of the image data, fusion of data from multiple sources, extraction of the features from multiple camera views or matching the features demand more processing power. It is challenging to execute these complex algorithms on the nodes with low processing power and energy resources [2].

1.4.6 Object Occlusion

The object occlusion occurs when a camera looses the sight of a target object due to the obstruction by another object. The occluding objects can be static [21] or dynamic. The static occluding objects can be handled easily but it is more difficult to handle the dynamic occluding objects. Multicamera networks provide multiple views of an object. Therefore, they can easily handle occlusion problems. It is challenging to avoid losing the tracked object, due to occlusions, when sufficient numbers of cameras are not available for tracking. The challenge is involved in designing the new sensor management policies that reduce the chances of object occlusion by selecting the minimum number of camera nodes which enable the multiple views of the target object.

1.4.7 Data Reliability

An important requirement of the VSNs and the other network systems is the reliable transport of data. The retransmission of the data increases the data latency which affects the real time operation. The solution to the problem is to increase the reliability of the data. The major challenges to achieve data reliability are the unreliable channels, data congestion in the network and the bursty and bulky data traffic of the VSNs. A transport scheme to increase the data reliability is discussed in [22], which combines the multipath data transport and error correction. Another work which increases the reliability of the transmitted data over multiple paths is presented in [23]. The congestion control is a dominant problem in the design of reliable protocols for the VSNs. The network congestion can cause significant loss of data in the VSNs. The work to control the congestion in wireless multimedia networks is presented in [24]. The data reliability is increased by the concurrent data flow. However, it increases the transmission cost of the data. Multimedia data can tolerate a certain degree of loss [24]. Thus, there is a tradeoff between the

quality of the received data and the cost required to transmit that data.

1.5 Energy Consumption in VSNs

Generally, the camera nodes in the VSNs are powered by the batteries. Therefore, the lifetime of these nodes is limited. A long lifetime is desirable as the VSNs are mostly installed in the remote areas and it is difficult to replace the batteries at remote sites. The lifetime of the energy constrained VSNs can be increased by reducing the energy, used for data transmission. This energy can be reduced by decreasing the data transmission. By decreasing the data transmission, the energy consumption is reduced but it decreases the QoS. This is because the quality of the image data and the application QoS depends on the amount of data. Thus, there is a tradeoff between the energy consumption and the QoS parameter in a VSN.

The common applications of the VSNs include monitoring of large areas, such as public places, parking areas and large stores. A large area is monitored completely for the entire duration of a given time. To balance the energy consumption of the camera nodes, a common strategy is to allocate the parts of the monitored region to the camera nodes. A strategy, which allocates the parts of the monitored region to the cameras and also maximizes the battery lifetime of the camera nodes, is discussed in [26]. In the redundantly deployed VSNs, a subset of cameras can perform continuous monitoring. With the passage of time, this subset of cameras can be changed with the other subset of cameras.

The energy consumption of the camera nodes can be reduced by the distributed power management of the camera nodes. Such a scheme based on the coordinated node wake-ups is discussed in [27]. The energy consumption of a node can be reduced considerably by limiting the idle periods of the nodes. The idle periods are the long durations when a node listens to the channel. The two important operating modes in the VSNs are duty-cycle mode and the event-driven mode. The effect of these operating modes on the lifetime of a camera node is analyzed in [29].

The lifetime of a battery-operated camera node is limited by its energy consumption and is determined by the hardware used and the working mode of the node. It can be estimated by calculating its power consumption for performing different tasks such as image capture, processing and transmission. Such an analysis is presented in [28]. The analysis describes important results, such as the time consumed in acquiring an image and processing that image is 2.5 times more than the time required for transmitting a compressed image, the energy cost for analyzing the image and compressing a portion of the image is about the same as for the compression of the full image. The transition between the states can be expensive in terms of time and energy.

The power consumption specifications of a camera node include the power consumption profiles of the Central Processing Unit (CPU), radio and the camera in the different operational modes such as sleep, idle and working mode. As

discussed before, if a node transmits raw data without processing or with very little processing, then more energy is required for communication. The data transmission is expensive operation in terms of energy. The solution to this problem is to reduce the size of the data before transmission. The size of the data can be reduced by using the data compression techniques. There are a number of compression techniques available. To select best compression method, an analysis is presented in [30]. It measures the current which is consumed in different states such as standby, sensing, processing, connection and communication. The selected compression method provides good compromise between the energy consumption and the quality of the image.

The energy consumption analysis of a camera node, when performing different tasks, is presented in [28] and the energy consumption analysis in different working modes is presented in [29]. These analyses are helpful in developing the effective resource management policies [2]. The analysis of the tradeoffs, between the energy costs for data processing and data communication, is presented in [30]. This analysis is helpful to choose the best vision processing techniques that provide the data of a certain quality and also prolong the lifetime of the camera node. To increase the lifetime of the camera nodes, the low-power features should be considered in the design of the camera nodes.

1.6 Overall Objective and Contributions

The objective of this thesis is to design a VSN to track the large birds such as golden eagle in the sky. The thesis presents a complete VSN design recipe in terms of node specification and camera placement for sky surveillance between the two given altitude limits. It discusses in detail the selection of the camera sensor for the bird surveillance, the focal length required for the chosen camera sensor to ensure the minimum resolution at the highest required altitude, the placement of the camera nodes to ensure the full coverage at the lowest required altitude and the cost required to cover a given area.

As the covered area is increased, the number of nodes to cover that area is also increased. The desirable objective is to increase the covered area at the decreased cost. The optimization techniques are used to reduce the cost. The final solution is presented with a heterogeneous VSN. To verify the above concepts, the measurements are performed in the field with actual cameras nodes. The salient features of the thesis are described below.

- To develop the model of a VSN by designing the specifications of the VSN components such as camera sensors, lens focal lengths, placement of camera nodes and the cost required to cover an area.
- To decrease the cost required to cover a given area by using optimization techniques by dividing a given range of altitudes into a number of sub ranges and covering each range with an individual sub VSN.

- To verify the minimum required resolutions by measuring at the higher required altitude(s) of a VSN or sub VSNs and the verification of full coverage above the lower required altitude(s) for a VSN or sub VSNs to confirm the accurate placement of the camera nodes.

1.7 THESIS OUTLINE

After the current discussion on the VSNs, the remaining thesis is organized as follows. The chapter 2 discusses the VSN applications and the prominent architectures of VSNs. The chapter 3 describes the camera placement in VSNs. The chapter 4 introduces about the eagle surveillance. Chapter 5 discusses model formation for the VSN. The chapter 6 describes the cost optimization for the VSN. The chapter 7 describes the practical measurements of different parameters of the VSN. The chapter 8 summarizes the papers that are included in this thesis work. Finally, the chapter 9 summarizes and concludes the complete thesis work.

2 VSN APPLICATIONS AND NODE ARCHITECTURES

The VSNs can be deployed in a wide range of practically useful applications. This chapter describes some of the examples including surveillance, traffic monitoring, sports, environmental monitoring, Parking Space Finder (PSF) and seabird monitoring. A number of professional VSN platforms/prototypes are designed by scientists and engineers. The platforms discussed in this chapter include SensEye, CITRIC, MeshEye, FireFly Mosaic, WisNAP, Panoptes and Cyclops.

2.1 APPLICATIONS OF VSNS

The rich sensing of the world by using the camera sensors can enable a wide range of applications. One application domain includes the traffic monitoring applications such as the congestion avoidance services that offer the traffic routing advice, inform about the available parking spaces etc. One application area includes the surveillance while the other area can be habitat and environmental monitoring, where the visual information can be used for direct observations. Additional applications include bus alert systems that inform the users when it is the time to leave for the bus stop, lost-and-found services that may report the most recent location recorded for a missing object, the family monitoring services that watches the children or aging people [41]. The VSNs can be deployed to monitor the coastal areas or the activities of the birds. They can provide the surveillance of the large parks, markets and public places. The following paragraphs describe some of the important applications of VSNs in the fields.

2.1.1 Surveillance

The common examples of VSNs applications in surveillance include the intrusion detection, healthcare, building monitoring, home security, traffic, habitat and environmental monitoring. These applications capture the images of the surroundings, which are processed for the identification, recognition and classification of the required objects. On the basis of the results, some precautionary measures are taken or some control is exercised. Because of the bandwidth constraints of the VSNs, these applications demand to process the images with the lowest possible processing and to transfer the processed images or the information extracted from these images with the least amount of data. The real time operation and the reliability of the collected data are very important objectives for the surveillance applications [31].

A good example of the system, designed for surveillance, is iMouse. It is an integrated mobile surveillance and wireless sensor system. The iMouse includes static sensors, mobile sensors and external server. The static sensors form a WSN to monitor the environment. A static sensor uses a mote for the communication and contains a sensor board which can collect the light, sound and temperature data. When the output received from a sensor is greater or lower than a predefined threshold value, it is interpreted as an event. A number of sensor outputs can be

considered together to interpret a new events. For example, the unusual sound, light or temperature readings in a home security system are the sure signs of some dangerous situation.

In case of some event, the mobile sensors can be moved to the event location, capture the images of the event and transmit them to the server. An example mobile sensor [32] contains a Stargate processing board, a mote for communication, a webcam to capture the images and an IEEE 802.11 WLAN card for communication. The mobility of the sensor is achieved by using a Lego car. The control of the car and the webcam is achieved by Stargate processing board. A user can interact with the system via an external server to obtain information and to issue the commands. The other functions of the server are to control the network, to interpret the events from the static sensors and to actuate the mobile sensors to move to the emergency site to capture the high-resolution images. The captured images of the site are transmitted to the server for further decisions.

2.1.2 Traffic Monitoring

The VSNs can be used in in traffic monitoring applications [33], [34], [35]. In addition to the vehicle count and speeds, the video monitoring systems can also provide additional information such as the vehicle classifications, travel times of the city links, lane changes count, rapid accelerations or decelerations of the vehicles, queue lengths at the urban intersections. The extra advantage of VSNs is that the cameras are less disruptive and less costly to install. For vision-based traffic surveillance systems [36], [37], the cameras can be mounted on the poles or other tall structures, looking down at the traffic scene. The video is captured by the camera nodes and is processed locally at the node. The extracted features are transmitted to the Central Base Station (CBS) for further processing.

The processing of the collected data can be performed in three stages. First, segmenting the scene into individual vehicles and tracking these vehicles to refine and update its position and velocity in 3D coordinates. Second, the track data is processed to compute the local traffic parameters such as vehicle count per lane, average speeds and the lane change frequencies. These parameters and the track information, such as time stamp, vehicle type, color, shape, position, are transmitted to the CBS at regular intervals of time. Third, the CBS can use the received information for a number of tasks such as controlling the signals or other traffic control devices, displaying the messages etc. The CBS can also process the received information to compute the long-distance parameters such as the link times, origin and destination counts.

2.1.3 Sports

The VSNs have a number of applications in sports and gaming field [38], [39]. There is a common need to collect the statistics about the players or about the games. For example, sometimes it is required to know that how much ground is covered by athletes, how quickly they have moved during the game. This

information can be used to design more specific training to suit the individual players. The interactions can be studied between the individual players or for a team as a whole. A VSN application for sport area is presented in [38] which describes a system to track the football players. The input to the system is the video data from static cameras, with overlapping FoVs, at a football stadium. The output of the system is the real-time positions of the players during a match. The system processes the data, first on the basis of a single camera and then on the basis of multiple cameras. The organization of the processing is designed to achieve sufficient synchronization between cameras, using a request-response pattern, invoked by the second stage multi-camera tracker.

The single-view processing includes the change detection against an adaptive background and image-plane tracking to improve the reliability of the measurements of occluded players. The multiview processing uses Kalman trackers to model the player position and velocity, to which the multiple measurements from the single-view stage are associated. The advantage of the underlying system over the existing single-view systems is the overall visibility of all the players. The dynamic occlusion problem is relieved greatly by using the single-view tracking with partial observations and multi-sensor tracking architecture. The estimate of each player position is biased automatically to the most accurate measurement by the closest camera and the fused measurement in the overlapping regions. The result is more accurate than that from an individual camera.

2.1.4 Environment Monitoring

The VSNs have applications in the environment monitoring. The applications collect data about animals and the environment which can be helpful to answer many science questions or to solve the nature conservation issues. The data can be used to improve the existence or absence of a species at a site. The information can be used to show the arrival of an invasive species or the conservation status of rare species. One such application of a camera network, to survey the diversity and abundance of the terrestrial mammal and bird communities is presented in [40]. The camera network was deployed at an island for about one year duration to record the spatio-temporal dynamics of the animals. A sensor network was designed by using the distributed, motion-sensitive cameras that can collect data about animal populations. The camera sensors capture the images of the animals when they pass in front of the cameras.

The camera sensor network for this application consists of a number of cameras, deployed on trees at some suitable heights, at the suggested locations with the help of a GPS unit. The camera view was maximized by aiming them in the most suitable direction, with the least vegetation to avoid obstructing the view. The cameras capture the image at the night time by using IR flashes. These flashes cannot be seen by animals and are helpful to avoid the animal disturbance and hesitation from the cameras. The data transmission is limited by the battery power,

needed to send the thousands of images from a remote camera. The cameras were deployed for about a week and then moved to the new locations to cover the maximum possible areas with the minimum number of cameras. A flash memory card is installed with each camera to store the images. The memory cards are replaced with new blank cards after every week and are returned to the lab where the images are organized in a database. The parameters such as the time, date, trigger event, trigger type are automatically extracted from the metadata of the images. The image sequences are processed to extract the required information.

2.1.5 Parking Space Finder

The PSF application [41] is designed to locate and direct a driver to the available parking spaces, near a desired destination. The system utilizes a set of cameras which are connected to the IrisNet, to detect the presence of cars in parking spaces and update the distributed database with this high-level semantic information. The IrisNet is a general purpose network architecture of the multimedia sensors. The IrisNet provides an extensible distributed database infrastructure to store the sensor readings, closer to their source. The database is organized according to a geographic hierarchy and is divided into region, city, neighborhood, block, etc. This hierarchical architecture is well suitable with the application and improves the scalability of the distributed system.

The front end of the PSF is a web based interface. The current location of a driver and the desired destination location are input to this front end. The query is sent to the IrisNet to find the information about an empty parking slot nearest to the destination place and the other related information about the empty slot such as if a permit is required, maximum hourly rate, etc. After locating the space, the front end uses the Yahoo Maps online service to generate driving paths to the available parking slot. This front end can be integrated into a car's navigation system which would be able to get the current location and destination directly from the system and then generate the driving path. If a single camera is not able to cover a particular parking lot, the PSF is able to use the views from multiple cameras and fuse them together to produce an image that covers an entire lot, before running the car detection routines. The detector uses the variance of pixel intensity in image regions to determine the occupancy of a parking space.

2.1.6 Seabird monitoring

The monitoring of the wild life is important to gain knowledge about the biological behaviors of the animals and the birds. A VSN application to monitor the seabirds, in an island, is presented in [42]. The VSN is of multimodal type as it uses different type of sensors with the server such as IR sensors, thermometers, sound sensors and network cameras. The network design of the VSN is server based which connects all the sensor nodes, provides the storage of the sensed data, processes the collected data, and so on. All the data is collected on the server. There is no need for autonomous routing as the configuration of the sensor nodes is pre-designed. Up to 16 sensor nodes can be connected to a server. Each sensor node

provides the input interfaces for analog and digital data. One sensor node can support up to 16 interfaces. The data is captured after intervals and is sent to the server. The VSN can be operated with a battery or AC power.

The purpose of an IR sensor is to study the nest leaving and returning habits of the birds. The sensors are installed at the front of the nests. The thermometers are installed within nests to monitor the activity of the birds. The sound detectors are installed near the nests to study the singing behavior of the birds. A sound sensor can also detect the presence of a group of seabirds. To study the number of birds at a place, the camera sensors are used. The cameras capture the JPEG pictures of the flying seabirds. To capture an image, a threshold value is used. A threshold value of the singing level of the bird sounds is defined. When the input sings exceeds the threshold value a camera is triggered which captures the image. The captured images are stored on the server and can be processed later for further analysis of the behavior of the birds.

2.2 VSN Node Architectures

A VSN sensor device is composed of several basic components such as sensing unit, CPU, communication subsystem, coordination subsystem, storage unit (memory), and optional mobility/actuation unit. The sensing units are usually composed of two subunits including the sensors and Analog to Digital Converters (ADCs). The ADCs convert the analog signals to digital signals. The digital signals are processed by a CPU. A communication subsystem interfaces the device to the network and is composed of a transceiver. The whole system is powered by a power unit. The power unit can be supported by an energy scavenging unit such as solar cells. Several commercial products are available that can function as a VSN device. They differ in the amount of processing power, communication capability and energy consumption [43]. A summary of common platforms is described in following paragraphs. The platforms include SensEye, CITRIC, MeshEye, FireFly Mosaic, WiSNAP, Panoptes and Cyclops.

2.2.1 SensEye

The SensEye [11] is a three-tier heterogeneous network of the wireless sensor nodes and camera sensors designed for surveillance application. The surveillance consists of the three tasks including object detection, recognition and tracking. The lowest tier contains Mote nodes [44], equipped with 900 MHz radios. The tier contains the low resolution camera sensors Cyclops or CMUcam. The second tier contains Stargate nodes [45] with a 400 MHz XScale embedded processor. The nodes in the tier 2 contain two radios. One radio is 802.11 which is used by Stargate nodes to communicate with each other. The other radio (900 MHz) is used by Stargate nodes to communicate with Motes in the tier 1. The third tier contains high resolution PTZ cameras connected to the embedded PCs. The small coverage gaps left by the tier 2 cameras can be filled with these cameras. These cameras provide additional redundancy for the tasks such as localization.

The design strategy of the SensEye is to employ the resource constrained, low-power elements to perform simpler tasks and to use the more capable and high power elements to perform more complex tasks. It results in more efficient use of precious energy resources. The multi-tier network design offers many advantages such as low cost, high coverage. It provides a better balance of cost, coverage, functionality and reliability by using different elements to perform different tasks.

The heterogeneous design of the SensEye optimizes the power consumption, to increase the network lifetime. The key to increase the lifetime is to use the energy resources efficiently and to save as much energy as possible. The SensEye uses many wise strategies to conserve power. For example, the sensing and processing tasks are mapped to the least powerful tier. It is assured that the tier is able to execute the tasks reliably and also fulfills the latency requirements of the application. The duty-cycle operation is implemented for the processor, radio and the sensor of each node. A node is wake-up only when it is required. The more energy consuming nodes in higher tiers are wake-up only when required by the lower tiers. The redundancy in the sensor coverage is utilized to save more power.

2.2.2 CITRIC

The CITRIC [46] is a wireless camera mote for the heterogeneous sensor networks. The hardware platform of this system integrates a 1.3 Mp camera, a PDA class frequency scalable processor, 54 MB RAM and 16 MB flash on a single device. The device connects to a standard sensor network mote to form a camera mote. The communication requirements in CITRIC are reduced by using the in-network processing instead of the centralized processing. The CITRIC uses the back-end client/server architecture to provide a user interface to the system and to support the centralized processing for higher-level applications. It has tighter integration of the components which results in more computing power and less power consumption. It can be employed for a wider variety of distributed pattern recognition applications. The applications demonstrated are image compression, target tracking and camera localization.

The CITRIC follows the modular design technique. It separates the image processing from the networking hardware. It results in easy development and testing of various image processing and computer vision algorithms. It also separates the functions in the client/server back-end software architecture. The mote can communicate over IEEE 802.15.4 protocol and can integrate with the existing low-bandwidth sensor networks. The CITRIC motes are wirelessly networked with the gateway computers that are connected to the internet. The images are captured by the camera sensor and then pre pre-processing is performed on these images. The results are sent to the central server over the network for further processing. The architecture allows various clients to interact with different subsets of the motes and support different high-level applications.

The CITRIC platform consists of a camera board connected to the Tmote Sky board [47]. The camera board is comprised of a processor board and an image sensor board and uses a small number of functional blocks to minimize the size, power consumption and manufacturing costs. The onboard processor is a general purpose processor running Linux. The PXA270 is a fixed-point processor with a maximum speed of 624 MHz, 256 KB internal SRAM and wireless MMX coprocessor to accelerate the multimedia operations. The processor is voltage and frequency scalable for low power operation and is connected to the 64MB SDRAM for storing the image frames during processing and 16MB flash for storing the code. A microphone is connected to the system making it a multi-model system.

2.2.3 MeshEye

The MeshEye [7] is energy efficient smart camera mote architecture, designed for in-node processing. It is designed for distributed intelligent surveillance. The important design considerations for the MeshEye architecture are the selection of low power parts, use of standard interfaces and minimization of the total component count. The important reasons for the small component count are the reduced power consumption and low cost. The reduced power consumption is important for the surveillance applications which are using battery-powered camera motes. The MeshEye contains the two boards, a base board and a sensor board. The sensor board sits on top of the base board. The base board comprises voltage regulators, microcontroller, radio, flash card and the external interface connectors. The sensor board contains two kilopixel imagers and the VGA camera module.

The core of the mote architecture is the Atmel AT91SAM7S family of microcontrollers, which incorporates an ARM7TDMI ARM Thumb processor. This microcontroller family has the power-efficient 32-bit RISC architecture that can be clocked up to 55 MHz. This architecture is suitable to perform the low to high processing task in real time. The AT91SAM7S family offers up to 64 KB of SRAM and up to 256 KB of flash memory. It has a built-in power management controller which can operate the processor in different power saving modes. It can power down the peripherals by disabling their clock source. An internal programmable PLL can operate the processor core at lower clock frequencies. It has a USB 2.0 port and a serial interface.

The mote can host up to eight kilopixel imagers and one high-resolution camera module. An optical mouse sensor is used for kilopixel imager. One of the kilopixel imagers will be used to continuously poll for the moving objects entering in its FoV. Once an object is detected, the stereo vision of the two kilopixel imagers is used to detect the size and position of the object. After determining the position, the microcontroller triggers the VGA camera to capture the high resolution image of the object. A CMOS VSA camera is used for the high-resolution image capture. The flash memory is used for the frame buffering and image storage. The CC2420 transceiver, implementing IEEE 802.15.4 standard, is used for the wireless

connection with other motes in the network. The mote can be powered by a stationary power supply as well as by the two rechargeable AA batteries.

2.2.4 FireFly Mosaic

The FireFly Mosaic [48] is a WSN image processing framework with operating system, networking and image processing primitives that assist in the development of the distributed vision-sensing tasks. Each FireFly Mosaic wireless camera consists of a FireFly node [49] coupled with a CMUcam3 embedded vision processor [50]. The FireFly Mosaic implements an assisted living application capable of fusing multiple cameras with overlapping views to discover and monitor the daily activities in a home. The multiple cameras provide greater coverage of a scene and also handle object obstruction problems. The system automatically combines the information extracted from multiple overlapping cameras to recognize various regions in the house. The prototype of the system consists of eight embedded vision cameras, using batteries for their operation. The image processing is performed in a distributed network.

The FireFly Mosaic hardware includes the CMUcam3 vision processing board, the FireFly sensor networking node and the FireFly gateway to the PC interface board. The hardware architecture of the CMUcam3 consists of a CMOS camera chip, a frame buffer and a microcontroller. The CMOS sensor used is OmniVision OV6620 camera. The images are buffered in AL440b FIFO chip which frees the microcontroller from the pixel-level timing details. The processing of the image is performed by ARM7TDMI microcontroller which contains the 64KB of on-chip RAM and 128KB of flash memory. The interface between the FireFly node and the CMUcam3 includes an in-circuit programming interface which can be used for wireless updates of the camera software over the sensor network. The CMUcam3 also contains four built-in servo controller outputs which can be used to actuate the pan-tilt head.

The FireFly sensor nodes contain low power 8-bit Atmega 1281 processor which is coupled with Chipcon CC2420 802.15.4 radio. The main processor contains the 8KB RAM and 128KB flash. The radio can transmit data at the rate of 250 Kbps up to 100 meters. The FireFly nodes have a mini-SD slot for the data storage and hardware expansion. The FireFly boards can be interfaced with a sensor board which can sense multiple variables such as light, temperature, acceleration and audio. The communication between the CMUcam3 and the FireFly node is performed over the TTL serial line with various extra GPIO pins which can be used for signaling purposes. The FireFly node uses an unregulated 3 volts supply from four AA battery split voltage. The CMUcam3 steps down the 6 volts to 5 volts by using an onboard regulator. The internal regulator of the CMUcam3 can also be used to power the FireFly board from the AC power.

2.2.5 WiSNAP

WiSNAP [51] is a MATLAB-based application platform for wireless image sensor networks. Its Application Program Interface (API) layer and the underlying device libraries facilitate the high-level algorithm and application development on the real image sensor and wireless mote hardware devices. WiSNAP's open system architecture can be readily accommodated with virtually any type of sensor or mote device. The two application examples presented, the event detection and the node localization, demonstrate the easy deployment of the WiSNAP for efficient application development and emulation of the wireless image sensor networks. The WiSNAP consists of two APIs. One API is the Image Sensor API which enables the frame capturing from image sensors. The other API is the Wireless Mote API which provides access to the wireless motes.

WiSNAP is an open-system development structure which can be extended to any image sensor or wireless mote. The developers can extend it for their particular application needs. The open architecture of the WiSNAP framework allows easy integration of additional APIs. For example, a separate API for sensors can be added to the existing application platform which can provide scalar outputs like temperature, pressure, acceleration or velocity. The device libraries access the low-level control of computer hardware and peripheral interfaces by using the functions provided by operating systems. The APIs and libraries facilitate easy extension to other image sensors and wireless motes.

The Agilent's ADCM-1670 camera module is a low power, medium resolution image sensor suitable for the energy constrained WSNs. The Agilent's ADNS-3060 optical mouse sensor is suitable for the low resolution image sensor for the image sensor networks. The Chipcon CC2420DB IEEE 802.15.4 compliant demonstration board pairs an Atmel 8-bit AVR ATmega128L microcontroller [52] with a Chipcon CC2420 2.4 GHz IEEE 802.15.4 RF transceiver [53] which makes it a powerful wireless mote. The current implementation of the WiSNAP includes the device libraries for Agilent's ADCM-1670 camera module [54], Agilent's ADNS-3060 optical mouse sensor [55] and Chipcon's CC2420DB IEEE 802.15.4 compliant demonstration board [56].

2.2.6 Panoptes

The Panoptes [57] is a video-based sensor networking architecture. A Panoptes sensor node is a low-power sensor. The initial video sensor developed was an Applied Data Bitsy board, utilizing the Intel StrongARM 206 MHz embedded processor. The sensor has a Logitech 3000 USB-based video camera, 64 MB memory and an 802.11 based networking card. The next version of the Panoptes sensor was based on Crossbow Stargate platform. The reason for this shift is that this platform has twice the processing power than the Bitsy board and less energy consumption. These video sensors can capture video at a reasonable frame rate of greater than 15 fps. The Panoptes video sensor uses the Linux operating system.

The Linux is flexible to modify the parts of the system for specific applications. Also, it is simple to access a device with Linux than other operating systems.

The video sensing functionality is split into a number of components including capture, compression, filtering, buffering, adaptation and streaming. A USB-based camera is used for video capture with Phillips Web Camera interface with video for Linux. To reduce the transmission cost, the video frames are compressed before the transmission. The data is decompressed from the USB device in the kernel before passing it to the user space. The priorities are used to manage the frame rate and frame quality. When the buffer is full, the data is discarded from the lowest priority layer to the highest priority layer until it is less than a critical value. The priority mapping can be dynamic over time. For example, a high resolution video may be required in an environment monitoring application during the low and high tides but a low quality video during the normal conditions.

A scalable video surveillance system is implemented using the Panoptes video sensor. The system allows the video sensor to connect with the system automatically and allows the sensors to be controlled through the user interface. The video surveillance system consists of a number of components such as video sensor, a video aggregating node and a client interface. The video aggregation node stores and retrieves the video data for the video sensors and the clients. The video sensors employ 802.11 wireless networking to network with the aggregation node. To maximize the scalability of the system, a change detection filtering algorithm is implemented. The motion filtering identifies the events of interest and captures them. For low-power operation, the highest priority information is transferred first from the sensor. This is the case when the network is intermittent or the sensor will be disconnected from the network to save power.

2.2.7 Cyclops

The Cyclops [5] is a vision sensor for wireless sensor networks that performs local image capture and analysis. Cyclopes is a small camera device that bridges the gap between the computationally constrained wireless sensor nodes such as Motes and the CMOS imagers which are designed to mate with the resource-rich hosts. The Cyclops enables the development of new class of vision applications that span across the WSN. Cyclops is an electronic interface between a camera module and a host. It contains a micro-controller that isolates the high-speed data transfer requirements of the camera module from the low-speed embedded controller, providing the still image frames at low rates. The major components of the Cyclopes include an imager, a micro-controller (MCU), a complex programmable logic device (CPLD), SRAM and flash. The MCU is ATmega 128L [2] which controls the Cyclops, communicates with the host and performs the image inference. The MCU controls the imager, sets its parameters and instructs it to capture a frame. The MCU can perform local processing on the captured image to extract some inference.

The camera module is a low power Agilent ADCM-1700, containing a CMOS image sensor and a processor with a high quality lens. The image sensor has a resolution of 352×288. The camera module contains a complete image processing pipeline. It also implements the automatic exposure control and the automatic white balancing. The Cyclops needs memory for image buffering and the local inference processing. To increase the memory space, it uses an external high speed, lower power 64KB CMOS SRAM. For extended battery operation, the device operates from a single 2.3V to 3.6V power supply. The memory is automatically placed in low-power mode when it is not in use. In addition, the Cyclops has 512KB CMOS flash programmable and erasable read only memory. The flash is used to permanently store the data for the functions such as template matching or local file storage.

The CPLD provides the high speed clock, synchronization and memory control for image capture. The CPLD can also perform a limited amount of image processing at capture time such as background subtraction, frame differentiation. When CPLD services are not required then its clock is set to halt state to reduce the power consumption. The reduced power consumption of Cyclops makes it feasible for large scale deployment and extended lifetime. It makes the Cyclops suitable for particular classes of applications such as the object detection and gesture recognition.

3 CAMERA PLACEMENT

This chapter presents an overview of existing camera placement research. After discussing this research, the chapter describes some limitations of the current research concerning the placement of cameras to cover a required area.

3.1 CAMERA PLACEMENT RESEARCH OVERVIEW

Camera sensors are used in many applications such as video surveillance, sensing rooms, conference rooms etc. These applications use arrays of camera sensors. The important issue in designing sensor arrays is the appropriate placement of the camera sensors for the complete coverage of a given space. The term space denotes a physical 2D or 3D room or area which is required to be covered by camera sensors array. The term coverage means that every point of a given space is sensed with a specified minimal resolution. The objective is to image an object in space with minimum resolution. The camera arrays are getting larger and larger day by day. This fact demands the development of efficient camera placement strategies [58].

The problem addressing the optimal placement of multiple visual sensors in a required space is very important. The main goal is to use the minimum number of cameras to completely cover a given space. The problem also relates to optimally positioning and posing the camera sensors. Usually, several different types of cameras are available which differ in their range of views, intrinsic parameters, image sensor resolutions, optics and costs. An important issue is to maintain the required resolution while minimize the cost of a camera sensor array. One objective of camera placement is to determine the minimum number of camera sensors of a certain type as well as their positions and poses in space such that the maximum coverage is achieved. The other objective of camera placement is to determine how to achieve the minimum required coverage while minimizing the total cost of the sensor array when different types of camera sensors are given [58].

The camera sensors can be mounted on mobile autonomous robots for surveillance purposes. The robots installed with camera sensors will be inexpensive as compared to the robots installed with more complex sensors such as lasers. A system that can control the placement of these mobile robots to collect the largest possible amount of information will enhance the usefulness of robots. The camera sensors can be used in automated assembly lines to replace the humans. Replacing the humans with automated systems will increase the production speed of the assembly line and reduce the risk of missing faulty products. For these systems to produce good results, it is necessary that they have best possible view of the products which are being monitored. The effectiveness of these systems is heavily dependent on their physical placement. Thus, it is necessary to determine optimal viewpoints for these systems [59].

The distributed networks provide surveillance of the environment and digitized battlefield. The important issue in the design of these networks is the placement of sensors in the surveillance zone. Several different type of sensors are available which can be appropriately placed for these surveillance applications. These sensors differ from each other in their monitoring range, detection capabilities, and cost. The sensors that can detect targets at longer distances are expensive. It may be impossible to use these sensors for a given application due to higher cost. On the other hand, if small range sensors are used then effective surveillance is possible by using a large number of such sensors. These facts dictate the need for efficient sensor placement strategies to minimize the cost and still be able to achieve the minimum required surveillance [60].

An important problem in sensor networks is to find location of a target. If the coverage area of a sensor is represented as a grid, then the target location is determined by determining the grid point in given space. For enhanced coverage, a large number of sensors are typically deployed in a monitoring area. If the coverage areas of multiple sensors overlap, they may all report a target in their respective zones. The precise location of the target must then be determined by examining the location of these sensors. In many cases, it is impossible to precisely locate the target. Finding the target location can be simplified if the sensors are placed in such a way that every grid point is covered by a unique subset of sensors. In this case, a set of sensors reporting a target uniquely identifies the grid location for the target. In this way, the trajectory of a moving target can be easily determined from time series data [60].

There is a close resemblance between the sensor placement problem and the guard placement problem addressed by the art gallery theorem [61]. The guard placement problem can be informally stated as determining the minimum number of guards required to cover the interior of an art gallery. Several variants of guard placement problem have been studied in the literature including mobile guards, exterior visibility, and polygons with holes. The sensor placement problem differs from guard placement problem in a way that the sensors can have different ranges and also that the target location identification problem requires more sensors than covering problem. The sensor placement problem is also closely related to the alarm placement problem described in [62]. It refers to the problem of placing alarms on the nodes of a graph G to diagnose a single fault in the system. The alarms are similar to the sensors in a monitoring area.

A design methodology for multimedia surveillance systems is proposed in [63] which help a system designer to optimally select and place the sensors to accomplish a given task with a specified performance. The proposed design methodology is direction aware. It means it realizes that only the images obtained from a certain direction may be useful. This design methodology can be scaled to multiple PTZ cameras as well as motion sensors. The design strategy is proposed for building heterogeneous surveillance systems.

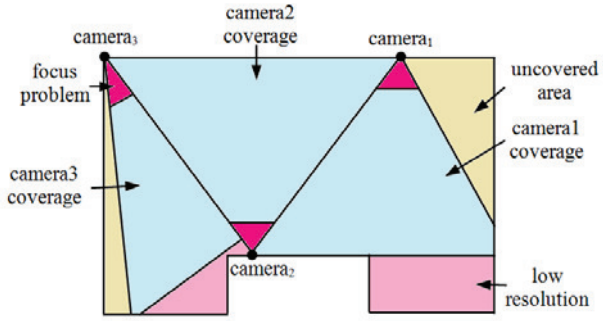

Figure 3.1. 2D Coverage model of a space.

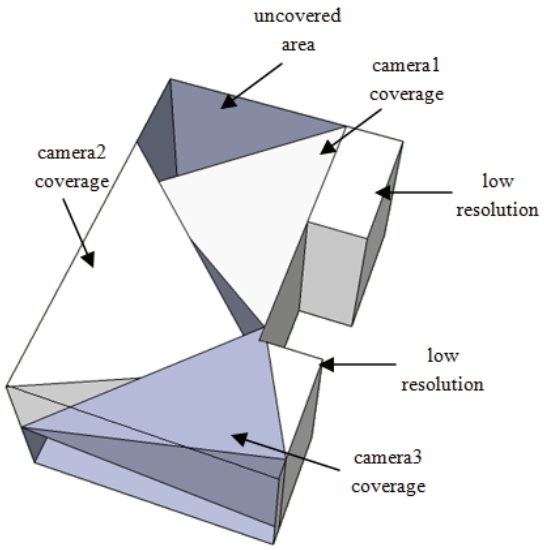

Figure 3.2. 3D Coverage model of a space.

3.2 Coverage Limitations of Existing Research

The problem with some of the research studies just mentioned is that the given area is not fully covered or the minimum required resolution is not assured in the given area. The concept is presented in Figure 3.1. The figure shows a room, the area of which is covered by a number of cameras including cam_1, cam_2 and cam_3. There are some parts in the room which are not being covered. Also, there are some corners in the room which are being covered by a resolution which is lower than the minimum required resolution. Figure 3.1 is the 2D diagram of the room. The coverage appears to be complete at least in the FoVs of given cameras.

However, in the 3D image of the same room, Figure 3.2, it can be seen that this is not the actual case. There are some places which are not being covered by cameras' FoVs. Moreover, there are focus problems in the covered space. Focus problems occur in the areas which are very near to the camera sensors. These areas are not imaged by cameras with accuracy. The research presented in this thesis ensures the full coverage of all the required area and also ensures the minimum required resolution. The research also addresses the camera focus problems.

4 EAGLE SURVEILLANCE

Many applications require characterizing the population behaviour of endangered species such as eagles. This chapter starts with the discussion of the facts about eagles which are relevant to this research. Then the threats to the life of eagle are discussed. The success of the wind energy has made the deployment of larger wind farms possible. The chapter discusses the effects of these wind farms on eagle populations. The next chapter will focus on the development of a VSN model to monitor the golden eagles. The eagle facts described here will be used in the design phase of the VSN model.

4.1 GOLDEN EAGLE FACTS

Golden eagles are the members of bird family. The unique features of these eagles are their larger size, more powerful build, and heavier head and beak. To design a VSN model to monitor the golden eagles, it is necessary to have knowledge about the bird facts which are relevant to the design of the required VSN. The important facts of eagle which are related to the VSN model include the bird size and its routine flight heights. The wingspan of the bird varies from 1.8 to 2.3 m. The bird flies in the altitudes range from 3000 to 5000 m above the ground. The size, wingspan [66], speed [67] and the altitudes of flight [68] of eagle are shown in TABLE 4.1.

TABLE 4.1. Facts about Eagle

Eagle parameters	Golden Eagle
Length	0.84-0.97 m
Wingspan	1.8-2.3 m
Flying speed	129 km/h
Diving speed	322 km/h
Normal Cruising altitude	3000 m
Maximum Cruising Altitude	5000 m

4.2 THREATS TO EAGLE

The largest populations of golden eagles in European areas are found in Alps, Scotland, Scandinavia and Spain. In European areas, the eagles prefer to live mostly in remote mountainous areas and on the lower ground. The eagle likes large territories with enough prey and builds the nests at the places which are free from human disturbance. It prefers the open country areas or the forests with a lot of open spaces where it can hunt. The nest is constructed either on large trees or cliffs. There are many threats to the existence of this beautiful bird. One major threat is the illegal persecution through shooting or poisoning. Sometimes, nests

are deliberately destroyed by game managers. There is a continuing threat from egg collectors in some areas. The poor habitat quality is a serious threat to the life of eagle. The extreme plantation or cutting of trees in eagle territories can disturb the habitat of this bird. There is a need to take measures to secure as well as increase the eagle populations.

4.3 Energy Crises and Human Disturbance

The world energy crises have diverted the engineers to think on renewable energy sources. One of these sources is the wind energy where the wind turbines convert the wind energy to electrical energy. This technology is so successful that the larger wind farms are being built on hills, in forests and even in sea areas. However, these wind farms are a constant threat for the golden eagle habitat. In 2004, it was scientifically estimated that a total of 2,300 golden eagles have been killed by a large wind farm at Altamont Pass, California, in its first 23 years of operation [74]. These are the figures which are collected from only a single area. If the data is collected from other world areas as well, the figures will be alarming. This situation dictates the need to perform the detailed environmental studies before building the wind farms to estimate their effects on eagle habitat. The studies should be performed in the eagle breeding areas as well as the locations which are visited by the eagles during migration season, especially the areas where eagles concentrate during migration. The results of these studies must be taken into account before building the new wind farms. The human disturbance must be reduced in the areas which are close to the nests as well as the important sites where the eagles hunt their prey [64]. Many organizations are working to ensure the survival of the golden eagle such as the Forestry Commission, England, Scottish Natural Heritage and the Royal Society for the Protection of Birds, to ensure the survival of this bird [65].

5 MODEL FORMULATION FOR VSN

This chapter discusses the development of a VSN model for the surveillance of the golden eagles in the sky. The chapter starts with a brief discussion of the 3D visualization of an area as covered by the VSN. The chapter also discusses the minimum resolution which is required to recognize an eagle flying at the higher altitude. Then the concepts of focal length and Angle of View (AoV) are described. Following this, a number of camera sensors are discussed which are used in this study. The development of the VSN model is presented in a number of steps. The steps include the camera sensor selection for the VSN, focal length calculation for the selected camera sensor, camera placement for the full coverage above a given lower altitude. To cover a given area, a number of camera nodes will work in collaboration with each other to track an eagle. The model will calculate the total number of nodes required to cover a given area. At the end of the chapter, the different area coverage regions are discussed.

5.1 COVERAGE VISUALIZATION

The 3D visualization of the coverage with a matrix of camera nodes is shown in Figure 5.1. The sharp tips at the bottom of the figure represent the camera nodes. A number of such nodes arranged in the form of a matrix will form the VSN. The Figure 5.1 contains two important altitude limits. One altitude limit is the dotted line which is called the lower altitude and is denoted by a_l in the figure. The other altitude limit is the dark surface at the top of the figure which is called the higher altitude and is denoted by a_h in the figure. The VSN can provide the full coverage of an eagle between these two altitude values.

The reason for the coverage to be limited at the higher altitude is the resolution of the eagle image on the camera sensor. The resolution is the number of pixels in the eagle image. The quality of an image depends on its resolution. A higher resolution image has better quality. An eagle flying at the lower altitudes will be captured with higher resolution images and vice versa. A certain minimum resolution is required to detect an eagle accurately. The coverage of the VSN is limited at the higher altitude due to the fact that above this altitude the resolution decreases below the minimum criterion and it is not possible to detect the eagle accurately.

The reason for the coverage to be limited at the lower altitude is the distance between the two neighbouring monitoring nodes. It is denoted by d_x on the x side and by d_y on the y side. The lower altitude and the distance between the two neighbouring nodes are related with each other. As the distance between the nodes is decreased, the lower altitude value is also decreased and vice versa. The distance between the neighbouring camera nodes is adjusted such that it ensures the full coverage at the required lower altitude.

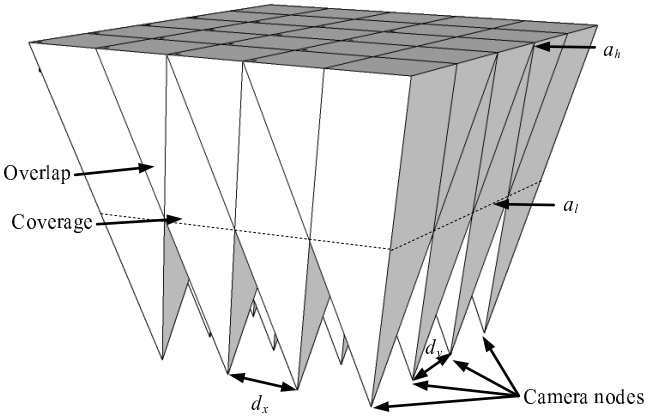

Figure 5.1. 3D Visualization of coverage.

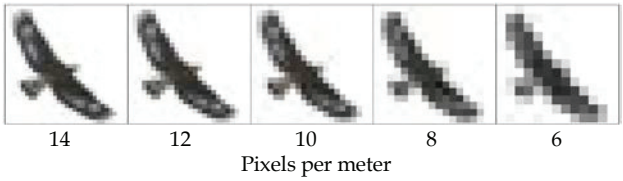

Figure 5.2. An eagle at different resolutions.

As the altitude from the cameras nodes is increased, the coverage of the area by the VSN is also increased. The coverage increases till the lower altitude, where it becomes 100%. Above the lower altitude, the overlap in the coverage is achieved which is useful to calculate the accurate size and exact altitude of an eagle flying in that area, by using the triangulation technique.

5.2 Resolution Effect

As discussed before the resolution is specified in terms of the number of pixels that an eagle contains in an image. It is expressed as the number of pixels per meter. The minimum resolution required to recognize an object, in an object recognition algorithm has been reported in the literature [69], to be about 10 pixels per meter. The images of an eagle object at different resolutions are shown in Figure 5.2. The degradation in the quality of an image with the decrease in the image resolution, as an eagle gradually flies towards higher altitudes, is shown in Figure 5.2. It can be seen that at the lowest resolution, it is almost impossible to recognize the eagle. The figure shows that to recognize an eagle at the highest altitude of 5000 m, a minimum resolution of 10 pixels per meter is required. From the above study, the following assumptions are considered to design the VSN.

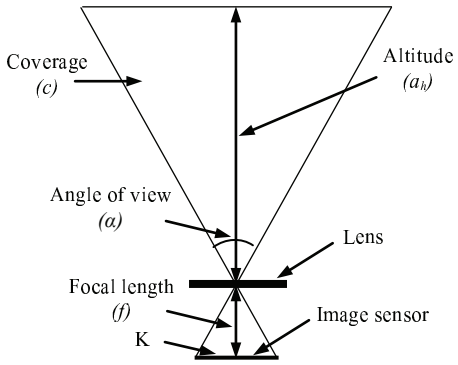

Figure 5.3. Image formation model of lens and camera sensor.

- It is assumed that an eagle flies in a range of altitudes from 3000 to 5000 m above the ground. So, the value of the lower altitude, a_l, is 3000 m and that of the higher altitude, a_h, is 5000 m.
- The *flat* topography of the ground is assumed.
- The distances between the camera nodes are d_x and d_y in the x and y directions, respectively.
- A minimum resolution of 10 pixels per meter is assumed to recognize an eagle at the highest altitude.
- The cameras are aligned such that the horizontal direction of the camera sensor is parallel to the x direction of the observed area.

5.3 IMPORTANT TERMS

The two important concepts related to the cameras and imaging are the focal length and AoV, also called the Field of View (FoV). These two concepts are described in the following paragraphs.

5.3.1 Focal Length

The focal length is the distance between a lens and the image of an object, when the object is infinitely far away from the lens. A lens of the long focal length is referred to as telephoto lens. It produces the larger sized image of a distant object at a larger distance from the lens. The image may cover the entire area of the sensor. A lens of the short focal length is referred to as wide angle lens. It produces the smaller sized image of a distant object at a smaller distance from the lens. The choice of the lens focal length for a camera depends on the size of the camera sensor used in the camera [70]. A model for the image formation with a lens on a camera sensor is shown in Figure 5.3. The small thick horizontal line is representing a lens, small horizontal line at the bottom of the small triangle is representing a camera sensor and the small vertical arrow between the camera sensor and the lens is showing the focal length f of the lens.

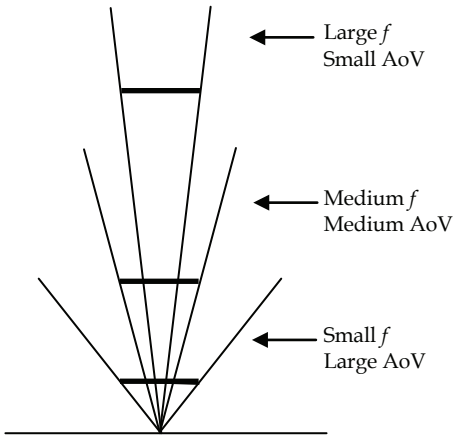

Figure 5.4. AoV versus focal length.

5.3.2 Angle of View

The AoV is defined as the angle subtended at the lens by the camera sensor when the lens is focused at infinity [71]. There exists an inverse relation between the focal length of a lens and the AoV. If a focal length is large, the AoV will be narrow and consequently a smaller area will be covered by the camera and vice versa. These concepts are shown graphically in Figure 5.4. An image sensor generally has a rectangular shape. If the larger side of the rectangle is defined as the horizontal side and the smaller side as the vertical side then the AoV can be measured from three different ways. It can be measured from the horizontal side, vertical side or the diagonal side of the sensor. The AoV shown in Figure 5.3 is measured from the horizontal side of the image sensor. The expression for the AoV can easily be derived by solving the two small right triangles at the bottom of Figure 5.3. The expression to calculate the AoV is given in the following equation.

$$\alpha = 2\arctan\frac{K}{2f} \qquad (5.1)$$

where K is the sensor length in the chosen direction (horizontal, vertical or diagonal), α is the AoV and f is the focal length of the lens. The Equation (5.1) shows that the longer is the focal length, the narrower is the AoV.

5.4 VSN Formulation

The formulation of the VSN consists of a number of steps. The first step is to select a suitable camera sensor for the VSN. The next step is the focal length calculation for the lens, to be used with this camera sensor. The camera sensor and the associated lens define a camera sensor node. Next, the placement of the camera

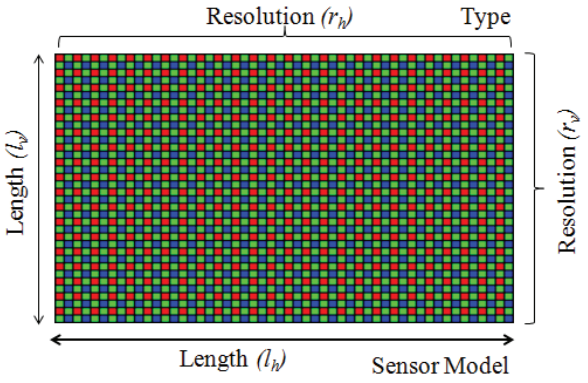

Figure 5.5. A camera sensor with parameters.

TABLE 5.1. Camera sensors used in study

No	Sensor	Type	Resolution		Size (mm)	
			r_h	r_v	l_h	l_v
1	MT9V011	VGA	640	480	3.58	2.69
2	MT9V032	WVGA	752	480	4.51	2.88
3	MT9M033	1.2Mp	1280	960	3.54	2.69
4	MT9M001	1.3Mp	1280	1024	6.66	5.32
5	MT9M032	1.6Mp	1472	1096	3.24	2.41
6	MT9D012	2Mp	1600	1200	3.56	2.68
7	MT9T031	3Mp	2048	1536	6.55	4.92
8	MT9P031	5Mp	2592	1944	5.70	4.28
9	MT9E013	8Mp	3264	2448	4.57	3.43
10	MT9J003	10Mp	3664	2748	6.119	4.589
11	MT9F002	14Mp	4384	3288	6.14	4.6

nodes is finalized to form the VSN. The last step is to calculate the total number of nodes to cover a given area. All these design steps are described below.

5.4.1 Camera Sensor Selection

The first step of VSN design is the selection of a suitable camera sensor. The diagram of a typical camera sensor is shown in Figure 5.5. A camera sensor has a rectangular shape with a number of parameters such as the type, model, horizontal length, vertical length, horizontal resolution and vertical resolution. The type parameter is used to recognize a camera sensor, such as 1 Mp, 2 Mp. The larger side of the sensor is called the horizontal length (l_h), the smaller side is called the vertical length (l_v). The number of pixels along the longer side is called the horizontal resolution (r_h) and the number of pixels along the smaller side is called the vertical resolution (r_v). The sensor is marketed with its model number, e.g., MT9V011. A number of camera sensors which will be used in this study are given in TABLE 5.1 along with their parameters. These parameters will be extensively

used in the design of the VSN. Any camera sensor can be chosen from the TABLE 5.1 to design the VSN.

5.4.2 Focal Length Calculation

The next VSN design step is the calculation of the focal length of the lens to be used with the chosen camera sensor. The camera sensor and the lens with this focal length will form a monitoring node. A lens of a smaller focal length will form a low resolution image of a distant eagle on the selected camera sensor whereas a lens of a larger focal length will form a high resolution image. The focal length of the lens, installed with the camera sensor, is adjusted such that the combination of the camera sensor and the lens focal length must ensure the minimum required resolution of an eagle, flying at the highest altitude.

Suppose the size of the eagle is assumed to be 1m x 2m, then the number of pixels required along the 1m side of the bird is 10. In other words, the resolution required for an eagle of the size 1m x 2m, flying at the higher required altitude, i.e., 5000m, is 10 pixels per meter. The number of the pixels occupied by an eagle on the camera sensor can be obtained by dividing the length of the eagle with the total length of the view, captured by the camera sensor on the x or y side and multiplying it with the total number of pixels contained by the sensor along l_h or l_v side.

$$p_x = \frac{l_{ox}}{l_{vx}} \cdot r_h \text{, or } p_y = \frac{l_{oy}}{l_{vy}} \cdot r_v \qquad (5.2)$$

Where p_x and p_y are the number of pixels occupied by the eagle, l_{ox} and l_{oy} are the lengths of the object, l_{vx} and l_{vy} are the lengths of the views on the x side and y side, respectively. The r_h and r_v are the camera sensor parameters as described above. The focal length that is required to obtain the minimum number of pixels for the given eagle size, at the given higher altitude can be derived by the symmetry of the triangles in the model of Figure 5.3. The value of the focal length, f, derived is given below.

$$f = \frac{l_h}{l_{vx}} \cdot a_h \text{, or } f = \frac{l_v}{l_{vy}} \cdot a_h \qquad (5.3)$$

Where a_h is the highest altitude. The l_h and l_v are the camera sensor parameters as described above. By combining the equations (5.2) and (5.3), the derived equation for the focal length, f, which fulfils all the criteria, is given below.

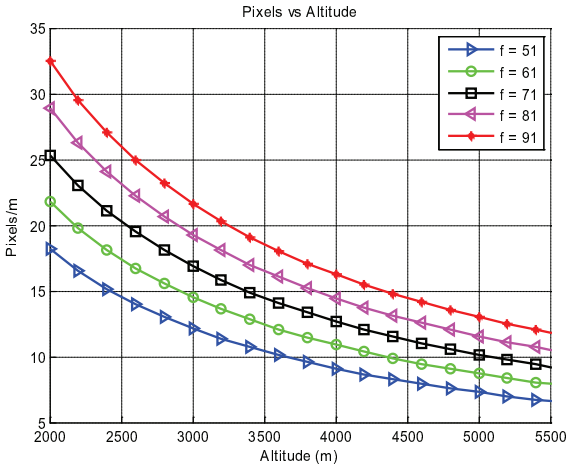

Figure 5.6. Resolution analysis of MT9E013 sensor versus *f*.

$$f = \frac{p_x}{r_h} \cdot \frac{l_h}{l_{ox}} \cdot a_h \text{, or } f = \frac{p_y}{r_v} \cdot \frac{l_v}{l_{oy}} \cdot a_h \qquad (5.4)$$

Both, the selection of a camera sensor, from TABLE 5.1, and the required focal length, calculated by using equation (5.4), form a monitoring node. The resolution of an eagle, in terms of pixels per meter, at an altitude a_h, can be verified for this node. Suppose a node is designed by using the 8 Mp camera sensor, MT9E013, to monitor an eagle of size 1m x 2m at an altitude of 5000 m. The focal length required by this camera sensor to monitor this eagle at the desired altitude is calculated by using equation (5.4), and is found to be 71 mm. The resolution versus altitude is simulated for a set of focal lengths, 51, 61, 71, 81 and 91 mm. The results are shown in Figure 5.6. The figure shows that the minimum lens focal length which fulfils the criterion of 10 pixels per meter, at the 5000 m altitude, is 71 mm.

Next, the lens of 71 mm focal length is chosen for all the sensors given in TABLE 5.1 to make the different monitoring nodes. The simulations are performed for the resolution versus altitude for all the nodes. The results are shown in Figure 5.7. From the simulation results it can be verified that only the two camera sensors, 8 Mp and 14 Mp, are suitable to design the camera nodes with 71 mm focal length.

5.4.3 Camera Node Placement

A camera sensor combined with a lens forms a monitoring node. A number of such nodes installed in the form of a matrix will form the final VSN. An example VSN developed by using the two monitoring nodes C_1 and C_2, is shown in Figure 5.8. The next step of the VSN design is to decide the placement of the monitoring nodes in the matrix. The placement will be finalized by calculating the distance between

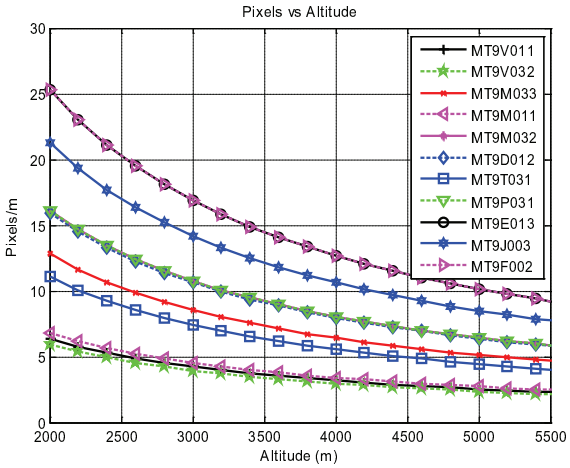

Figure 5.7. Resolution analysis of different sensors at 71 mm *f*.

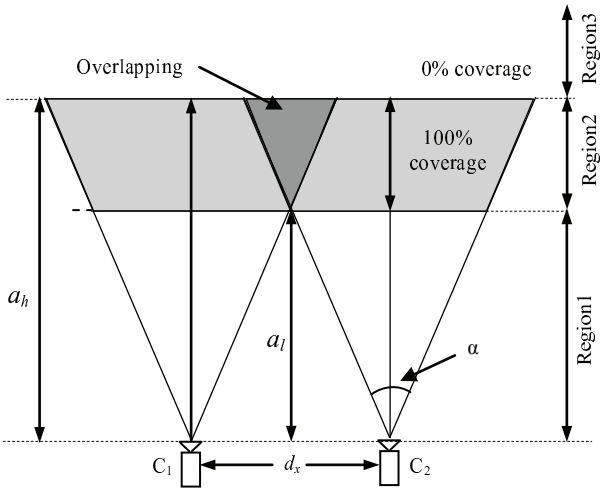

Figure 5.8. VSN model with two camera nodes.

the two neighbouring nodes. The expressions for the distances d_x and d_y along x and y direction can be calculated by solving the triangles involving the distances d_x, d_y and the lower altitude a_l and by placing the expression of the AoV from equation (5.1). The derived equations to calculate d_x and d_y are given below.

$$d_x = \frac{a_l \cdot l_h}{f}, \text{ and } d_y = \frac{a_l \cdot l_v}{f} \qquad (5.5)$$

where l_h and l_v are the horizontal and the vertical lengths of the camera sensor, used for the node design, and f is the focal length of the associated lens.

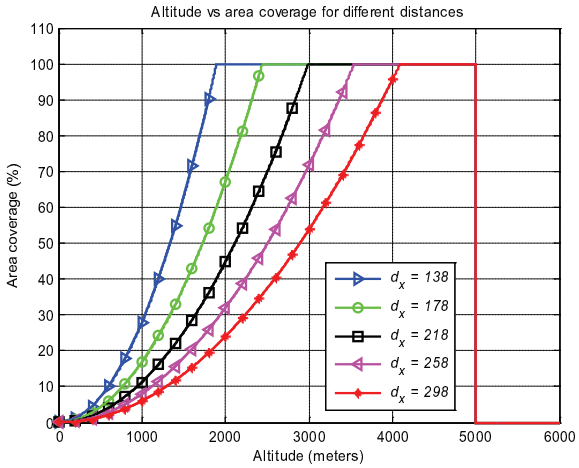

Figure 5.9. Coverage versus distance between nodes analysis.

Example 5.1

To illustrate the coverage model of Figure 5.8, a two node network is designed in this example. Suppose the 10 Mp camera sensor, MT9J003, is selected for this VSN to monitor the eagle. The equation (5.4) is used to calculate the focal length required for this camera sensor to achieve a resolution of 10 pixels per meter. The calculated focal length is 84 mm. The equation (5.5) is used to calculate the distance between the camera nodes, to achieve the full coverage at the lower altitude a_l of 3000 m. The distance is calculated along the x side, as the nodes are placed along the x axis. The value of the d_x is found to be 218 m. The distances 138, 178, 218, 258 and 298 m are chosen between the model nodes and the coverage is simulated for a range of altitude from 0 to 6000 m. The simulation results are shown in Figure 5.9. The simulation results show that for smaller distances between the camera nodes, the full area coverage is achieved at the lower altitudes. Also, for larger distances between the camera nodes, the full area coverage is achieved at the higher altitudes.

5.4.4 Area Coverage Cost

The last step in the design of the VSN is to calculate the total number of nodes to cover a given area. The coverage model can be used to minimize the number of nodes needed in a deployment for the surveillance of a given area. If A is the area to be covered by the VSN then the equation to calculate the number of nodes n (cost of VSN), required to cover the given area is given below.

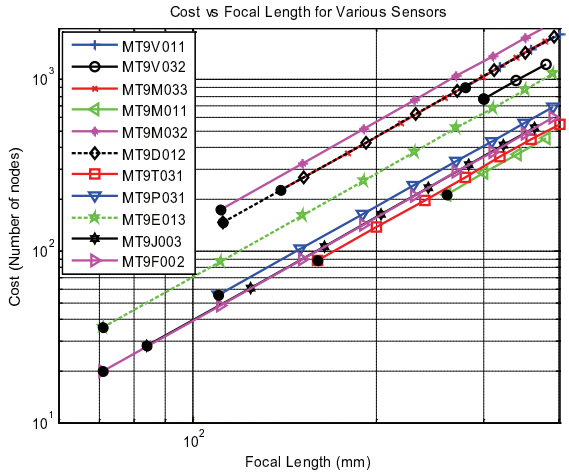

Figure 5.10. Optimization results of homogeneous VSN.

$$n = \frac{A}{\frac{l_v}{l_h}\left(\frac{a_l \cdot r_h}{a_h \cdot p}\right)^2}. \qquad (5.6)$$

The calculated number of nodes is a good index to determine the surveillance cost of a given area. To cover an area of 1 km², by using the camera sensors given in the TABLE 5.1, and to achieve the full coverage the altitude 3000-5000 m, the coverage model and the equation (5.6) are combined. The cost of the VSN for the evaluated optics and the camera sensors, that provides the 100% coverage at the 3000 m altitude is illustrated in Figure 5.10. The small black dot at the starting of a curve shows the minimum focal length which assures 10 pixels per meter resolution at the 5000 m altitude. This minimum focal length can also be calculated by using equation (5.4). As the focal length is increased from this minimum value, the cost of the network is also increased. To cover the given area of 1 km², the focal length of the lens and the type of the camera sensor can be known from the simulation results of Figure 5.10. The distance between the nodes is calculated from equation (5.5) and the total number of nodes, required to cover the given area, can be calculated from equation (5.6) or seen from Figure 5.10. The results in Figure 5.10 show that the camera node, using a 14 Mp camera sensor MT9F002, with the lens focal length of 71mm, uses the minimum cost for the surveillance of 1 km² area. This combination of the camera sensor and the lens requires a total of 20 camera nodes for the surveillance of 1 km² area between the altitude values of 3000 and 5000 m.

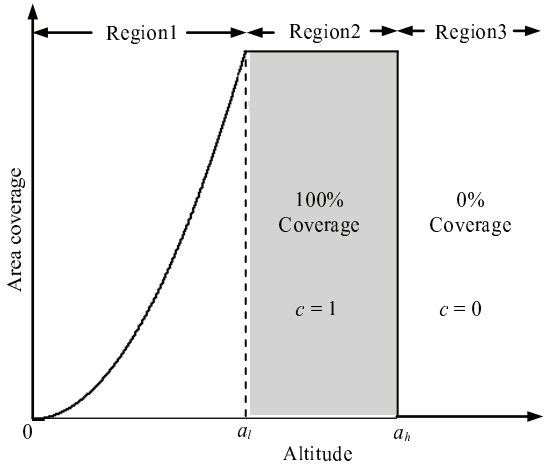

Figure 5.11. Aree coverage regions.

5.5 COVERAGE REGIONS

The coverage of the VSN shown in Figure 5.8 can be summarized in three area coverage regions, Region 1, Region 2 and Region 3. These regions are shown in Figure 5.11.

5.5.1 Region 1

The Region 1 starts from the altitude 0 and ends at the altitude a_l. The value of the altitude a_l is 3000 m. The area coverage increases from 0 to 100% as the altitude increases from 0 to a_l. The relation between the area coverage and the altitude, in Region1, can be expressed as follows.

$$c = \frac{a^2}{f^2} \cdot \frac{l_h \cdot l_v}{d_x \cdot d_y} \qquad (5.7)$$

For $0 \le a \le a_l$,

where c is the coverage, a is the altitude, d_x and d_y are the distances along x and y directions, f is the focal length, l_h and l_v are the horizontal and vertical lengths of the camera sensor, respectively. Equation (5.7) shows that the coverage will be increased by increasing the altitude and/or the sensor area and by decreasing the focal length and/or the distance between the nodes. By increasing the altitude, the coverage will be increased but the resolution will be decreased. To overcome this problem, the lenses with larger focal length will be required but it will increase the number of camera nodes as well as the price of the VSN. Also, by decreasing the distance between the nodes, the number of nodes will be increased. The design

objective is be to achieve the full coverage with the smaller focal length and the larger distance between the cameras nodes. This will result in the decreased cost.

5.5.2 Region 2

The Region 2 starts from the altitude a_l and ends at the altitude a_h. The value of a_h is 5000 m. For the altitudes above a_h, the resolution reduces to less than the minimum criterion. The resolution can be increased by increasing the focal length and/or the resolution of the camera sensor or by decreasing the camera sensor area. Region 2 is the desired region for this surveillance application. It assures the full coverage of the eagle for a range of altitudes from 3000 to 5000 m. The coverage remains constant in this region and can be represented as follows.

$$c = 1 \qquad (5.8)$$

For $a_l \le a \le a_h$.

5.5.3 Region 3

The Region 3 starts from the altitude a_h and continues onward. The coverage is zero in this region because the resolution reduces below the criterion. The coverage can be represented as follows.

$$c = 0 \qquad (5.9)$$

For $a \ge a_h$.

This region is useless for this surveillance application. The reason is that an eagle cannot be tracked in this region due to the zero coverage.

6 COST OPTIMIZATION FOR VSN

Chapter 5 describes the design of a VSN, for the surveillance of the golden eagle, between the higher altitude of 3000 m and the higher altitude of 5000 m. This chapter describes the design of a VSN which ensures the monitoring of an eagle in the altitude ranges from 500 to 5000 m, covering an area of $1km^2$. The surveillance area of the VSN is increased by increasing the higher altitude and/or decreasing the lower altitude. The drawback is that it increases the covered area but it also increases the VSN cost. The optimization techniques are used in this chapter to increase the covered area at the decreased cost.

The costs required by each camera sensor of TABLE 5.1, to cover the given area, for the 10 pixels per meter resolution at the given higher altitude, are calculated by using equation (5.6). The costs required by all the camera sensors are given in TABLE 6.1. From the table it is evident that a large cost of the respective camera sensor is required to cover the given area. The minimum costs of 994 and 694 are required by the camera sensors of type 10 Mp and 14 Mp, respectively. Even these minimum costs are very high to design a VSN for the eagle surveillance application. Thus, the need arises to design the techniques to reduce the number of camera nodes to cover the given area.

The main objective of this chapter is to reduce the cost of a VSN, required to cover a given area, as low as possible. This chapter will describe the techniques to reduce the cost to cover an area. As the 10 Mp and 14 Mp camera sensors require minimum cost to cover a given area, these camera sensors will be used for the analysis in this chapter. The results derived with these camera sensor types will be equally applicable to the other camera sensor types as well.

6.1 OPTIMIZATION PRINCIPLE

The basic idea to reduce the cost required to cover a given area is splitting a given range of altitudes into the sub-ranges of altitudes and then covering these individual sub-ranges of the altitudes with sub VSNs. This technique will be helpful to reduce the cost required to cover a given area between the two given altitudes limits. The individual sub VSNs required to cover the sub-ranges of altitudes may use the similar or different camera sensors but the different optics. One sub VSN will use the optics which will be suitable for one sub-range of altitudes while the other sub VSN will use the optics which will be suitable for the other sub-range of altitudes. Thus, the combined VSN will be a heterogeneous VSN of the individual sub VSNs. The major task is to find the specific altitude points where to split a given range of altitudes. These points will be used to divide the given altitudes range into sub ranges, such that a minimum cost will be required to cover a given area, on the basis of the partitioning of the range of the altitudes [73].

TABLE 6.1. Cost for homogeneous VSN

No	Sensor	Type	Cost
1	MT9V011	VGA	32553
2	MT9V032	WVGA	27704
3	MT9M033	1.2Mp	8139
4	MT9M001	1.3Mp	7630
5	MT9M032	1.6Mp	6199
6	MT9D012	2Mp	5209
7	MT9T031	3Mp	3179
8	MT9P031	5Mp	1985
9	MT9E013	8Mp	1252
10	MT9J003	10Mp	994
11	MT9F002	14Mp	694

6.2 DESIGNING SUB VSNS USING OPTIMIZATION

If the range of given altitudes is larger than a certain value then a higher cost is involved to cover this range with a homogeneous VSN. The solution to reduce this cost is to divide this range into sub ranges and cover these sub ranges with sub VSNs. In the following paragraphs the optimization techniques, to divide a VSN into two, three and four VSNs are presented. The values of the altitude points which are used to divide this range are calculated. The sub VSNs are designed by using these altitude points. The optical components are also calculated for each individual sub VSN.

6.2.1 Optimization with Two VSNs

To find the optimum altitude points to split the given altitudes range, the costs of the camera sensors to cover a given area are simulated against the respective altitude values in the given altitudes range. The cost of a camera sensor to cover a given area can be calculated by using the equation (5.6). Suppose the camera sensors of types 10 Mp and 14 Mp are chosen and the simulations for the cost are performed against an altitude range of 500 to 5000 m to cover an area of 1 km^2. It is assumed that the 10 Mp camera sensor will cover the lower sub-range of altitudes. For this camera sensor the simulations are performed by fixing the a_{min} value to 500 m and the values of a_{max} are varied from 501 to 5000 m. It is further assumed that the 14 Mp camera sensor will cover the higher sub-range of altitudes. For this camera type, the simulations are performed by fixing the value of a_{max} to 5000 m and the values of a_{min} are varied from 500 to 4999 m. During simulations, the costs achieved for the two camera sensor types are added and are plotted against the respective altitudes along with the cost plots of the individual camera sensor types. A resolution of 10 pixels per meter is assumed for the above simulations.

The simulation results are shown in Figure 6.1. The figure shows that the two plots for the 10 Mp and 14 Mp camera sensors intersect at an altitude of 1445 m. It is also

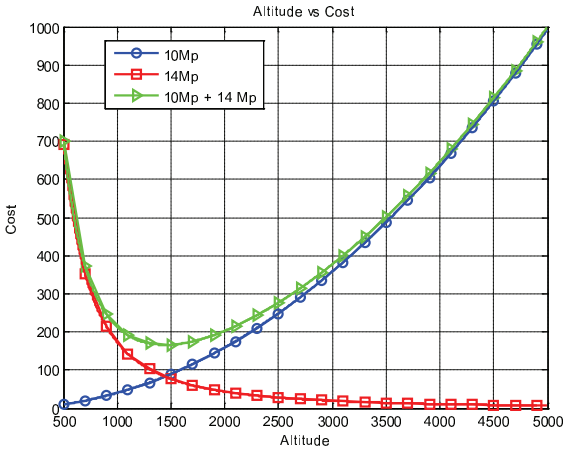

Figure 6.1. Optimization with two camera nodes.

evident that the combined cost for the two camera sensors has minimum value at this altitude. Also, both the camera sensors use equal cost to cover the given area at this altitude point, which is 83 for each camera sensor type in this case. For this particular case, the 1445 m altitude point is the optimum altitude point which provides the minimum combined cost for the two camera types. This point can be used as a partition point for the given altitudes range from 500 to 5000 m. By partitioning the given range into two ranges, the two sub-ranges of altitudes are obtained. The coverage of these sub ranges with the two sub VSNs, VSN_1 and VSN_2, will use the minimum cost to cover the given area.

The altitude values for the first sub range will be from 500 to 1445 m. This sub-range will be covered by a sub VSN, say VSN_1, by using the 10 Mp camera sensor, as was assumed before. The VSN_1 requires a total cost of 83 nodes to cover the given area as shown in the simulation results of Figure 6.1. This cost can also be calculated by using the equation (5.6). The focal length of the lens to be used with the 10 Mp camera sensor to achieve a minimum resolution of 10 pixels per meter at the 1445 m altitude can be calculated by using the equation (5.4), and is found to be 24 mm. The other sub-range of altitudes is from 1445 to 5000 m. This sub-range will be covered by the second sub VSN, say VSN_2, by using the 14 Mp camera sensor, as assumed before. The VSN_2 requires a total of 83 nodes to cover the given area as shown in the simulation results of Figure 6.1. This cost can also be calculated by using the equation (5.6). The focal length of the lens to be used with the 14 Mp camera sensor, to achieve a minimum required resolution of 10 pixels per meter at the 5000 m altitude can be calculated by using equation (5.4), and is found to be 70 mm.

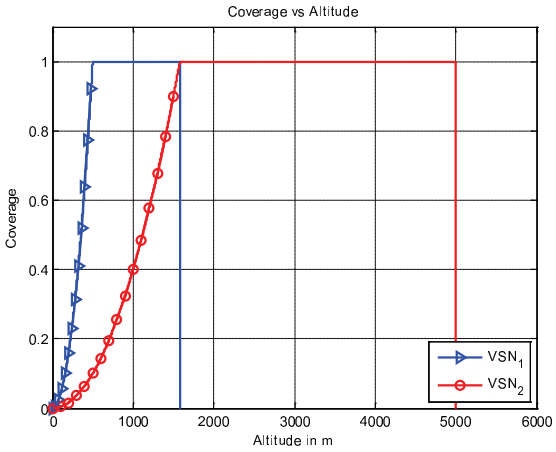

Figure 6.2. Coverage graph of heterogeneous VSN with 2 sub VSNs.

The resultant VSN will be a heterogeneous network of sub VSNs, VSN_1 and VSN_2. It will be heterogeneous because of the different camera sensor types and the lenses of the different focal lengths used in the sub VSNs. If the same types of camera sensors are used for the two sub VSNs, even then the resultant VSN will be heterogeneous because of using the different types of optics for the two sub VSNs. By using this technique of partitioning the altitudes range, an area of $1km^2$ between the altitudes range from 500 to 5000 m can be covered with a total of 166 camera nodes. The coverage graph of the two VSNs is shown in Figure 6.2. If the altitudes range partitioning technique is not used and a homogeneous VSN is used to cover the altitudes range from 500 to 5000 m, then the homogeneous VSN using the 10 Mp camera sensor will cost 994 nodes while the homogeneous VSN using the 14 Mp camera sensor will cost 694 nodes.

For the VSN_1, the a_{l1} and a_{h1} are the lower and higher altitude values, respectively. Similarly, for the VSN_2, the a_{l2} and a_{h2} are the lower and higher altitude values, respectively. The a_{12} is the optimized altitude point in the given range of altitudes. The VSN_1 will cover the altitudes range from a_{min} to a_{12}. Thus, the a_{h1} value of the VSN_1 will be equal to the a_{12} point as shown in Figure 6.3. The VSN_2 will cover the range from a_{12} to a_{max}. Thus, the a_{l2} value of the VSN_2 will be equal to the a_{12} point, as shown in Figure 6.3. The equation for the optimized altitude point a_{12} can be derived as follows. The cost for the VSN_1 for the altitudes range from a_{min} to a_{12} can be calculated by using equation (5.6). Similarly, the cost for the VSN_2 for altitudes range from a_{l2} to a_{max} can be calculated. The expression for the optimized altitude point a_{12} is derived by equating the two costs and simplifying for the optimized point. The derived equation for this point is given below.

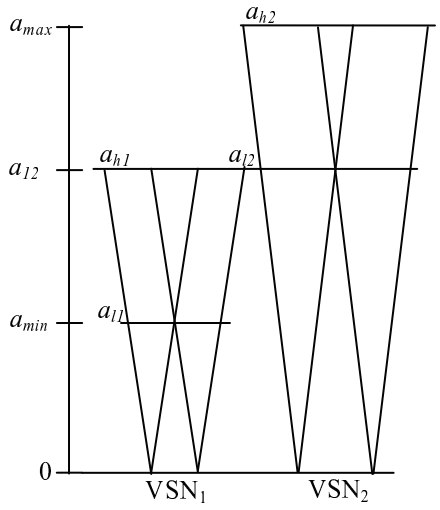

Figure 6.3. Heterogeneous VSN design with 2 sub VSNs.

$$a_{12} = \left(a_{\min} \cdot a_{\max} \cdot \sqrt{\frac{s_1}{s_2}} \right)^{\frac{1}{2}} \qquad (6.1)$$

Where a_{min} is the minimum altitude and a_{max} is the maximum altitude of the given range. The s_1 and s_2 are equal to the multiplication of r_h and r_v parameters of the camera sensors used for VSN_1 and VSN_2, respectively. In this equation the first expression, containing the a_{min} and a_{max} terms, calculates the altitude value, while the second expression $\sqrt{\frac{s_1}{s_2}}$ is related to the camera sensors. If both camera sensors are of similar type then this expression reduces to 1. In that case the equation (6.1) reduces to the following form.

$$a_{12} = \left(a_{\min} \cdot a_{\max} \right)^{\frac{1}{2}} \qquad (6.2)$$

Thus, when the camera sensors for both the sub VSNs are similar, the value of the optimized altitude point depends only on the values of a_{min} and a_{max} and is independent of the camera sensor types used for the VSN_1 and VSN_2.

6.2.2 Optimization with Three VSNs

The cost of a VSN to cover a given area can be reduced further if a given range of altitudes is divided into three sub-ranges and covering these individual sub-ranges

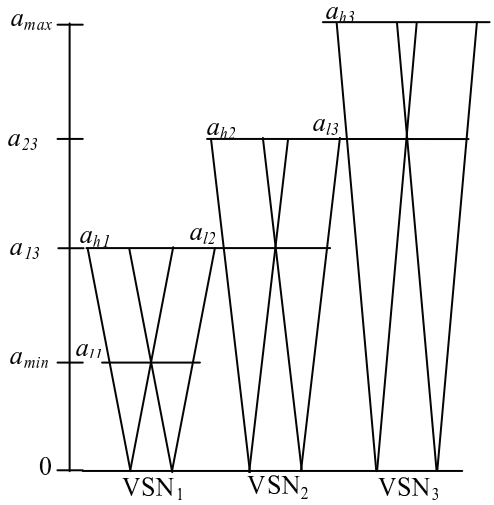

Figure 6.4. Heterogeneous VSN design with 3 sub VSNs.

by using three sub VSNs. Suppose there are three sub VSNs, VSN_1, VSN_2 and VSN_3, to cover the given area. For VSN_1, the a_{l1} is the lower altitude value and a_{h1} is the higher altitude value. For VSN_2, the a_{l2} is the lower altitude value and a_{h2} is the higher altitude value. Similarly, for VSN_3, the a_{l3} is the lower altitude value and a_{h3} is the higher altitude value. The a_{13} and a_{23} are the two optimized altitude points in the given range of altitudes, as shown in Figure 6.4. The a_{13} is the lower optimum altitude value while the a_{23} is the higher optimum altitude. The VSN_1 will cover the altitudes range from a_{min} to a_{13}. Thus, the a_{h1} value of VSN_1 will be equal to the a_{13} point as shown in Figure 6.4. The VSN_2 will cover the range from a_{13} to a_{23}. Thus, the a_{l2} value of VSN_2 will be equal to the a_{13} point and the a_{h2} value will be equal to the a_{23} point as shown in Figure 6.4. The VSN_3 will cover the range from a_{23} to a_{max}. Thus, the a_{l3} value of VSN_3 will be equal to the a_{23} point and the a_{h3} value will be equal to the a_{max} point as shown in Figure 6.4. The coverage graph of the three sub VSNs is shown in Figure 6.5.

To derive the equation for the optimum altitude point a_{13}, the cost for the VSN_1 for the altitudes range from a_{min} to a_{13} is calculated by using equation (5.6). Similarly, the cost for the VSN_2 for the altitudes range from a_{13} to a_{23} is calculated. The expression for the optimized altitude point a_{13} is derived by equating the two costs and simplifying for the optimized point a_{13}. The derived equation for this point is given below.

$$a_{13} = \left(a_{\min}^{2} . a_{\max} \cdot \frac{s_1}{\sqrt{s_2 s_3}} \right)^{\frac{1}{3}} \qquad (6.3)$$

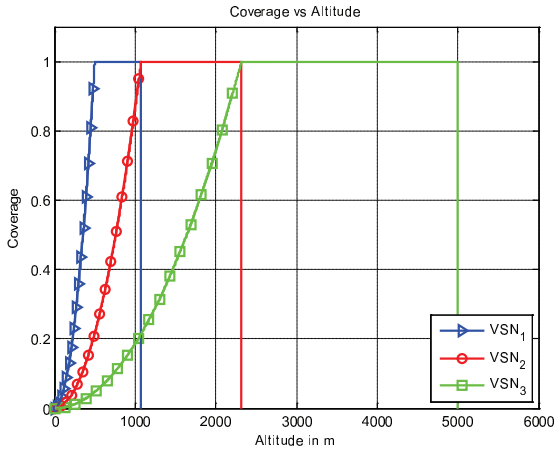

Figure 6.5. Coverage graph of heterogeneous VSN with 3 sub VSNs.

Where a_{min}, a_{max}, s_1, s_2 are described above for equation (6.1). The s_3 is equal to the multiplication of r_h and r_v of the camera sensor used for VSN_3.

To derive the equation for the optimum altitude point a_{23}, the cost for the VSN_2 for the altitudes range from a_{13} to a_{23} is calculated by using equation (5.6). Similarly, the cost for the VSN_3 for the altitudes range from a_{23} to a_{max} is calculated. The expression for the optimized altitude point a_{23} is derived by equating the two costs and simplifying for the optimized point a_{23}. The derived equation for this point is given below.

$$a_{23} = \left(a_{\min} \cdot a_{\max}^2 \cdot \frac{\sqrt{s_1 s_2}}{s_3} \right)^{\frac{1}{3}} \qquad (6.4)$$

Where a_{min}, a_{max}, s_1, s_2 and s_3 are as described above for equations (6.1) and (6.3).

In equations (6.3) and (6.4), the first expression, containing the a_{min} and a_{max}, calculates the altitude value, while the second expression containing the s_1, s_2 and s_3 is related to the camera sensor types used for the VSN_1, VSN_2 and VSN_3, respectively. If similar cameras are used for all the three sub VSNs, then this expression reduces to 1 and the equations (6.3) and (6.4) reduce to the following equations.

$$a_{13} = \left(a_{\min}^2 \cdot a_{\max} \right)^{\frac{1}{3}} \qquad (6.5)$$

$$a_{23} = \left(a_{\min} \cdot a_{\max}^2 \right)^{\frac{1}{3}} \qquad (6.6)$$

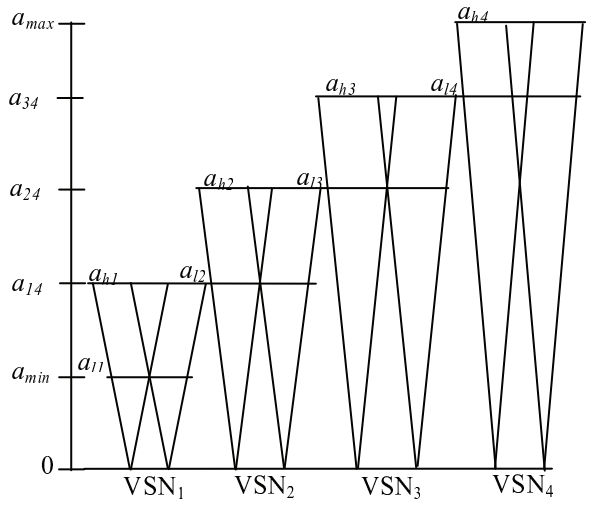

Figure 6.6. Heterogeneous VSN design with 4 sub VSNs.

Thus, when similar camera types are used for all the three VSNs, the values of the optimum altitude points no longer depend on the camera sensor types used for the VSN$_1$, VSN$_2$ and VSN$_3$ and depend only on the a_{min} and a_{max} values.

6.2.3 Optimization with Four VSNs

Suppose a given range of altitudes is divided into the four sub-ranges and the individual sub-ranges are covered by using the four sub VSNs, VSN$_1$, VSN$_2$, VSN$_3$ and VSN$_4$, to cover a given area. For VSN$_1$, the a_{l1} is the lower altitude value and the a_{h1} is the higher altitude value. For VSN$_2$, the a_{l2} is the lower altitude value and the a_{h2} is the higher altitude value. For VSN$_3$, the a_{l3} is the lower altitude value and the a_{h3} is the higher altitude value. Similarly, For VSN$_4$, the a_{l4} is the lower altitude value and the a_{h4} is the higher altitude value. The a_{14}, a_{24} and a_{34} are the optimized altitude points in the given range of altitudes, as shown in Figure 6.6. The a_{14} is the lower optimum point, a_{24} is the middle optimum point and the a_{34} is the higher optimum point.

The VSN$_1$ will cover the altitudes range from a_{min} to a_{14}. Thus, the a_{l1} value of VSN$_1$ will be equal to the a_{min} and the a_{h1} value will be equal to the a_{14} point as shown in Figure 6.6. The VSN$_2$ will cover the range from a_{14} to a_{24}. Thus, the a_{l2} value of VSN$_2$ will be equal to the a_{14} point and the a_{h2} value will be equal to the a_{24} point. The VSN$_3$ will cover the range from a_{24} to a_{34}. Thus, the a_{l3} value of VSN$_3$ will be equal to the a_{24} point and the a_{h3} value will be equal to the a_{34}. The VSN$_4$ will cover the range from a_{34} to a_{max}. Thus, the a_{l4} value of VSN$_4$ will be equal to the a_{34} point and the a_{h3} value will be equal to the a_{max}. The coverage graph of four sub VSNs is shown in Figure 6.7.

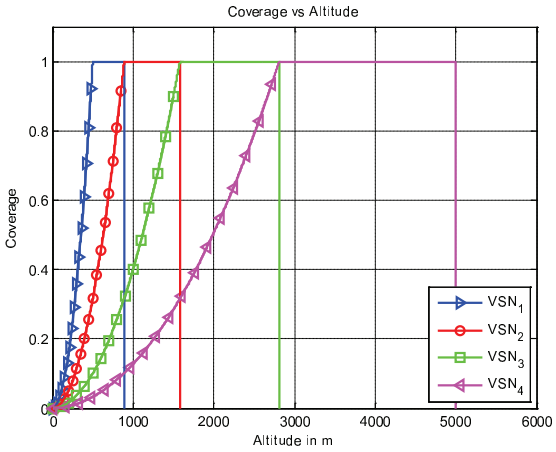

Figure 6.7. Coverage graph of heterogeneous VSN with 4 sub VSNs.

To derive the equation for the optimum altitude point a_{14}, the cost for the VSN_1 for the altitudes range from a_{min} to a_{14} and the cost for the VSN_2 for the altitudes range from a_{14} to a_{24} are calculated by using equation (5.6). The expression for the optimized altitude point a_{14} is derived by equating the two costs and simplifying for the optimized point a_{14}. The derived equation for this point is given below.

$$a_{14} = \left(a_{\min}^{3} . a_{\max} \cdot s_1 \cdot \sqrt{\frac{s_1}{s_2 s_3 s_4}} \right)^{\frac{1}{4}} \qquad (6.7)$$

Where a_{min}, a_{max}, s_1, s_2 and s_3 are as described above for equation (6.4). The s_4 is equal to the multiplication of r_h and r_v of the camera sensor used for VSN_4.

To derive the equation for the optimum altitude point a_{24}, the cost for the VSN_2 for the altitudes range from a_{14} to a_{24} and the cost for the VSN_3 for the altitudes range from a_{24} to a_{34} are calculated by using equation (5.6). The expression for the optimized altitude point a_{24} is derived by equating the two costs and simplifying for the optimized point a_{24}. The derived equation for this point is given below.

$$a_{24} = \left(a_{\min} \cdot a_{\max} \cdot \sqrt{\frac{s_1 s_2}{s_3 s_4}} \right)^{\frac{1}{2}} \qquad (6.8)$$

Where a_{min}, a_{max}, s_1, s_2 and s_3 and s_4 are as described above.

To derive the equation for the optimum altitude point a_{34}, the cost for the VSN_3 for the altitudes range from a_{24} to a_{34} and the cost for the VSN_4 for the altitudes range from a_{34} to a_{max} are calculated by using equation (5.6). The expression for the optimized altitude point a_{34} is derived by equating the two costs and simplifying for the optimized point a_{34}. The derived equation for this point is given below.

$$a_{34} = \left(a_{\min} \cdot a_{\max}^3 \cdot \frac{1}{s_4} \cdot \sqrt{\frac{s_1 s_2 s_3}{s_4}} \right)^{\frac{1}{4}} \qquad (6.9)$$

Where a_{min}, a_{max}, s_1, s_2 and s_3 and s_4 are as described above.

In equations (6.7), (6.8) and (6.9), the first expression, containing a_{min} and a_{max}, calculates the altitude value, while the second expression containing s_1, s_2, s_3 and s_4 is related to the camera sensor types. If similar cameras are used for all the four sub VSNs, then these expressions reduce to 1 and the equations (6.7), (6.8) and (6.9) reduce to the following equations.

$$a_{14} = \left(a_{\min}^3 . a_{\max} \right)^{\frac{1}{4}} \qquad (6.10)$$

$$a_{24} = \left(a_{\min} \cdot a_{miax} \right)^{\frac{1}{2}} \qquad (6.11)$$

$$a_{34} = \left(a_{\min} \cdot a_{\max}^3 \right)^{\frac{1}{4}} \qquad (6.12)$$

Thus, when similar camera types are used for all the four sub VSNs, the values of the optimum altitude points become independent of the camera sensor types used to design the sub VSNs and depend only on the values of a_{min} and a_{max}.

6.3 SELECTION CRITERIA FOR 1, 2, 3 OR 4-VSNS

The next design task is to decide that how many partitions will be suitable for a given range of altitudes that will required the minimum cost to cover a given area. The following paragraphs will describe the procedure to decide for one, two, three of partitions to cover a given area.

Suppose a range of altitudes with lower altitude a_{min1} and higher altitude a_{max}. Suppose the given range of altitudes is divided into two sub-ranges with the a_{12} as the optimum point for this division. To make a decision whether to cover the given range with one homogeneous VSN or two sub VSNs, the cost to cover the given range with one VSN from a_{min1} to a_{max} is calculated. Also, the cost to cover the given range with the two sub VSNs, from a_{min1} to a_{12} and from a_{12} to a_{max} is calculated. The

minimum criterion is that the two costs are equal. The above two costs are equalized and solved for the value of a_{min1}. The derived value of a_{min1}, when s_1 is used to design the sub VSN_1 and s_2 is used to design the sub VSN_2, is given below.

$$a_{\min 1} = \frac{a_{\max}}{2} \cdot \sqrt{\frac{s_2}{s_1}} \qquad (6.13)$$

The first term in this equation is used to calculate the altitude value while the second term $\sqrt{\frac{s_2}{s_1}}$ is related to the sensors. If the camera sensors used to design both the sub VSNs, VSN_1 and VSN_2, are of the same type, then the $\sqrt{\frac{s_2}{s_1}}$ term reduces to 1 and the equation (6.13) reduces to the following form.

$$a_{\min 1} = \frac{a_{\max}}{2} \qquad (6.14)$$

The a_{min1} value can be used to verify whether the given range of altitude is feasible to cover with one partition to divide the given range into more segments. If a given a_{min} value is higher than the a_{min1} then the one partition will use the minimum cost to cover the given altitudes range.

After deciding the lower limit for the one partition case, the limit for the two partitions is calculated. Suppose a range of altitudes with the lower altitude a_{min2} and the higher altitude a_{max}. Suppose the given range of altitudes is divided into three sub-ranges with a_{13}, a_{23} are the optimum points for this division. To make a decision to cover the given range with two or three sub VSNs, the cost to cover the given range with two sub VSNs, from a_{min2} to a_{12} with sensor s_1 and from a_{12} to a_{max} with sensor s_2 is calculated. Also, the cost to cover the given range with three sub VSNs, from a_{min} to a_{13} with sensor s_1, from a_{13} to a_{23} with sensor s_2, and from a_{23} to a_{max} with sensor s_3 is calculated. The minimum criterion is that the two costs are equal. The above two costs are equalized and solved for the value of a_{min2}. The derived value of the a_{min2} is given below.

$$a_{\min 2} = \frac{2^3}{3^3} \cdot a_{\max} \cdot \frac{s_3}{\sqrt{s_1 s_2}} \qquad (6.15)$$

The first term in equation (6.15) is used to calculate the altitude value while the second term $\frac{s_3}{\sqrt{s_1 s_2}}$ is related to the camera sensor types. If the camera sensors used to design the sub VSNS, VSN_1, VSN_2 and VSN_3, are of the same type, then the $\frac{s_3}{\sqrt{s_1 s_2}}$ term reduces to 1 and the equation (6.15) is reduced to the following form.

$$a_{\min 2} = \frac{2^3}{3^3} \cdot a_{\max} \qquad (6.16)$$

The a_{min2} is the lower limit for the two partitions. If the value of a given a_{min} is higher than the value of a_{min2}, then two partitions will be a feasible solution to cover the given ranges of altitude. If the value of the given a_{min} is lower than a_{min2} then more than two partitions will give better solution.

After deciding the limit for the two partition case, the lower limit for the three partitions is calculated. Suppose a range of altitudes with lower altitude a_{min3} and higher altitude a_{max}. Suppose the given range of altitudes is divided into four sub-ranges with a_{14}, a_{24}, and a_{34} as the optimum points for this division. To make a decision to cover the given range with three sub VSNs or four sub VSNs, the cost to cover the given range with three sub VSNs, from a_{min3} to a_{13} with camera sensor s_1, from a_{13} to a_{23} with camera sensor s_2, and from a_{23} to a_{max} with camera sensor s_3 is calculated. Also, the cost to cover the given range with four sub VSNs, from a_{min} to a_{14} with camera sensor s_1, from a_{14} to a_{24} with camera sensor s_2, from a_{24} to a_{34} with camera sensor s_3, and from a_{34} to a_{max} with camera sensor s_4 is calculated. The minimum criterion is that the two costs are equal. The above two costs are equalized and solved for the value of a_{min3}. The derived value of a_{min3} is given below.

$$a_{\min 3} = \frac{3^6}{4^6} \cdot a_{\max} \cdot s_4 \cdot \sqrt{\frac{s_4}{s_1 s_2 s_3}} \qquad (6.17)$$

The first term in equation (6.17) is used to calculate the altitude value while the second term $s_4 \cdot \sqrt{\frac{s_4}{s_1 s_2 s_3}}$ is related to the camera sensors. If the camera sensors used to design the sub VSNs, VSN_1, VSN_2, VSN_3 and VSN_4, are of the same type, then the $s_4 \cdot \sqrt{\frac{s_4}{s_1 s_2 s_3}}$ term reduces to 1 and the equation (6.17) is reduced to the following form.

$$a_{\min 3} = \frac{3^6}{4^6} \cdot a_{\max} \qquad (6.18)$$

The a_{min3} is the limit for the three partitions. If the value of a given a_{min} is higher than the value of a_{min3}, then the three partitions will be a feasible solution to cover the given ranges of altitude. If the value of the given a_{min} is lower than a_{min3} then more than three partitions will give better solution. The costs for one, two, three and four sub partitions are calculated for a range of altitudes from 500 to 3000 m against the maximum altitude of 5000 m as shown in TABLE 6.2. The validity of the results is evident from TABLE 6.2.

6.4 VSN Design for Different Altitude Ranges

The optimization techniques developed above for two, three, and four sub VSNs can be used to minimize the cost to cover a given area for a given range of altitudes. These techniques are applied to calculate the costs for various ranges of altitudes by using one, two, three and four sub VSNs and the results are shown in TABLE 6.2. The minimum cost is achieved when the camera sensor used for all the sub VSNs is 14 Mp. So, all the results given in TABLE 6.2 are calculated on the basis of the 14 Mp camera sensor.

The first altitudes range selected is from 3000 to 5000 m, where the value for a_{min} is 3000 m and for a_{max} is 5000 m. By using equation (6.16), the a_{min1} value obtained is 2500 m. As the value of a_{min} is higher than the a_{min1} value, the best design is to cover this range with a homogeneous VSN, without partitioning the given range. The minimum possible cost obtained is 20 by using the homogeneous VSN, as shown in TABLE 6.2. As the given altitudes range is not divided into sub ranges, 0% reduction in cost is obtained, as shown in TABLE 6.3. The focal length of the lens required to be used with the selected camera sensor to design this VSN is calculated by using equation (5.4) and is found to be 70 mm.

The second altitudes range selected is from 2500 to 5000 m, where the value for a_{min} is 2500 m and for a_{max} is 5000 m. By using equation (6.16), the a_{min1} value obtained is 2500 m. As the value of a_{min} is higher than the a_{min1} value, the best design is to cover this range with a homogeneous VSN, without partitioning the given range. The minimum possible cost obtained is 28 by using homogeneous VSN as shown in TABLE 6.2. As the given altitudes range is not divided into sub ranges, 0% reduction in cost is obtained, as shown in TABLE 6.3. The focal length of the lens required to be used with the selected camera sensor to design this VSN is calculated by using equation (5.4) and is found to be 70 mm.

The third altitudes range selected is from 2000 to 5000 m, where the value for a_{min} is 2000 m and for a_{max} is 5000 m. By using the equation (6.16), the a_{min1} value obtained

TABLE 6.2. Cost for different altitudes

Range	1 VSN	2VSN	3VSN	4VSN
3000-5000	20	23	29	36
2900-5000	20	23	30	36
2800-5000	22	24	31	37
2700-5000	23	25	31	38
2600-5000	25	26	32	38
2500-5000	28	28	33	39
2400-5000	30	29	34	40
2300-5000	33	30	35	41
2200-5000	36	31	36	42
2100-5000	39	33	37	43
2000-5000	44	36	38	44
1900-5000	48	37	39	45
1800-5000	53	38	41	46
1700-5000	60	41	43	47
1600-5000	68	43	44	49
1500-5000	78	48	48	50
1400-5000	88	49	48	52
1300-5000	102	54	51	54
1200-5000	120	58	54	56
1100-5000	143	63	57	59
1000-5000	174	70	63	64
900-5000	214	77	65	65
800-5000	271	87	71	70
700-5000	353	99	77	74
600-5000	481	115	85	80
500-5000	694	140	99	88

TABLE 6.3. Cost for different sub VSNs

No.	Altitudes	1-Cam	2-Cam	3-Cam	4-Cam
1	3000-5000	20	-	-	-
2	2500-5000	28	-	-	-
3	2000-5000	44	36	-	-
4	1500-5000	78	48	-	-
5	1000-5000	174	70	63	-
6	500-5000	694	140	99	88

is 2500 m. As the value of a_{min} is lower than the a_{min1} value, the homogeneous VSN is not suitable for this range of altitudes. By using the equation (6.17), the a_{min2} value obtained is 1481 m. As the value of a_{min} is higher than the a_{min2} value, the best design is to cover this range by using two partitions and cover this range with two sub VSNs, VSN_1 and VSN_2. The optimum point, a_{12}, to divide the range of altitudes can be calculated by using equation (6.1) or (6.2). The value of a_{12} is found to be 3162 m, which will divide the given range into two sub ranges. The altitude range from 2000 to 3162 m will be covered by VSN_1 while the altitude range from 3162 to 5000 m will be covered by VSN_2. The cost required by the VSN_1 and VSN_2 is calculated by using equation (5.6) and is 18 for each sub VSN. The combined cost by the two sub VSNs is 36. If the given range is covered by a homogeneous VSN, the cost required will be 44, as shown in TABLE 6.2. By using the optimization, 18% reduction in cost is obtained as shown in TABLE 6.3. The focal lengths of the lenses required to be used with the camera sensors selected for both the sub VSNs are calculated by using equation (5.4) and are found to be 45 mm for VSN_1 and 70 mm for VSN_2.

The fourth altitudes range selected is from 1500 to 5000 m, where the value for a_{min} is 1500 m and for a_{max} is 5000 m. By using equation (6.17), the a_{min2} value obtained is 1481 m. As the value of a_{min} is higher than the a_{min2} value, the best design is to cover this range by using two partitions and cover this range with two sub VSNs, VSN_1 and VSN_2. The optimum point, a_{12}, to divide the range of altitudes can be calculated by using equation (6.1) or (6.2). The value of a_{12} is found to be 2738 m, which will divide the given range into two sub ranges. The altitude range from 1500 to 2738 m will be covered by VSN_1. The altitude range from 2738 to 5000 m will be covered by VSN_2. The cost required by VSN_1 and VSN_2 is calculated by using equation (5.6) and is 24 for each sub VSN. The combined cost by the two sub VSNs is 48. If the given range is covered by homogeneous VSN, the cost required will be 78, as shown in TABLE 6.2. By using the optimization, 38% reduction in the cost is obtained as shown in TABLE 6.3. The focal lengths of the lenses required to be used with the camera sensors selected for both the sub VSNs are calculated by using equation (5.4) and are found to be 39 mm for VSN_1 and 70 mm for VSN_2.

The fifth altitudes range selected is from 1000 to 5000 m, where the value for a_{min} is 1000 m and for a_{max} is 5000 m. By using the equation (6.17), the a_{min2} value obtained is 1481 m. As the value of a_{min} is lower than the a_{min2} value, the two partitions are not suitable for this range of altitude as they will use more cost to cover this range of altitudes. By using the equation (6.18), the a_{min3} value obtained is 890 m. As the value of a_{min} is higher than the a_{min3} value, the best design is to cover this range by using three partitions and cover this range with three sub VSNs, VSN_1, VSN_2 and VSN_3. The two optimum points, a_{13} and a_{23} to divide the range of altitudes can be calculated by using equations (6.3) and (6.4) or from equations (6.5) and (6.6). The value of a_{13} is found to be 1709 m and the value of a_{23} is found to be 2924 m. These values will divide the given range into three sub ranges. The altitudes range from

1000 to 1709 m will be covered by VSN_1, the altitudes range from 1709 to 2924 m will be covered by VSN_2 and the altitudes range from 2924 to 5000 m will be covered by VSN_3. The cost required by VSN_1, VSN_2, and VSN_3 is calculated by using equation (5.6) and is 21 for each sub VSN. The combined cost by the three sub VSNs is 63. If the given range is covered by homogeneous VSN, the cost required will be 174. If the given range is covered by two sub VSNs, the cost required will be 70 as shown in TABLE 6.2. By using the optimization, 63% reduction in cost is obtained as shown in TABLE 6.3. The focal lengths of the lenses required to be used with the camera sensors selected for the three sub VSNs are calculated by using equation (5.4) and are found to be 24 mm for VSN_1, 41 mm for VSN_2 and 70 mm for VSN_3.

The last altitudes range selected is from 500 to 5000 m, where the value for a_{min} is 500 m and for a_{max} is 5000 m. By using the equation (6.18), the a_{min3} value obtained is 890 m. As the value of a_{min} is lower than the a_{min2} value, the three partitions are not suitable for this range of altitude as they will use more cost to cover this range of altitudes. The best design is to cover this range by using four partitions and cover this range with four sub VSNs, VSN_1, VSN_2, VSN_3 and VSN_4. The three optimum points, a_{14}, a_{24} and a_{34} to divide the given range of altitudes can be calculated by using equations (6.7), (6.8) and (6.9) or from equations (6.11), (6.12) and (6.13). The values of a_{14}, a_{24} and a_{34} are found to be 889, 1581 and 2812 m, respectively. These values will divide the given range into four sub ranges. The altitudes range from 500 to 889 m will be covered by the VSN_1, the altitude range from 889 to 1581 m will be covered by the VSN_2, the altitude range from 1581 to 2812 m will be covered by the VSN_3, and the altitude range from 2812 to 5000 m will be covered by VSN_4. The cost required by the VSN_1, VSN_2, VSN_3, and VSN_4 is calculated by using equation (5.6) and is 22 for each sub VSN. The combined cost by the four VSNs is 88. If the given range is covered by the homogeneous VSN the cost required will be 694, if the given range is covered by the two sub VSNs the cost required will be 140 and if the given range is covered by the three sub VSNs the cost required will be 99 as shown in TABLE 6.2. By using optimization, 87% reduction in cost is obtained as shown in TABLE 6.3. The focal lengths of the lenses required to be used with the camera sensors selected for four sub VSNs are calculated by using equation (5.4) and are found to be 13 mm for VSN_1, 22 mm for VSN_2, 39 mm for VSN_3 and 70 mm for VSN_4.

6.5 PERCENT COST REDUCTION BY USING OPTIMIZATION

The percent reduction in the cost for different ranges of altitudes is calculated and is shown in TABLE 6.4. In case of altitudes range from 3000 to 5000 m and from 2500 to 5000 m, only homogeneous VSN is feasible. The costs for the homogeneous VSNs from 3000 to 5000 and from 2500 to 5000 are 20 and 28, respectively. In case of altitudes range from 2000 to 5000 m, the cost for the homogeneous VSN is 44. By

TABLE 6.4. Percent cost reduction

No.	Altitudes (m)	Single VSN Optimization	Multi VSN Optimization	Reduction (%)
1	3000-5000	20	24	0
2	2500-5000	28	28	0
3	2000-5000	44	36	18
4	1500-5000	78	48	38
5	1000-5000	174	63	63
6	500-5000	694	88	87

using optimization, the cost reduces to 36, which is 18% reduction in cost. In case of altitudes range from 1500 to 5000 m, the cost for homogeneous VSN is 78. By using optimization, the cost reduces to 48, which is 38% reduction in cost. In case of altitudes range from 1000 to 5000 m, the cost for homogeneous VSN is 174. By using optimization, the cost reduces to 63, which is 63% reduction in cost. In case of altitudes range from 500 to 5000 m, the cost for homogeneous VSN is 694. By using optimization, the cost reduces to 88, which is 87% reduction in cost.

The optimization techniques give best results when a given range of altitudes is large, i.e., when there is a larger gap between a_{min} and a_{max}. A large range of altitudes for monitoring is desirable because a larger area can be tracked. The homogeneous VSN design gives worst results for large altitudes range while the optimization techniques give best results for large altitudes range. The optimization techniques are very promising to reduce the cost of a VSN. The reduced cost is always desirable as it reduces the price for a VSN design, the management overhead, the communication overhead and the energy requirements for a VSN.

7. MEASUREMENTS OF VSN MODELS

A VSN model was developed in chapter 5 for the eagle tracking application. The optimization techniques were used to reduce the cost of the VSN model to cover a given area between the two altitude limits. This chapter implements the real VSNs by using the design techniques presented in chapters 5 and 6. The critical VSN parameters are measured to verify the VSN models presented in the previous chapters. There are two critical parameters in a given VSN. The first parameter is the coverage above a given lower altitude and the second parameter is the minimum resolution at a given higher altitude. When both of these parameters are satisfied then it is verified that the complete VSN model will cover each and every point in a given area, between the give lower and higher altitudes. Thus, the first main objective of this chapter is to measure the coverage of a VSN above a given lower altitude and verify it whether it is 100% or not. The second main objective of this chapter is to measure the resolution of the VSN at a given higher altitude and to verify that whether it is fulfilling the minimum required criterion. Two VSN models will be discussed in this chapter. The first model is a homogeneous VSN and the second model is a heterogeneous VSN.

7.1 The Components Involved in VSN Designs

A monitoring node of a VSN is formed by a camera sensor and a lens of suitable focal length. The cameras and the lenses used for the implementation of the VSNs are shown in Figure 7.1. The first camera sensor selected for the VSN design is a 5 Mp sensor. The camera model UI-5480CP-M from UEye is using this camera sensor. The actual image sensor chip used in this camera is the Aptina image sensor having model number MT9P031STM. The horizontal length (l_h) of this chip is 5.632 mm while the vertical length (l_v) is 4.224 mm. The chip resolution along the horizontal side (r_h) is 2560 while along the vertical side (r_v) is 1920. These parameters are given in TABLE 7.1. The power is applied to the camera module via Hirose connector. The data is received from this camera with Ethernet link.

The second camera sensor selected for the VSN design is a WVGA type. The camera model UI-1220SE-M from UEye is using this camera sensor. The actual image sensor chip used in this camera is the Aptina image sensor having model number MT9V032STM. The horizontal length (l_h) of this chip is 4.512 mm while the vertical length (l_v) is 4.880 mm. The chip resolution along the horizontal side (r_h) is 752 while along the vertical side (r_v) is 480. These parameters are given in TABLE 7.1. The camera has a USB interface, which is used to receive data as well as supplying the power to the camera.

The lenses of the fixed focal lengths, 8.5 mm and 12 mm, from Edmund Optics are selected for the VSN design. A lens of the variable focal length, in the range from 8 mm to 48 mm, from Pentax is also used for the VSN. All these lenses are shown in

Figure 7.1. Cameras and lenses used for measurements.

TABLE 7.1. Camera sensors parameters

Model	MT9P031STM	MT9V032STM
Type	5Mp	WVGA
l_h	5.632 mm	4.512 mm
l_v	4.224 mm	2.880 mm
r_h	2560	752
r_v	1920	480

Figure 7.1. The remaining part of this chapter discusses the two VSNs, the homogeneous VSN and the heterogeneous VSN.

7.2 The Homogeneous VSN

A homogeneous VSN is implemented by using 5 Mp camera sensors. An eagle of size (1.08x0.54) cm, shown in Figure 7.2, is used to perform the measurements for this VSN. The higher monitoring altitude, a_h, for this VSN is assumed to be 293 cm. To monitor the given eagle with the given sensor at the given higher altitude, the focal length which ensures the minimum required resolution of 10 pixels per meter is calculated by using equation (5.4) and is found to be 12 mm. A lens of fixed focal length of 12 mm is used for this design. The selected camera and lens form a monitoring node. A laptop machine is used with this monitoring node as data storage and analysis platform. The monitoring node is connected to the laptop by using CAT 6 Ethernet cable. The Hirose 6 pin connector supplies the power to the camera module. The power is supplied to the camera module and the laptop by a 12 volt rechargeable battery. The camera is connected to the laptop by using an Ethernet cable as client while the laptop is used as a server. All this setup forms a complete standalone monitoring node and is shown in Figure 7.3. Two such nodes are used to design this homogeneous VSN. The images of the eagle are captured by

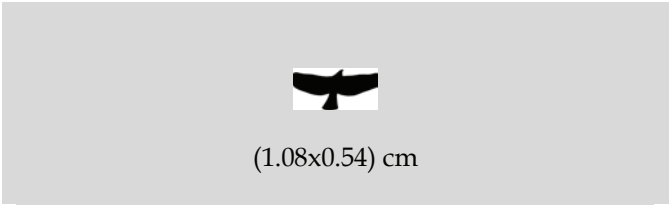

Figure 7.2. Bird dimensions used for measurements.

Figure 7.3. A complete monitoring node.

using the UEye Cockpit software, which is the camera interface to capture the images/videos or to change the camera controlling parameters.

The lower altitude, a_l, where the full coverage is required is assumed to be 176 cm. This value of the lower altitude is about 60% of the higher altitude value and is selected just for demonstration purpose. To achieve the full coverage at this lower altitude, the distance between the two nodes along x direction is calculated by using equation (5.5) and is found to be 82.5 cm. The AoV of the 5 Mp camera sensor with the 12 mm focal length is calculated by using equation (5.1). The value of the AoV obtained is 26.4^0.

7.2.1 Coverage Model for Homogeneous VSN

The coverage model of the homogeneous VSN, based on all the above specifications is shown in Figure 7.4. The cam_1 and cam_2 represent the two monitoring nodes. The VSN model shows the five horizontal lines A, B, C, D and E. These lines represent the specific altitude values. The line A represents the ground surface and the monitoring nodes will be installed on this line. The line B represents the altitude value, which is below the lower altitude value where the full coverage is required. The coverage on the line B will be less than 100 %. The coverage will be measured

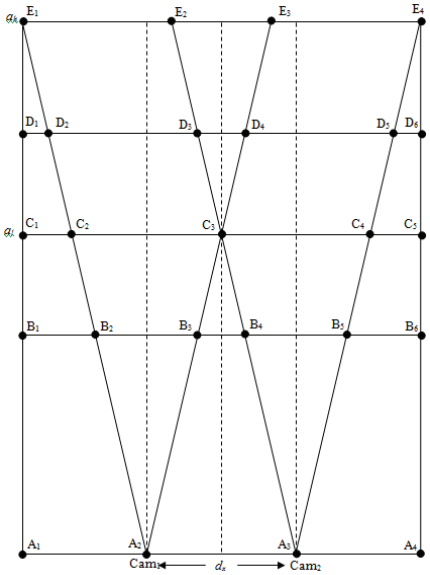

Figure 7.4. Homogeneous VSN Model.

on this line to show this fact. The line C is the required lower altitude where the full coverage is required. The coverage will be measured on this line, to verify whether it is 100% or not. The line D is an altitude value where the overlap in the coverage is verified. The line E is the higher altitude value where minimum required resolution is verified.

The line A contains four points A_1, A_2, A_3 and A_4. The two monitoring nodes will be placed on A_2 and A_3 points. The line B contains six points B_1, B_2, B_3, B_4, B_5 and B_6. The coverage will be achieved between the points B_2 - B_3 and B_4 - B_5 points. The line C contains five points C_1, C_2, C_3, C_4 and C_5. The coverage will be achieved between the C_2 - C_4 points. The line D contains six points D_1, D_2, D_3, D_4, D_5 and D_6. The coverage will be achieved between the D_2 - D_5 points. The line E contains four points E_1, E_2, E_3 and E_4. The coverage will be achieved between the E_1 - E_4 points.

7.2.2 Altitude Values of the Lines

To measure the coverages on the altitude lines A, B, C, D and E, the exact altitude values of these lines are required. The line A represents the ground plane so it is at the 0 cm altitude. The line C represents the lower altitude, so it at the 176 cm altitude from the line A, as discussed before. The line E represents the higher altitude, so it is at the 293 cm altitude above the ground. The line B is chosen 55 cm below the line C, so it is at the 121 cm altitude above the ground. The line D is chosen 55 cm above the line D, so it is at the 231 cm altitude above the ground. All these altitudes are summarized in Figure 7.5.

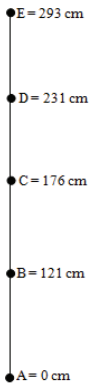

Figure 7.5. Altitude values in homogeneous VSN.

TABLE 7.2. Values of points in homogeneous VSN

	A (cm)	B (cm)	C (cm)	D (cm)	E (cm)
1	0	0	0	0	0
2	68.75	40.3	27.5	14.5	82.5
3	151.25	97.1	110	97.1	137.5
4	220	122.9	192.5	123	220
5	-	179.7	220	205.4	-
6	-	220	-	220	-

7.2.3 Values of Points on the Lines

To measure the coverages on the altitude lines A, B, C, D and E, the exact values of the points on the respective altitude lines are required. The value of a given point on a given altitude line is calculated from the left edge of the line. For example, the distance of the point A_2 from the point A_1 can be calculated by solving the triangle $E_1A_1A_2$ in Figure 7.4. The distance of the point A_2 from A_1 is calculated and is found to be 68.75 cm. The distance between the points A_2 and A_3 is the d_x which is 82.5 cm, as calculated before. Thus, the distance of the point A_3 from point A_1 is 151.25 cm. The distance of point A_4 from A_1 is 220 cm. Similarly, the distances of all the points on all other lines are calculated. The distances of the points B_2, B_3, B_4, B_5 and B_6 from B_1 are 40.3, 97.1, 122.9, 179.7 and 220 cm, respectively. The distances of the points C_2, C_3, C_4, and C_5 from C_1 are 27.5, 110, 192.5 and 220 cm, respectively. The distances of the points D_2, D_3, D_4, D_5 and D_6 from D_1 are 14.5, 97.1, 123, 205.4 and 220 cm, respectively. The distances of the points E_2, E_3 and E_4, from E_1 are 82.5, 137.5 and 220 cm, respectively. The values of all these points are given in TABLE 7.2.

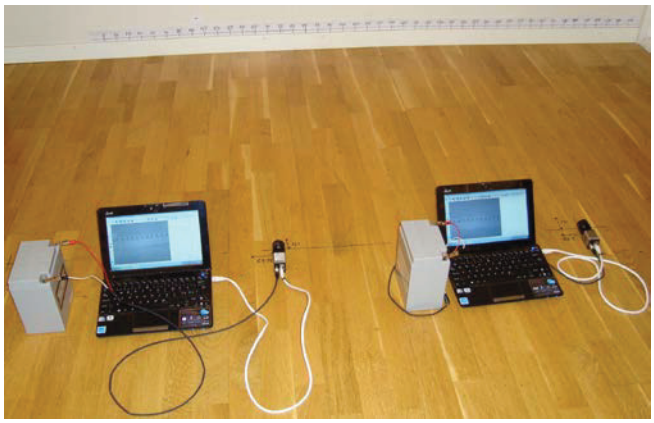

Figure 7.6. VSN installation.

7.2.4 Measurements in Homogeneous VSN

After designing the homogeneous VSN model, finding the altitude values of all the horizontal lines and the values of points on the respective lines, the actual VSN will be installed and measurements will be performed to verify the typical parameters as discussed before. To measure all the distances, a scale of about 240 cm long is made on a long strip of paper. The markings on the scale are marked after every 5 cm. The scale is glued on a wall in a room.

7.2.5 Measurements at Line B

The measurements are performed at the line B to verify the coverage between the points B_2 (40.3 cm) - B_3 (97.1 cm) and B_4 (122.9 cm) - B_5 (179.7 cm). The line B has an altitude of 121 cm from the line A. To perform the measurements, the wall is treated as the line B. A 220 cm long line is drawn parallel to the wall at a distance of 121 cm from the wall, which is treated as the line A. The monitoring nodes are fixed on this line at the points A_2 (68.75 cm) and A_3 (151.25 cm), facing towards the wall such that the lenses axes are perpendicular to the wall. The complete setup is shown in Figure 7.6. Next, the images of the wall are captured where the measuring strip is attached by using the camera interface software. The images captured by the monitoring nodes 1 and 2 are shown in Figure 7.7 and Figure 7.8, respectively. The analysis of the captured images is performed in the next paragraphs to measure the coverages of the monitoring nodes.

The measurements in Figure 7.7 show that a total of 225 pixels represent a 5 cm distance. There are about 214 pixels from the left edge of the figure to the 45 cm point, representing about a distance of 4.75 cm long. Thus, the B_2 point has a value of 40.25 cm. Similarly, there are about 112 pixels from the right edge of the figure to the 95 cm point, representing about a distance of 2.49 cm long. Thus, the B_3 point has a value of 97.49 cm. Thus, the practical coverage obtained by the monitoring

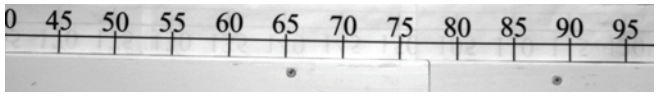

Figure 7.7. Measurements at line B by using node 1.

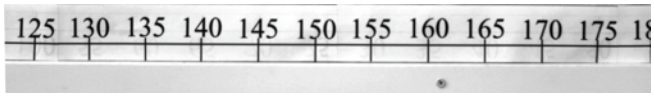

Figure 7.8. Measurements at line B by using node 2.

node 1 is B_2 (40.25 cm) - B_3 (97.49 cm) while the expected coverage as calculated before was B_2 (40.3 cm) - B_3 (97.1 cm). The calculated and measured values are almost equal.

The measurements in Figure 7.8 show that a total of 227 pixels represent a 5 cm distance. There are about 114 pixels from the left edge of the figure to the 125 cm point, representing about a distance of 2.62 cm long. Thus, the B_4 point has a value of 122.38 cm. Similarly, there are about 214 pixels from the right edge of the figure to the 175 cm point, representing about a distance of 4.71 cm long. Thus, the B_5 point has a value of 179.71 cm. Thus, the practical coverage obtained by the monitoring node 2 is B_4 (122.38 cm) - B_5 (179.71) while the expected coverage as calculated before was B_4 (122.9 cm) - B_5 (179.7 cm). The calculated and the measured values are almost equal. All these measured values are summarized in TABLE 7.3.

7.2.6 Measurements at Line C

The measurements are performed at the line C to verify the coverage between the points C_2 (27.5 cm) - C_3 (110 cm) and C_3 (110 cm) – C_4 (192.5 cm). The line C has an altitude of 176 cm from the line A. To perform the measurements, the wall is treated as the line C. A 220 cm long line is drawn parallel to the wall at a distance of 176 cm from the wall, which is treated as the line A. The monitoring nodes are fixed on this line at the points A_2 (68.75 cm) and A_3 (151.25 cm), as discussed before. Next, the images of the wall are captured where the measuring strip is attached. The images captured by the monitoring nodes 1 and 2 are shown in Figure 7.9 and Figure 7.10, respectively. The analysis of the captured images is performed in the next paragraphs to measure the coverages of the monitoring nodes.

The measurements in Figure 7.9 show that a total of 154 pixels represent a 5 cm distance. There are about 90 pixels from the left edge of the figure to the 30 cm point, representing about a distance of 2.92 cm long. Thus, the C_2 point has a value of 27.08 cm. Similarly, there are about 161 pixels from the right edge of the figure to the 105 cm point, representing about a distance of 5.23 cm long. Thus, the C_3 point has a value of 110.23 cm. Thus, the practical coverage obtained by the monitoring node 1 is C_2 (27.08 cm) - C_3 (110.23 cm) while the expected coverage as calculated

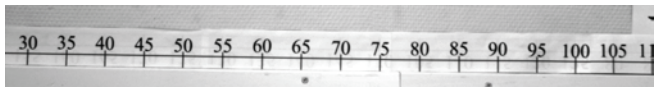

Figure 7.9. Measurements at line C by using node 1.

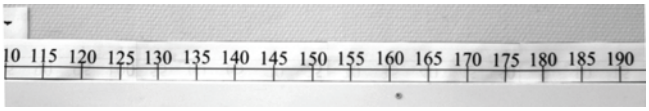

Figure 7.10. Measurements at line C by using node 2.

before was C_2 (27.5 cm) - C_3 (110 cm). The calculated and measured values are almost equal.

The measurements in Figure 7.10 show that a total of 152 pixels represent a 5 cm distance. There are about 156 pixels from the left edge of the figure to the 115 cm point, representing about a distance of 5.13 cm long. Thus, the C_3 point has a value of 109.87 cm. Similarly, there are about 103 pixels from the right edge of the figure to the 190 cm point, representing about a distance of 3.39 cm long. Thus, the C_4 point has a value of 193.39 cm. Thus, the practical coverage obtained by the monitoring node 2 is C_3 (109.87 cm) – C_4 (193.39) while the expected coverage as calculated before was C_3 (110 cm) – C_4 (192.5 cm). The calculated and the measured values are almost equal. All these measured values are summarized in TABLE 7.3.

7.2.7 Measurements at Line D

The measurements are performed at the line D to verify the coverage between the points D_2 (14.5 cm) – D_4 (123 cm) and D_3 (97.1 cm) – D_5 (205.4 cm). The line D has an altitude of 231 cm from the line A. To perform the measurements, the wall is treated as the line D. A 220 cm long line is drawn parallel to the wall at a distance of 231 cm from the wall, which is treated as the line A. The monitoring nodes are fixed on this line at the points A_2 (68.75 cm) and A_3 (151.25 cm), as discussed before. Next, the images of the wall are captured where the measuring strip is attached. The images captured by the monitoring nodes 1 and 2 are shown in Figure 7.11 and Figure 7.12, respectively. The analysis of the captured images is performed in the next paragraphs to measure the coverages of the monitoring nodes.

The measurements in Figure 7.11 show that a total of 118 pixels represent a 5 cm distance. There are about 116 pixels from the left edge of the figure to the 20 cm point, representing about a distance of 4.92 cm long. Thus, the D_2 point has a value of 15.08 cm. Similarly, there are about 99 pixels from the right edge of the figure to the 120 cm point, representing about a distance of 4.19 cm long. Thus, the D_4 point has a value of 124.19 cm. Thus, the practical coverage obtained by the monitoring node 1 is D_2 (15.08 cm) – D_4 (124.19 cm) while the expected coverage as calculated

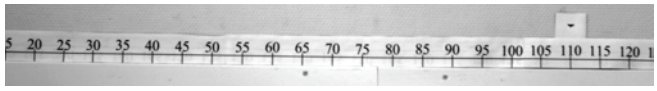

Figure 7.11. Measurements at line D by using node 1.

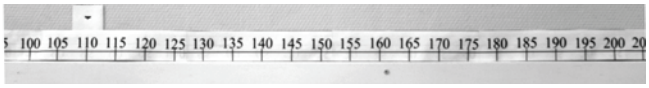

Figure 7.12. Measurements at line D by using node 2.

before was D_2 (14.5 cm) – D_4 (123 cm). The calculated and measured values are almost equal.

The measurements in Figure 7.12 show that a total of 119 pixels represent a 5 cm distance. There are about 103 pixels from the left edge of the figure to the 100 cm point, representing about a distance of 4.32 cm long. Thus, the D_3 point has a value of 95.68 cm. Similarly, there are about 125 pixels from the right edge of the figure to the 200 cm point, representing about a distance of 5.25 cm long. Thus, the D_5 point has a value of 205.25 cm. Thus, the practical coverage obtained by the monitoring node 2 is D_3 (95.68 cm) – D_5 (205.25) while the expected coverage as calculated before was D_3 (97.1 cm) – D_5 (205.4 cm). The calculated and the measured values are almost equal. All these measured values are summarized in TABLE 7.3.

7.2.8 Measurements at Line E

The measurements are performed at the line E to verify the coverage between the points E_1 (0 cm) - E_3 (137.5 cm) and E_2 (82.5 cm) – E_4 (220 cm). The line E has an altitude of 176 cm from the line A. To perform the measurements, the wall is treated as the line E. A 220 cm long line is drawn parallel to the wall at a distance of 293 cm from the wall, which is treated as the line A. The monitoring nodes are fixed on this line at the points A_2 (68.75 cm) and A_3 (151.25 cm), as discussed before. Next, the images of the wall are captured where the measuring strip is attached. The images captured by the monitoring nodes 1 and 2 are shown in Figure 7.13 and Figure 7.14, respectively. The analysis of the captured images is performed in the next paragraphs to measure the coverages of the monitoring nodes.

The measurements in Figure 7.13 show that a total of 95 pixels represent a 5 cm distance. There are about 101 pixels from the left edge of the figure to the 5 cm point, representing about a distance of 5.32 cm long. Thus, the E_1 point has a value of -0.32 cm. Similarly, there are about 67 pixels from the right edge of the figure to the 135 cm point, representing about a distance of 3.53 cm long. Thus, the E_3 point has a value of 138.53 cm. Thus, the practical coverage obtained by the monitoring node 1 is E_1 (-0.32 cm) - E_3 (138.53 cm) while the expected coverage as calculated

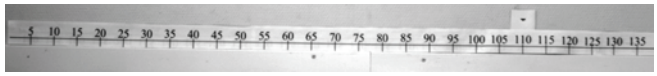

Figure 7.13. Measurements at line E by using node 1.

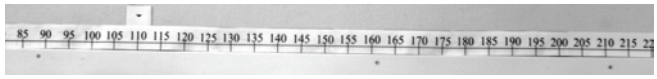

Figure 7.14. Measurements at line E by using node 2.

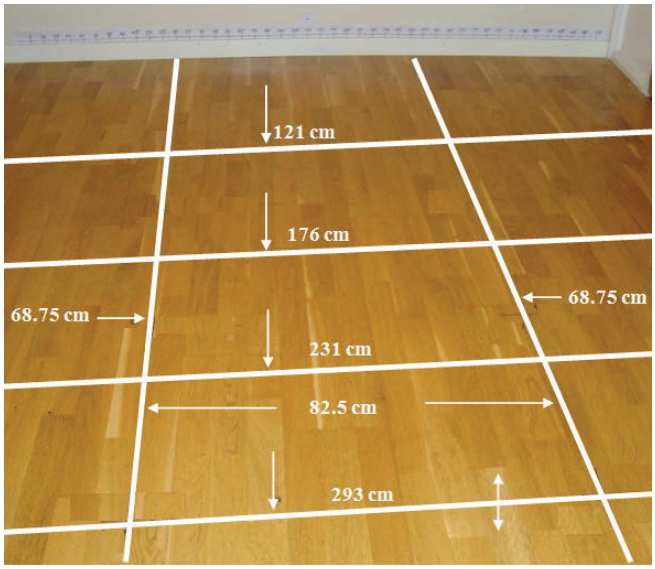

Figure 7.15. Marking lines on floor for homogeneous VSN.

before was E_1 (0 cm) - E_3 (137.5 cm). The calculated and measured values are almost equal.

The measurements in Figure 7.14 show that a total of 94 pixels represent a 5 cm distance. There are about 70 pixels from the left edge of the figure to the 85 cm point, representing about a distance of 3.72 cm long. Thus, the E_2 point has a value of 81.28 cm. Similarly, there are about 102 pixels from the right edge of the figure to the 215 cm point, representing about a distance of 5.43 cm long. Thus, the E_4 point has a value of 220.43 cm. Thus, the practical coverage obtained by the monitoring node 2 is E_2 (81.28 cm) – E_4 (220.43) while the expected coverage as calculated before was E_2 (82.5 cm) – E_4 (220 cm). The calculated and the measured values are almost equal. All these measured values are summarized in TABLE 7.3. The markings of the different lines on the floor, as discussed before are shown in Figure 7.15.

TABLE 7.3. Calculated and measured values for homogeneous VSN

Point	Cal. Values	Meas. Values
Altitude Line B		
B_2 (node 1)	40.3	40.25
B_3 (node 1)	97.1	97.49
B_4 (node 2)	122.9	122.38
B_5 (node 2)	179.7	179.71
Altitude Line C		
C_2 (node 1)	27.5	27.08
C_3 (node 1)	110.0	110.23
C_3 (node 2)	110.0	109.87
C_4 (node 2)	192.5	193.39
Altitude Line D		
D_2 (node 1)	14.5	15.08
D_4 (node 1)	123.0	124.19
D_3 (node 2)	97.1	95.68
D_5 (node 2)	205.4	205.25
Altitude Line E		
E_1 (node 1)	0	-0.32
E_2 (node 1)	82.5	81.28
E_3 (node 2)	137.5	138.53
E_4 (node 2)	220.0	220.43

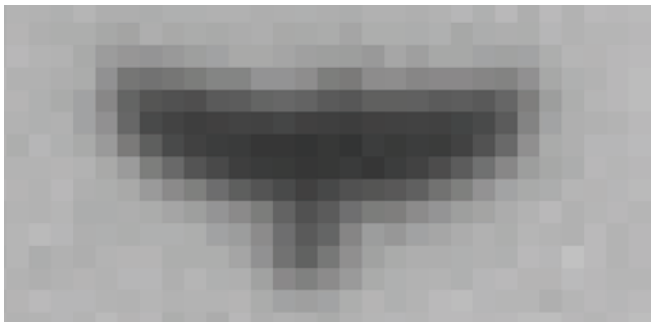

Figure 7.16. Bird resolution at highest altitude in homogeneous VSN.

7.2.9 Measurement of Resolution

The minimum resolution of the eagle image on the camera sensor, when it is 293 cm far from the monitoring nodes, is required to be 10 pixels per meter. To measure this resolution, a small portion of the image which contains the eagle is separated from Figure 7.13. The magnified image of the separated portion is shown in Figure 7.16. The segmentation of this image is performed and the number of pixels is

counted in the eagle along the wings side. It is found that the number of pixels is about 19 and is according to the plan. The number of pixels can also be directly counted from Figure 7.16.

7.3 The Heterogeneous VSN

A heterogeneous VSN is designed by using the 5 Mp and WVGA camera sensors. The heterogeneous VSN is designed to monitor the area between the lower and the higher altitude values of 46.93 and 293 cm, respectively. This given altitudes range is divided into the three sub ranges of altitudes and these sub ranges will be covered by the three sub VSNs called VSN_1, VSN_2 and VSN_3. The coverage model of this heterogeneous VSN is shown in Figure 7.17. The VSN_1 is covering the highest sub range. Thus, the higher altitude value for this sub VSN is 293 cm. The same eagle as used for the homogeneous VSN is used to perform the measurements for this heterogeneous VSN. To monitor the given eagle with the 5 Mp camera sensor at the 293 cm altitude, the focal length which ensures the minimum required resolution of 10 pixels per meter is calculated by using equation (5.4). The focal length is found to be 12 mm. A lens of fixed focal length of 12 mm is used with the given camera sensor to form the monitoring node for VSN_1.

The lower altitude limit for VSN_1 is assumed to be 208 cm. To achieve the full coverage above this lower altitude, the distance between the two nodes along x direction is calculated by using equation (5.2). The value of d_x obtained is 97.62 cm. The AoV of the given camera sensor with the 12 mm focal length is calculated by using equation (5.1). The value of the AoV obtained is 52.28^0. The VSN_1 will provide the full coverage above 208 cm altitude. To cover an area below the 208 cm altitude, the VSN_2 is used. Thus, for the VSN_2 the value of the higher altitude is 208 cm. Suppose the 5 Mp camera sensor is used to design the monitoring nodes for this sub VSN. The focal length required to track the given eagle at 208 cm altitude with a minimum resolution of 10 pixels per meter, by using the selected image sensor is calculated by using equation (5.2) and is found to be 8.5 mm. A lens of fixed focal length of 8.5 mm is used with the given camera sensor to form the monitoring node for VSN_2. The AoV of the given camera sensor with 8.5 mm focal length is calculated by using equation (5.1). The value of the AoV obtained is 67.06^0.

The distance between the two nodes of the VSN_2 is chosen to be the same as for the VSN_1, i.e., 97.62 cm. For this value of d_x, the value of the lower altitude for VSN_2 is calculated by using equation (5.3). The lower altitude value obtained is 147.33 cm. However, more coverage will be obtained due to the intersection of the sub VSNs, VSN_1 and VSN_2 The value of the lower altitude for VSN_2 can be calculated by solving the triangle $C_4A_2A_4$ or $C_7A_4A_6$ in Figure 7.17. The triangles can easily be solved with the help of the AoVs as calculated for both VSNs. The value of the intersection altitude of VSN_1 and VSN_2 obtained by solving these triangles is found to be 86.39 cm. Thus, the lower altitude value for VSN_2 is 86.39 cm.

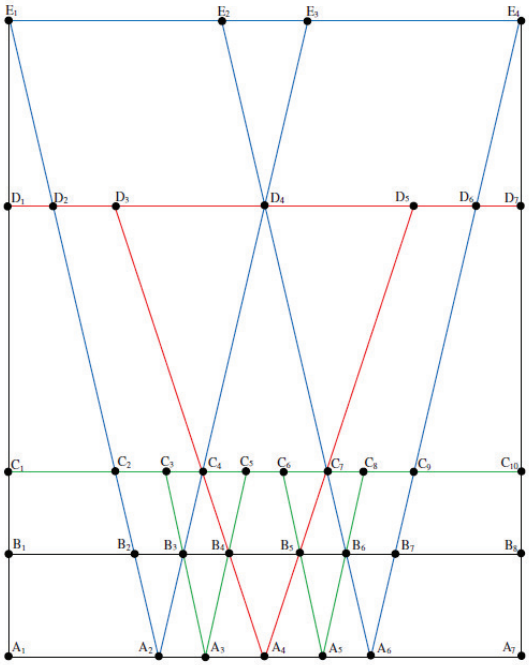

Figure 7.17. Heterogeneous VSN Model.

The VSN_2 will provide the full coverage above the 86.39 cm altitude. To cover an area below 86.39 cm, the VSN_3 is used. Thus, for VSN_3 the value of the higher altitude is 86.39 cm. Suppose the WVGA camera sensor is used to design the monitoring nodes for this sub VSN. The focal length required to track the given eagle at 86.39 cm altitude with a minimum resolution of 10 pixels per meter, by using the selected image sensor is calculated by using equation (5.2) and is found to be 9.5 mm. A variable focal length lens is used for this purpose. The focal length of this lens is set to 9.5 mm. The AoV of the given camera sensor with 9.5 mm focal length is calculated by using equation (5.1). The value of the AoV obtained is 50.81^0.

The placement of the monitoring nodes for VSN_3 can be determined by solving the triangles $A_2B_2B_3$, $A_2B_2B_3$ and $A_2B_2B_3$ in Figure 7.17. The solution of these triangles will also provide the information about the lower altitude where full coverage is achieved for VSN_3. Again, the AoVs as calculated above will be helpful to solve these triangles. By solving these triangles, the placement of the VSN_3 nodes is obtained. They should have a distance of 22.14 cm from the VSN_1 nodes and a distance of 26.68 cm from the VSN_2 nodes. The value of the lower altitude calculated for the VSN_3 is 46.93 cm. The laptop machines are also be used with the monitoring nodes as the data storage and analysis platform with the heterogeneous VSN as for the homogeneous VSN.

7.3.1 Coverage Model for Heterogeneous VSN

The coverage model of the heterogeneous VSN based on all the above design specifications is shown in Figure 7.17. The VSN model shows the five horizontal lines A, B, C, D and E. These lines represent the specific altitude values. The line A represents the ground surface and the monitoring nodes will be installed on this line. The line B represents the lower altitude value for the VSN_3. The VSN_3 provides the full coverage at this altitude by making the intersections with the sub VSNs, VSN_1 and VSN_2. The line C represents the higher altitude value for VSN_3. The line C also represents the lower altitude value for VSN_2. The VSN_2 provides the full coverage at this altitude by making the intersection with the VSN_1. The line D represents the higher altitude value for VSN_2. The line D also represents the lower altitude value for VSN_1. The VSN_1 provides the full coverage at this altitude. The line E is higher altitude value for VSN_1. Above this line the coverage of the heterogeneous VSN drops to zero due to the reduction in the resolution below the minimum criterion.

The line A contains the seven points A_1, A_2, A_3, A_4, A_5, A_6 and A_7. The monitoring nodes will be placed on these points. The monitoring nodes for the VSN_1 are placed at the points A_2 and A_6, the monitoring node for the VSN_2 is placed at the points A_4 and the monitoring nodes for the VSN_3 are placed at the points A_3 and A_5. The line B contains the eight points B_1, B_2, B_3, B_4, B_5, B_6, B_7 and B_8. The coverage will be achieved between the points the B_2 - B_7. The line C contains the ten points C_1, C_2, C_3, C_4, C_5, C_6, C_7, C_8, C_9 and C_{10}. The coverage will be achieved between the C_2 - C_9 points. The line D contains the seven points D_1, D_2, D_3, D_4, D_5, D_6 and D_7. The coverage will be achieved between the D_2 - D_6 points. The line E contains the four points E_1, E_2, E_3 and E_4. The coverage will be achieved between the E_2 - E_4 points.

7.3.2 Altitude Values for the Lines

To measure the coverage on the altitude lines A, B, C, D and E, the exact altitude values of these lines are required. The line A represents the ground plane so it is at the 0 cm altitude. The line B represents the lower altitude for VSN_3. Thus, it is at the altitude 46.93 cm above the ground. The line C represents the lower altitude for VSN_3. Thus, it is at the altitude 86.39 cm above the ground. The line D represents the higher altitude for VSN_2. Thus, it is at the altitude 208 cm above the ground. The line E represents the higher altitude for VSN_1. Thus, it is at the altitude 293 cm above the ground. All these altitudes are summarized in Figure 7.18.

7.3.3 Values of Points on the Lines

To measure the coverages on the altitude lines A, B, C, D and E, the exact values of the points on the respective altitude lines are required. The value of a given point on a given altitude line is calculated from the left edge of the line. For example, the distance of the point A_2 from the point A_1 can be calculated by solving the triangle $E_1A_1A_2$ in Figure 7.17. The distance of point A_2 from point A_1 is calculated and is

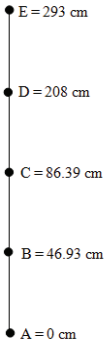

Figure 7.18. Altitude values in heterogeneous VSN.

68.76 cm. The distance between the points A_2 and A_6 is d_x which is 97.62 cm, as calculated before. Thus, the distance of the point A_6 from the point A_1 is 166.4 cm. The distance of the point A_7 from A_1 is 235.16 cm. The point A_4 is the half of d_x distance away from A_2. Thus, the point A_4 is at 117.26 cm from A_1. The point A_3 is at 22.14 cm distance from A_2 and the point A_5 is at 22.14 cm distance from A_6. Thus, the points A_3 and A_5 are at distances 90.9 and 144.26 cm from A_1, respectively.

Similarly, the distances of all the points on all other lines are calculated. The distances of the points B_2, B_3, B_4, B_5, B_6, B_7 and B_8 from B_1 are 57.75, 79.77, 102.03, 133.13, 155.39, 177.41 and 235.16 cm, respectively. The distances of the points C_2, C_3, C_4, C_5, C_6, C_7, C_8, C_9 and C_1 from C_1 are 48.49, 70.38, 89.03, 111.41, 123.74, 146.13, 164.77, 186.67 and 235.16 cm, respectively. The distances of the points D_2, D_3, D_4, D_5 D_6 and D_7 from D_1 are 19.95, 48.67, 117.58, 186.49, 215.21 and 235.16 cm, respectively. The distances of the points E_2, E_3 and E_4, from E_1 are 97.64, 137.52 and 235.16 cm, respectively. The values of all these points are shown in TABLE 7.4.

7.3.4 Measurements in Heterogeneous VSN

After designing the heterogeneous VSN model, finding the altitude values of all the horizontal lines and the values of all the points on the respective lines, the actual VSN will be installed and measurements will be performed for the sub VSNs, VSN_1, VSN_2 and VSN_3, to verify the typical parameters as discussed before.

7.3.5 Measurements for VSN_1

The VSN_1 is covering the highest sub range. The higher altitude value for VSN_1 is 293 cm and the lower altitude value is 208 cm. For simplicity, the VSN_1 is separated from the main heterogeneous VSN, shown in Figure 7.17. The separated VSN_1 from the main VSN is shown in Figure 7.19. For VSN_1, the full coverage is achieved at the altitude line D, so it is treated as the lower altitude for VSN_1. The first measurement task in VSN_1 is to verify the full coverage at the altitude line D. The measurements

TABLE 7.4. Values of points in heterogeneous VSN

	A (cm)	B (cm)	C (cm)	D (cm)	E (cm)
1	0	0	0	0	0
2	68.76	57.75	48.49	19.95	97.64
3	90.9	79.77	70.38	48.67	137.52
4	117.58	102.03	89.03	117.58	235.16
5	144.26	133.13	111.41	186.49	-
6	166.4	155.39	123.74	215.21	-
7	235.16	177.41	146.13	235.16	-
8	-	235.16	164.77	-	-
9	-	-	186.67	-	-
10	-	-	235.16	-	-

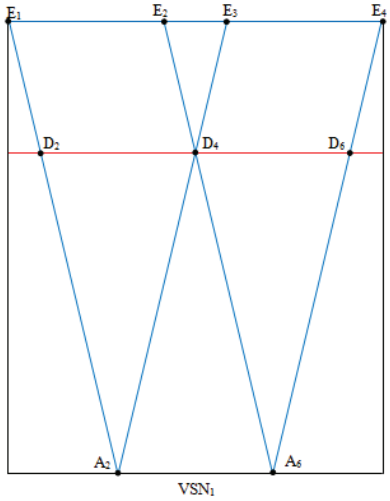

Figure 7.19. Sub VSN_1 in heterogeneous VSN.

at the line D are performed to verify the coverage between the points D_2 (19.95 cm) – D_4 (117.58 cm) and D_4 (117.58 cm) – D_6 (215.21 cm). The line D has an altitude of 208 cm from the line A. To perform the measurements, the wall is treated as the line D. A 235.16 cm long line is drawn parallel to the wall at a distance of 208 cm from the wall, which is treated as the line A. The monitoring nodes are fixed on this line at the points A_2 (68.76 cm) and A_6 (166.4 cm), according to the Figure 7.19. The monitoring node 1 is fixed at the point A_2 while the monitoring node 2 is fixed at A_6. Both these nodes are of similar type, having the 5 Mp camera sensor and the lens of 12 mm focal length.

Next, the images of the wall are captured where the measuring strip is attached by using the camera interface software. The images captured by the monitoring nodes 1 and 2 are shown in Figure 7.20 and Figure 7.21, respectively. The analysis of

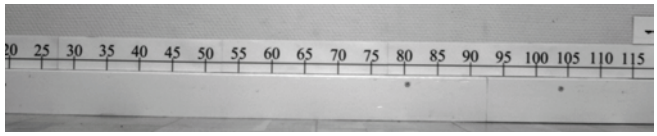

Figure 7.20. Measurements for VSN_1 at altitude D by using node 1.

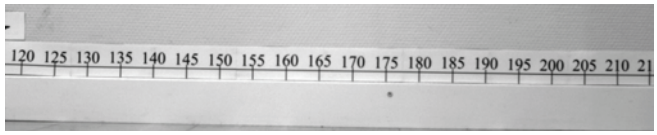

Figure 7.21. Measurements for VSN_1 at altitude D by using node 2.

the captured images is performed in the next paragraphs to measure the coverages of the monitoring nodes.

The measurements in Figure 7.20 show that a total of 131 pixels represent a 5 cm distance. There are about 145 pixels from the left edge of the figure to the 25 cm point, representing about a distance of 5.53 cm long. Thus, the D_2 point has a value of 19.47 cm. Similarly, there are about 84 pixels from the right edge of the figure to the 115 cm point, representing about a distance of 3.21 cm long. Thus, the D_4 point has a value of 118.21 cm. Thus, the practical coverage obtained by the monitoring node 1 is D_2 (19.47 cm) – D_4 (118.21 cm) while the expected coverage as calculated before was D_2 (19.95 cm) – D_4 (117.58 cm). The calculated and the measured values are almost equal.

The measurements in Figure 7.21 show that a total of 131 pixels represent a 5 cm distance. There are about 66 pixels from the left edge of the figure to the 120 cm point, representing about a distance of 2.52 cm long. Thus, the D_4 point has a value of 117.48 cm. Similarly, there are about 146 pixels from the right edge of the figure to the 210 cm point, representing about a distance of 5.57 cm long. Thus, the D_6 point has a value of 215.57 cm. Thus, the practical coverage obtained by the monitoring node 2 is D_4 (117.48 cm) – D_6 (215.57 cm) while the expected coverage as calculated before was D_4 (117.58 cm) – D_6 (215.21 cm). The calculated and the measured values are almost equal. All these measurements are given in TABLE 7.5.

For the VSN_1, the higher altitude line is E, which is 293 cm far from the line A, where the minimum resolution criterion must be met. The minimum resolution of the eagle image on the camera sensor, when the eagle is 293 cm far from the monitoring nodes, is required to be 10 pixels per meter. To perform the measurements, the wall is treated as line E. A 235.16 cm long line is drawn parallel to the wall at a distance of 293 cm from the wall, which is treated as the line A. The monitoring node 1 is fixed at the point A_2 while the monitoring node 2 is fixed at A_6. The image captured by the monitoring node 1 at altitude E is shown in Figure 7.22.

TABLE 7.5. Measurement values for sub VSN_1

Node	Point	Pix. for 5cm	Pix	Dist. (cm)	Ref. Point (cm)	Cal. Dist. (cm)	Meas. Dist. (cm)
1	D_2	131	145	-5.53	25	19.95	19.47
1	D_4	131	84	+3.21	115	117.58	118.21
2	D_4	131	66	-2.52	120	117.58	117.48
2	D_6	131	146	+5.57	210	215.21	215.57

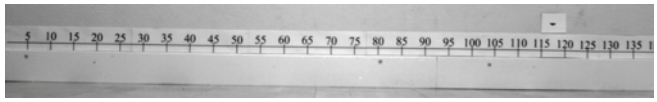

Figure 7.22. Measurements for VSN_1 at altitude E by using node 1.

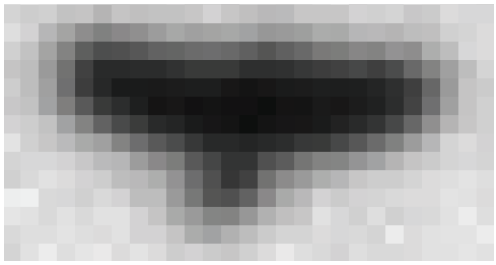

Figure 7.23. Bird resolution at highest altitude in sub VSN_1.

To measure the resolution, a small portion of the image, which contains the eagle, is separated from Figure 7.22. The magnified image of the separated portion is shown in Figure 7.23. The segmentation of this image is performed and the number of pixels is counted in the eagle along the wings side. It is found that the number of pixels is about 19 and is according to the plan. The number of pixels can also be directly counted from Figure 7.23.

7.3.6 Measurements for VSN_2

The VSN_2 is covering the middle sub range. The higher altitude value for VSN_2 is 208 cm and the lower altitude value is 86.39 cm. For simplicity, the VSN_2 is separated from the main heterogeneous VSN. The separated VSN_2 is shown in Figure 7.24. For VSN_2, the full coverage is achieved at the altitude line C, so it is treated as the lower altitude for the VSN_2. The first measurement task in VSN_2 is to verify the full coverage at the altitude line C. The measurements at the line C are performed to verify the coverage between the points C_2 (48.49 cm) – C_4 (89.03 cm) and C_4 (89.03 cm) – C_7 (146.13 cm). The line C has an altitude of 86.39 cm from the line A. To perform the measurements, the wall is treated as the line C. A 235.16 cm long line is drawn parallel to the wall at a distance of 86.39 cm from the wall, which

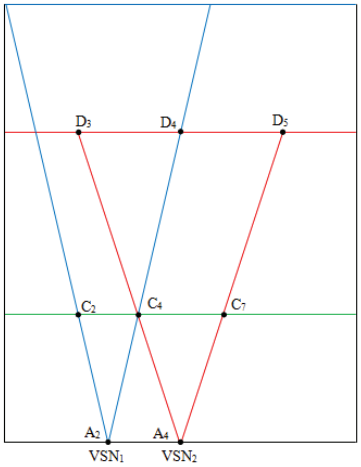

Figure 7.24. Sub VSN_2 in heterogeneous VSN.

is treated as the line A. The monitoring nodes are fixed on this line at the points A_2 (68.76 cm) and A_4 (117.58 cm), according to the Figure 7.24. The monitoring node 1 is fixed at the point A_2 while the monitoring node 2 is fixed at A_4. Both these nodes are using the 5 Mp camera sensor but different lenses. The node 1 is using the 12 mm focal length lens while the node 2 is using the 8.5 mm focal length lens. Next, the images of the wall are captured where the measuring strip is attached. The images captured by the monitoring nodes 1 and 2 are shown in Figure 7.25 and Figure 7.26, respectively. The analysis of the captured images is performed in the next paragraphs to measure the coverages of the monitoring nodes.

The measurements in Figure 7.25 show that a total of 317 pixels represent a 5 cm distance. There are about 52 pixels from the left edge of the figure to the 50 cm point, representing a distance of about 0.82 cm long. Thus, the C_2 point has a value of 49.18 cm. Similarly, there are about 308 pixels from the right edge of the figure to the 85 cm point, representing a distance of about 4.85 cm long. Thus, the C_4 point has a value of 89.86 cm. Thus, the practical coverage obtained by the monitoring node 1 is C_2 (49.18 cm) – C_4 (89.86 cm) while the expected coverage as calculated before was C_2 (48.49 cm) – C_4 (89.03 cm). The calculated and the measured values are almost equal.

The measurements in Figure 7.26 show that a total of 224 pixels represent a 5 cm distance. There are about 227 pixels from the left edge of the figure to the 95 cm point, representing a distance of about 5.07 cm long. Thus, the C_4 point has a value of 89.93 cm. Similarly, there are about 261 pixels from the right edge of the figure to the 147 cm point, representing about a distance of 5.83 cm long. Thus, the C_7 point has a value of 145.83 cm. Thus, the practical coverage obtained by the monitoring node 2 is C_4 (89.93 cm) – C_7 (145.83 cm) while the expected coverage as calculated

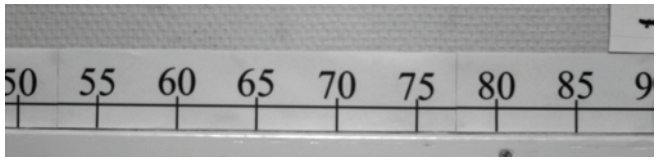

Figure 7.25. Measurements for VSN_2 at altitude C for node 1.

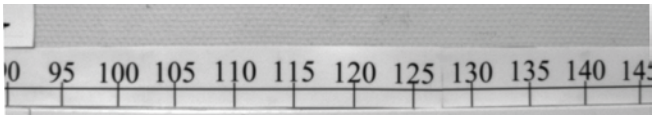

Figure 7.26. Measurements for VSN_2 at altitude C for node 2.

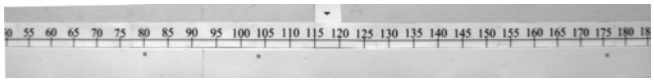

Figure 7.27. Measurements for VSN_2 at altitude D for node 1.

TABLE 7.6. Measurement values for sub VSN_2

Node	Point	Pix. for 5cm	Pix	Dist. (cm)	Ref. Point (cm)	Cal. Dist. (cm)	Meas. Dist. (cm)
1	C_2	317	52	-0.82	50	48.49	49.18
1	C_4	317	308	+4.85	85	89.03	89.86
2	C_4	224	227	-5.07	95	89.03	89.93
2	C_7	224	261	+5.83	140	146.13	145.83

before was C_4 (89.03 cm) – C_7 (146.13 cm). The calculated and the measured values are almost equal. All these measurements are given in TABLE 7.5.

For the VSN_2, the higher altitude line is D, which is 208 cm far from the line A, where the minimum resolution criterion must be met. The minimum resolution of the eagle image on the camera sensor, when the eagle is 208 cm far from the monitoring nodes, is required to be 10 pixels per meter. To perform the measurements, the wall is treated as the line D. A 235.16 cm long line is drawn parallel to the wall at a distance of 208 cm from the wall, which is treated as the line A. The monitoring node 1 is fixed at the point A_2 while the monitoring node 2 is fixed at A_4. The image captured by the monitoring node 1 at the altitude D is shown in Figure 7.27. To measure the resolution, a small portion of the image which contains the eagle is separated from Figure 7.27. The magnified image of the separated portion is shown in Figure 7.28. The segmentation of this image is performed and the number of pixels is counted in the eagle along the wings side. It is found that the number of pixels is about 19 and is according to the plan. The number of pixels can also be directly counted from Figure 7.28.

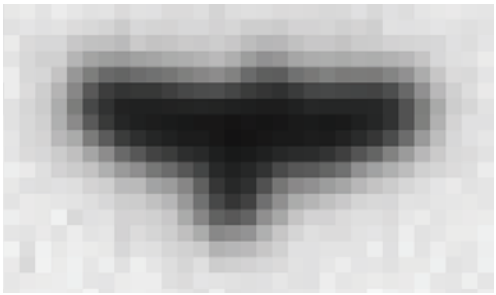

Figure 7.28. Bird resolution at highest altitude in sub VSN_2.

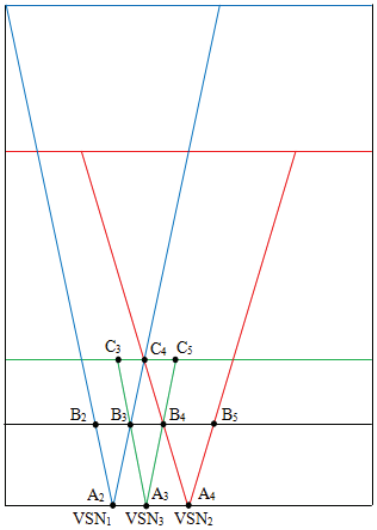

Figure 7.29. Sub VSN_3 in heterogeneous VSN.

7.3.7 Measurements for VSN_3

The VSN_3 is covering the lowest sub range. The higher altitude value for VSN_3 is 86.39 cm and the lower altitude value is 46.93 cm. For simplicity, the VSN_3 is separated from the main heterogeneous VSN. The separated VSN_3 is shown in Figure 7.29. For VSN_3, the full coverage is achieved at the altitude line B, so it is treated as the lower altitude for VSN_3. The first measurement task in VSN_3 is to verify the full coverage at the altitude line B. The measurements at the line B are performed to verify the coverage between the points B_2 (57.75 cm) – B_3 (79.77 cm), B_3 (79.77 cm) – B_4 (102.03 cm) and B_4 (102.03 cm) – B_5 (133.13 cm). The line B has an altitude of 46.93 cm from the line A. To perform the measurements, the wall is treated as line B. A 235.16 cm long line is drawn parallel to the wall at a distance of 46.93 cm from the wall, which is treated as line A. The monitoring nodes are fixed on this line at the points A_2 (68.76 cm), A_3 (90.9 cm) and A_4 (117.58 cm), according to the Figure 7.29. The monitoring node 1 is fixed at the point A_2, The monitoring

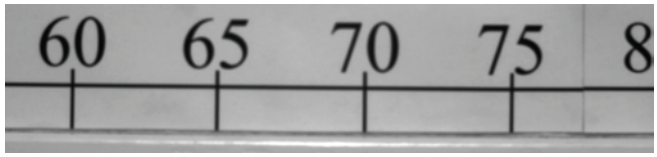

Figure 7.30. Measurements for VSN_3 at altitude B for node 1.

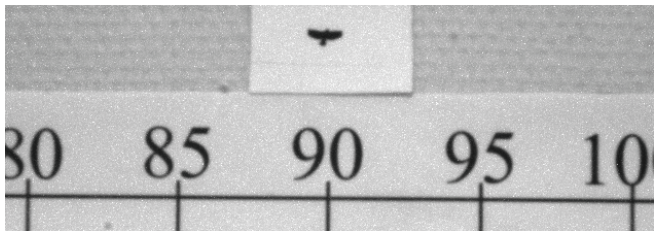

Figure 7.31. Measurements for VSN_3 at altitude B for node 3.

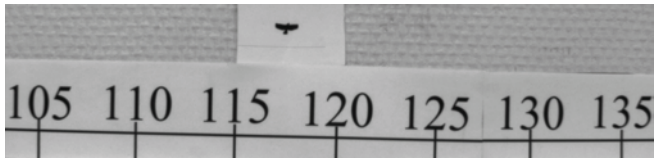

Figure 7.32. Measurements for VSN_3 at altitude B for node 2.

node 2 is fixed at the point A_4 while the monitoring node 3 is fixed at A_3. The nodes 1 and 2 are using are using the 5 Mp camera sensors but different lenses. The node 1 is using the 12 mm focal length lens while the node 2 is using the 8.5 mm focal length lens. The node 3 is using WVGA camera sensors and the 9.5 mm focal length lens.

Next, the images of the wall are captured where the measuring strip is attached. The images captured by the monitoring nodes 1, 3 and 2 are shown in Figure 7.30, Figure 7.31 and Figure 7.32, respectively. The analysis of the captured images is performed in the next paragraphs to measure the coverages of the monitoring nodes.

The measurements in Figure 7.30 show that a total of 573 pixels represent a 5 cm distance. There are about 267 pixels from the left edge of the figure to the 60 cm point, representing about a distance of 2.33 cm long. Thus, the B_2 point has a value of 57.67 cm. Similarly, there are about 562 pixels from the right edge of the figure to the 75 cm point, representing about a distance of 4.9 cm long. Thus, the B_3 point has a value of 79.9 cm. Thus, the practical coverage obtained by the monitoring node 1

TABLE 7.7. Measurement values for sub VSN_3

Node	Point	Pix. for 5cm	Pix	Dist. (cm)	Ref. Point (cm)	Cal. Dist. (cm)	Meas. Dist. (cm)
1	B_2	573	267	-2.33	60	57.75	57.67
1	B_3	573	562	+4.9	75	79.77	79.9
2	B_3	149	29	-0.97	80	79.77	79.03
2	B_4	149	26	+0.87	100	102.03	100.87
3	B_4	403	134	+1.66	105	102.03	103.34
3	B_5	403	128	+1.6	135	133.13	136.6

is B_2 (57.67 cm) – B_3 (79.9 cm) while the expected coverage as calculated before was B_2 (57.75 cm) – B_3 (79.77 cm). The calculated and the measured values are almost equal.

The measurements in Figure 7.31 show that a total of 149 pixels represent a 5 cm distance. There are about 29 pixels from the left edge of the figure to the 80 cm point, representing about a distance of 0.97 cm long. Thus, the B_3 point has a value of 79.03 cm. Similarly, there are about 26 pixels from the right edge of the figure to the 100 cm point, representing about a distance of 0.87 cm long. Thus, the B_4 point has a value of 100.87 cm. Thus, the practical coverage obtained by the monitoring node 1 is B_3 (79.03 cm) – B_4 (100.87 cm) while the expected coverage as calculated before was B_3 (79.77 cm) – B_4 (102.03 cm). The calculated and the measured values are almost equal.

The measurements in Figure 7.32 show that a total of 403 pixels represent a 5 cm distance. There are about 734 pixels from the left edge of the figure to the 105 cm point, representing about a distance of 1.66 cm long. Thus, the B_4 point has a value of 103.34 cm. Similarly, there are about 128 pixels from the right edge of the figure to the 135 cm point, representing about a distance of 1.6 cm long. Thus, the B_5 point has a value of 136.6 cm. Thus, the practical coverage obtained by the monitoring node 1 is B_4 (103.34 cm) – B_5 (136.6 cm) while the expected coverage as calculated before was B_4 (102.03 cm) and B_5 (133.01 cm). The calculated and the measured values are almost equal. All these measurements are given in TABLE 7.7.

For the VSN_3, the higher altitude line is C, which is 86.39 cm far from the line A, where the minimum resolution criterion must be met. The minimum resolution of the eagle image on the camera sensor, when the eagle is 86.39 cm far from the monitoring nodes, is required to be 10 pixels per meter. To perform the measurements, the wall is treated as the line C. A 235.16 cm long line is drawn parallel to the wall at a distance of 86.39 cm from the wall, which is treated as the line A. The monitoring nodes are fixed on this line at the points A_2, A_3 and A_4, according to the Figure 7.29. The image captured by the monitoring node 3 at the altitude C is shown in Figure 7.33. To measure the resolution, a small portion of the image which contains the eagle is separated from Figure 7.33. The magnified image of the separated portion is shown in Figure 7.34. The segmentation of this image is

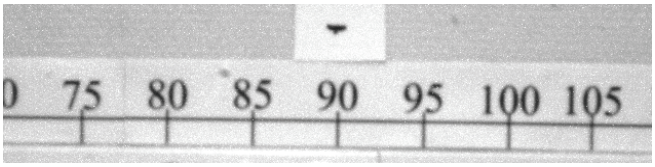

Figure 7.33. Measurements for VSN_3 at altitude C for node 3.

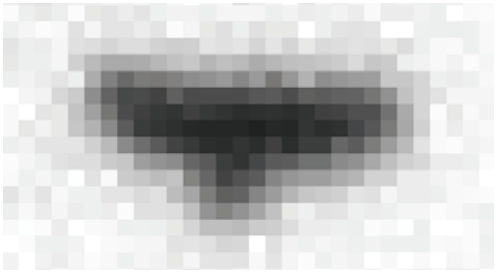

Figure 7.34. Bird resolution at highest altitude in sub VSN_3.

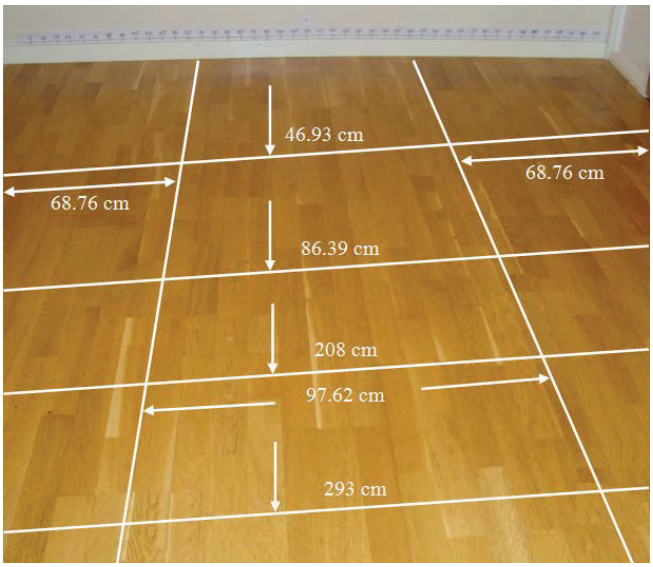

Figure 7.35. Marking lines on floor for heterogeneous VSN.

performed and the number of pixels is counted in the eagle along the wings side. It is found that the number of pixels is about 19 and is according to the plan. The number of pixels can also be directly counted from Figure 7.34. The marking lines on the floor for the heterogeneous VSN are shown in Figure 7.35.

8 PAPERS SUMMARY

8.1 PAPER 1 - MODELLING A VSN

This paper discusses the development of a VSN model to track the golden eagle in the sky. A number of camera sensors are explored along with the optics such as lens of suitable focal length which ensures a minimum required resolution at the required higher altitude in the sky. The combination of camera sensor and lens formulate a monitoring node. The camera node model is used to optimize the placement of the nodes for full coverage of a given area above a given lower altitude. The model presents the solution to minimize the cost required full coverage of a given area between the two extremes, higher and lower altitudes, in terms of camera sensor, lens focal length, camera node placement and actual number of nodes for sky surveillance application.

8.2 PAPER 2 - COST OPTIMIZATION OF A VSN

The area covered by a VSN can be increased by increasing the higher altitude and/or decreasing the lower. However, it increases the cost of VSN. The desirable objective is to increase the covered area at the decreased cost. This objective is achieved by using optimization techniques to design a heterogeneous VSN. This paper presents the cost reduction techniques. The core idea is to divide a given monitoring range of altitudes into a number of sub-ranges of altitudes. The sub-ranges of altitudes are monitored by individual sub VSNs, the VSN_1 covers the lower sub-range, the VSN_2 covers the next higher sub-range and so on, such that a minimum cost is used to cover a given area.

8.3 PAPER 3 – MEASUREMENTS OF A HOMOGENEOUS VSN

This paper discusses the verification of the VSN model presented in paper 1. The selection of the camera sensor, calculation of the lens focal length for the selected camera sensor, the distance between the camera nodes for their proper placement and the cost of the VSN to cover a given area are calculated by using the VSN model developed in paper 1. The measurements are performed by installing the actual cameras and optics with proper nodes placements. The laptop machines are used as data storage and analysis platforms. The VSN coverage is verified at the given lower altitude for 100% coverage. Moreover, the resolution is measured at the given higher altitude to verify whether it is fulfilling the minimum required resolution criterion. The verification of these parameters ensures that the designed VSN is able to rack the bird in the given area.

8.4 PAPER 4 - MEASUREMENTS OF A HETEROGENEOUS VSN

In this paper, a small heterogeneous VSN is designed based on the concepts developed in papers 1 and 2. The main VSN is a combination of three sub-VSNs, VSN_1, VSN_2 and VSN_3. VSN_1 monitors the lowest altitudes range, VSN_2 monitors

the middle altitudes range and the VSN_3 monitors the higher altitudes range. The VSNs are installed by using the actual cameras and lenses. The selection of the camera sensors, lenses focal lengths for the selected camera sensors, the placement of camera nodes and the costs are calculated on the basis of the concepts developed in papers 1 and 2. The coverages are verified above the given lower altitudes of the respective sub VSNs for 100% coverage. Also, the measurements are performed for the verification of minimum resolution at the higher altitudes of the respective sub VSNs. The laptop machines are used as data storage and analysis platforms. After verification of these parameters, it is ensured that the designed heterogeneous VSN, based on the model presented in paper 1 and the techniques given in paper 2, is able to rack the bird in the given area.

8.5 AUTHORS CONTRIBUTIONS

The thesis includes ten papers out of which four are included in this thesis. The contributions of the authors in these main papers are described in TABLE 8.1 on the next page.

TABLE 8.1. Contributions of the Authors

Paper	Main Author	Co-Authors	Contributions	
I	NA	NL BO MO MI KK	NA MO BO NL MI KK	Modelling, Optimization, Simulations, Analysis, Results, Writing Main Supervisor Co-Supervisor Co-Supervisor Discussions and review Discussions and review
II	NA	KK MI NL MO	NA MO NL MI KK	Mathematical modelling, Simulations, Analysis, Results, Writing Main Supervisor Co-Supervisor Discussions and review Discussions and review
III	NA	MI KK NL MO	NA MO BO NL MI KK	Measurements, Analysis, Results, Writing Main Supervisor Co-Supervisor Co-Supervisor Discussions and review Discussions and review
IV	NA	KK MI NL MO	NA MO NL MI KK	Measurements, Analysis, Results, Writing Main Supervisor Co-Supervisor Discussions and review Discussions and review

1. Naeem Ahmad (NA)
2. Mattias O'Nils (MO)
3. Bengt Oelmann (BO)
4. Najeem Lawal (NL)
5. Muhammad Imran (MI)
4. Khursheed Khursheed (KK)

9 THESIS SUMMARY AND CONCLUSIONS

9.1 THESIS SUMMARY

The thesis presents the design of a VSN for sky surveillance application. The objective of this VSN is to track golden eagle in the sky. Generally, a VSN consists of the basic components including sensing unit, CPU, communication subsystem, coordination subsystem, storage unit and power supply unit. The sensing unit senses the environment and collects data from it, the CPU processes the data, the communication subsystem interfaces the device to the network. The power unit supplies the power to the system. VSNs can be homogeneous or heterogeneous. The homogeneous VSNs use similar type of nodes while heterogeneous VSNs use different type of nodes. Each type has its pros and cons. The major data transmission techniques in VSNs are single hop transmission, multihop transmission and multipath transmission.

The VSNs can be deployed in many useful applications such as surveillance, traffic monitoring, sports, environmental monitoring etc. The surveillance applications can be applied in home, traffic monitoring on roads, building monitoring. The applications of VSNs in sports and games can be used to monitor or study the performance of players. VSNs can be successfully employed to study nature and environment. They can guide the drivers towards the empty parking slots, saving lot of time, energy and prevent frustration. They can monitor seabirds, wild life, animals and plants. A number of VSN platforms are developed. The common platforms include SensEye, a heterogeneous VSN system, a wireless camera mote CITRIC, MeshEye implementing in-node processing technique, FireFly Mosaic consisting of eight embedded cameras to monitor a house, WisNAP an application platform for image sensor networks, Panoptes platform designed for surveillance and Cyclops a vision based wireless network.

Although the VSNs offer new opportunities for many applications, they also raise new challenges. Camera sensors generate large amount of data as compared to scalar sensors. The camera nodes are generally low-power and have severe resource constraints. The processing and transmitting such data by these nodes is a challenging task. The VSNs are unique and more challenging in many ways. The major challenges which are faced in the context of VSNs are resource constraints, real time performance, time synchronization, coverage optimization, algorithmic constraints, object occlusion and data reliability.

The VSN model developed in this thesis explores a number of camera sensors along with the optics such as lenses of suitable focal lengths which ensure minimum required resolution at the highest altitude in the sky. The combination of a camera sensor and lens formulate a camera node. The camera node model is used to optimize the placement of the nodes for full coverage of a given area above a lower altitude. The model presents the solution to minimize the cost, number of

sensor nodes, required to fully cover a given area between the two extremes, higher and lower altitudes, in terms of camera sensor, lens focal length, camera node placement and actual number of. The first step of VSN design is the camera sensor selection from a number of camera sensors which are used in the study. The second step of VSN design phase is the focal length calculation for the selected camera sensor for the minimum required resolution at the required higher altitude. These two steps finalize the model of a node. A matrix of a number of such nodes is used to design the VSN to cover a given area. The third step of VSN design decides the nodes placement, which can be finalized by calculating the distance between them. The last step of VSN design phase is to calculate the cost to cover a given area.

The surveillance area of VSN is increased by increasing the higher altitude and/or decreasing the lower altitude. It increases the covered area but it also increases the VSN cost. The optimization techniques are used to decrease the VSN cost. The resultant VSN is a heterogeneous design. The strategy is to divide a given monitoring range of altitudes into a number of sub-ranges of altitudes and to cover them with individual sub VSNs such that a minimum cost is used to monitor a given area. The measurements are performed to verify the techniques and concepts developed by VSN model and optimization techniques. The coverage above a given lower altitude is verified for 100% coverage. Also, the resolution is measured at the higher specified altitude to ensure that whether it is fulfilling the minimum resolution criterion.

9.2 CONCLUSIONS

This thesis presents the general solution of camera placement problem to cover a given space. It ensures the coverage of every point in the given space. In addition to coverage of every point, the thesis also ensures the minimum required resolution at theses points. Another major issue of space coverage is the camera focus. The points which are very near to the camera sensors are not clearly captured by cameras. This thesis also resolves the camera focus issues in the coverage of the given space.

REFERENCES

[1] Y. Charfi, N. Wakamiya and M. Murata, "Challenging issues in visual sensor networks," IEEE Wirel. Commun. Vol. 16, No. 2, pp. 44 - 49, 2009.

[2] S. Soro and W. Heinzelman, "A survey of visual sensor networks," Hindawi Publishing Corporation Advances in Multimedia Volume 2009, Article I D 640386, 21 pages doi:10.1155/2009/640386.

[3] K. Obraczka, R.Manduchi, and J. Garcia-Luna-Aceves, "Managing the information flow in visual sensor networks," in Proceedings of the 5th International Symposium on Wireless Personal Multimedia Communication, 2002.

[4] H. Medeiros, J. Park, and A. Kak, "A light-weight event-driven protocol for sensor clustering in wireless camera networks," in Proceedings of the 1st ACM/IEEE International Conference on Distributed Smart Cameras (ICDSC '07), pp. 203–210, 2007.

[5] M. Rahimi, R. Baer, O. I. Iroezi, et al., "Cyclops: in situ image sensing and interpretation in wireless sensor networks," in Proceedings of the 3rd International Conference on Embedded Networked Sensor Systems, 2005.

[6] R. Kleihorst, B. Schueler, A. Danilin, and M. Heijligers, "Smart camera mote with high performance vision system," in Proceedings of ACM SenSys Workshop on Distributed Smart Cameras (DSC '06), 2006.

[7] S. Hengstler, D. Prashanth, S. Fong, and H. Aghajan, "MeshEye: a hybrid-resolution smart camera mote for applications in distributed intelligent surveillance," in Proceedings of the 6th International Symposium on Information Processing in Sensor Networks (IPSN '07), pp. 360–369, 2007.

[8] F. Lau, E. Oto, and H. Aghajan, "Color-based multiple agent tracking for wireless image sensor networks," in Proceedings of the Advanced Concepts for Intelligent Vision Systems (ACIVS '06), pp. 299–310, 2006.

[9] T. H. Ko and N. M. Berry, "On scaling distributed low-power wireless image sensors," in Proceedings of the 39th Annual Hawaii International Conference on System Sciences, 2006.

[10] A. Mainwaring, J. Polastre, R. Szewezyk, D. Culler. Wireless sensor networks for habitat monitoring.

[11] P. Kulkarni et al., "SensEye: A Multi-Tier Camera Sensor Network," Proc. 13th Annual ACM Int'l. Conf. Multimedia, 2005, pp. 229–38.

[12] W. Yu, Z. Sahinoglu, and A. Vetro, "Energy Efficient JPEG 2000 Image Transmission over Wireless Sensor Networks," Proc. IEEE GLOBECOM '04, 2004.

[13] C. D.-F. Vincent Lecuire and N. Krommenacker, "Energy Efficient Transmission of Wavelet-based Images in Wireless Sensor Networks," EURASIP J. Image Video Process., 2007.

[14] H. Wu and A. Abouzeid, "Error Resilient Image Transport in Wireless Sensor Networks," Comp. Net., vol. 50, Oct. 2006, pp. 2873–87.

[15] W. Wang, D. Peng, H. Wang, and H. Sharif, "Adaptive image transmission with p-v diversity in multihop wireless mesh networks," International Journal of Electrical, Computer, and Systems Engineering, vol. 1, no. 1, 2007.

[16] P. Djukic and S. Valaee, "Minimum Energy Reliable Multipath Ad Hoc Networks," 22nd Biennial Symp. Commun., June 2004.

[17] Y. Charfi, N. Wakamiya, and M. Murata, "Trade-Off Between Reliability and Energy Cost for Content-Rich Data Transmission in Wireless Sensor Networks," Proc. BROADNETS, Oct. 2006.

[18] Z. Yang and K. Nahrstedt, "A bandwidth management framework for wireless camera array," in Proceedings of the International Workshop on Network and Operating System Support for Digital Audio and Video (NOSSDAV '05), pp. 147–152, 2005.

[19] G. J. Pottie and W. J. Kaiser, "Wireless Integrated Network Sensors," Commun. ACM, vol. 43, May 2000, pp. 51–58.

[20] K. Römer, P. Blum, and L. Meier, "Time synchronization and calibration in wireless sensor networks," in Handbook of Sensor Networks: Algorithms and Architectures, I. Stojmenovic, Ed., pp. 199–237, John Wiley & Sons, New York, NY, USA, 2005.

[21] A. Ercan, A. E. Gamal, and L. Guibas, "Camera network node selection for target localization in the presence of occlusions," in Proceedings of the ACM SenSys Workshop on Distributed Smart Cameras, 2006.

[22] H. Wu and A. A. Abouzeid, "Error resilient image transport in wireless sensor networks," Computer Networks, vol. 50, no. 15, pp. 2873–2887, 2006.

[23] M. Chen, V. C. M. Leung, S. Mao, and Y. Yuan, "Directional geographical routing for real-time video communications in wireless sensor networks," Computer Communications, vol. 30, no. 17, pp. 3368–3383, 2007.

[24] M. Maimour, C. Pham, and J. Amelot, "Load repartition for congestion control in multimedia wireless sensor networks with multipath routing," in Proceedings of the 3rd International Symposium on Wireless Pervasive Computing (ISWPC '08), pp. 11–15, 2008.

[25] M. van der Schaar and P. Chou, Multimedia over IP and Wireless Networks: Compression, Networking, and Systems, Academic Press, New York, NY, USA, 2007.

[26] J. C. Dagher, M. W. Marcellin, and M. A. Neifeld, "A method for coordinating the distributed transmission of imagery," IEEE Transactions on Image Processing, vol. 15, no. 7, pp. 1705–1717, 2006.

[27] N. H. Zamora and R. Marculescu, "Coordinated distributed power management with video sensor networks: analysis, simulation, and prototyping," in Proceedings of the 1st ACM/IEEE International Conference on Distributed Smart Cameras (ICDSC '07), pp. 4–11, 2007.

[28] C. B. Margi, R. Manduchi, and K. Obraczka, "Energy consumption tradeoffs in visual sensor networks," in Proceedings of 24th Brazilian Symposium on Computer Networks (SBRC '06), 2006.

[29] D. Jung, T. Teixeira, A. Barton-Sweeney, and A. Savvides, "Model-based design exploration of wireless sensor node lifetimes," in Proceedings of the 4th European Conference on Wireless Sensor Networks, pp. 277–292, 2007.

[30] L. Ferrigno, S. Marano, V. Paciello, and A. Pietrosanto, "Balancing computational and transmission power consumption in wireless image sensor networks," in Proceedings of the IEEE International Conference on Virtual Environments, Human-Computer Interfaces, and Measurement Systems (VECIMS '05), pp. 61–66, 2005.

[31] M. Chitnis, Y. Liang, J.Y. Zheng, P. Pagano, and G. Lipari. Wireless line sensor network for distributed visual surveillance.

[32] Y.C. Tseng, Y.C. Wang, K.Y. Cheng, and Y.Y. Hsieh. iMouse: An integrated mobile surveillance and wireless sensor system.

[33] D. Beymer, P. McLauchlan, B. Coifman, and J. Malik. A Real-time Computer Vision System for Measuring Traffic Parameters. 1997.

[34] K.H. Lim, L.M. Ang, K.P. Seng, and S.W. Chin. Lane-Vehicle Detection and Tracking. Hong Kong, March 2009.

[35] J.M. Ferryman, S.J. Maybank, and A.D. Worrall. Visual Surveillance for Moving Vehicles. Mumbai, India, January 1998.

[36] D. Koller, J. Weber, and J. Malik. Robust multiple car tracking with occlusion reasoning. In ECCV, pp. 189-196, Stockholm, Sweden, May 2-6, 1994.

[37] D. Koller, J. Weber, T. Huang, J. Malik, G. Ogasawara, B. Rao, and S. Russell. Towards robust automatic traffic scene analysis in real-time. In ICPR, Israel, November 1994.

[38] D. Xu , J. Orwell, L. Lowey , and D. Thride. Architecture and Algorithms for Tracking Football Players with Multiple Cameras. In IEEE Proc.-Vis. Image Signal Process., Vol. 152, No. 2, April 2005.

[39] C.J. Needham and R.D. Boyle. Tracking multiple sports players through occlusion, congestion and scale.

[40] R. Kays, S. Tilak, B. Kranstauber, P.A. Jansen, C. Carbone, M. Rowcliffe, T. Fountain, J. Eggert, and Z. He. Camera Traps as Sensor Networks for Monitoring Animal Communities. International Journal of Research and Review in Wireless Sensor Networks, June 2011.

[41] J. Campbell, P. B. Gibbons, and S. Nath. Irisnet: An internet-scale architecture for multimedia sensors. In Proceedings of ACM Multimedia, November 2005.

[42] S. Uchiyama, H. Yamamoto, M. Yamamoto, K. Nakamura, K. Yamazaki, "Sensor Network for Observation of Seabirds in Awashima Island", International Conference on Information Networking, Barcelona 2011.

[43] I. F. Akyildiz, T. Melodia, and K. R. Chowdhury, "Wireless Multimedia Sensor Networks: Applications and Testbeds, "Proc. IEEE, vol. 96, no. 10, pp. 1588-1605, Oct. 2008.

[44] Crossbow wireless sensor platform. http://www.xbow.com/Products/Wireless Sensor Networks.htm

[45] Stargate platform. http://www.xbow.com/Products/XScale.htm

[46] P. W.-C. Chen, P. Ahammad, C. Boyer, S.-I. Huang, L. Lin, E. J. Lobaton, M. L. Meingast, S. Oh, S. Wang, P. Yan, A. Yang, C. Yeo, L.-C. Chang, D. Tygar, and S. S. Sastry, "CITRIC: A Low-Bandwidth Wireless Camera Network Platform," in Proceedings of the International Conference on Distributed Smart Cameras, 2008.

[47] Moteiv Corp. Tmote Sky Datasheet, 2003.

[48] A. Rowe, D. Goel, and R. Rajkumar, "FireFly Mosaic: a vision enabled wireless sensor networking system," in Proceedings of 28th IEEE International Real-Time Systems Symposium (RTSS '07), 2007.

[49] A. Rowe, A. Goode, D. Goel, I. Nourbakhsh, "CMUcam3: An Open Programmable Embedded Vision Sensor", International Conferences on Intelligent Robots and Systems, Oct. 2007.

[50] A. Eswaran, A. Rowe, R, Rajkumar, "Nano-RK: an Energy-aware Resource-centric RTOS for Sensor Networks", IEEE Real-Time Systems Symposium, Dec. 2005.

[51] S. Hengstler and H. Aghajan, "WiSNAP: a wireless image sensor network application platform," in Proceedings of the 2nd International Conference on Testbeds and Research Infrastructures for the Development of Networks and Communities (TRIDENTCOM '06), pp. 7–12, 2006.

[52] Atmel Corporation, "ATmega128(L) 8-bit AVR® Microcontroller," Data Sheet, Revision 2467M-AVR-11/04, November 2004. Available: http://www.atmel.com/dyn/resources/prod_documents/doc2467.pdf

[53] Chipcon AS, "Smart RF® CC2420 2.4 GHz IEEE 802.15.4 / ZigBee ready RF Transceiver," Preliminary Data Sheet, Revision 1.2, June 2004. Available: http://www.chipcon.com/files/CC2420_Data_Sheet_1_2.pdf

[54] Agilent Technologies, "Agilent ADCM-1670 CIF CMOS Camera Module," Technical Specification, Preliminary Draft 0.10, August 2002.

[55] Agilent Technologies, "Agilent ADNS-3060 High-Performance Optical Mouse Sensor," Data Sheet, October 2004. Available: http://cp.literature.agilent.com/litweb/pdf/5989-3421EN.pdf

[56] Chipcon AS, "Smart RF® CC2420DBK Demonstration Board Kit," User Manual, Revision 1.3, November 2004. Available: http://www.chipcon.com/files/CC2420DBK_User_Manual_1_3.pdf

[57] W.-C. Feng, B. Code, E. Kaiser, M. Shea, W.-C. Feng, and L. Bavoil, "Panoptes: scalable low-power video sensor networking technologies," in Proceedings of the 11th ACM International Multimedia Conference and Exhibition (MM '03), pp. 562–571, Berkeley, Calif, USA, November 2003.

[58] E. Hörster and R. Lienhart, "Approximating optimal visual sensor placement", in IEEE ICME2006, 2006.

[59] D. Fehr, L. Fiore, and N. Papanikolopoulos, "Issues and solutions in surveillance camera placement," in Proc. IEEE Conf. Intelligent Robots and Systems, pp. 3780–3785, 2009.

[60] K. Chakrabarty, S. S. Iyengar, H. Qi, and E. Cho, "Grid coverage for surveillance and target location in distributed sensor networks", IEEE Transactions on Computers, 51(12): 1448–1453, 2002.

[61] J. O'Rourke, "Art Gallery Theory and Algorithms", New York: Oxford Univ. Press, 1987.

[62] N.S.V. Rao, "Computationa1 complexity Issues in Operative Diagnosis of Graph-Based Systems," IEEE Trans. Computers, vol. 42, no. 4, pp. 447-457, Apr. 1993.

[63] S. Rama, K. Ramakrishnan, P.K. Atrey, V.K. Singh, and M.S. Kankanhalli, "A design methodology for selection and placement of sensors in multimedia surveillance systems", ACM VSSN'06, October 27, 2006, Santa Barbara, California, USA.

[64] http://www.europeanraptors.org/raptors/golden_eagle.html.

[65] http://www.forestry.gov.uk/forestry/goldeneagle.

[66] J. L. Dunn and J. Alderfer, "National Geographic Field Guide to the Birds of North America," 5th Edition, 2006, pp.124-125.

[67] Golden Eagle, King of Birds. http://www.associatedcontent.com/article/610611/golden_eagles_king_of_the_birds.html.

[68] Golden Eagle. http://proeco.visti.net/naturalist/falconry/ geagl.htm.

[69] H. Glasl, D. Schreiber, N. Viertl, S. Veigl, and G. Fern´andez, "Video based traffic congestion prediction on an embedded system," In Proc. of the 11th International IEEE Conference on Intelligent Transportation Systems, Beijing, China, Oct. 2008.

[70] H. D. Young, R. A. Freedman, and A. L. Ford, Sears and Zemansky's University Physics: With Modern Physics, 12th ed., Pearson Addison Wesley, 2007, pp.1157-1206.

[71] R.E. Jacobson, S.F. Ray, G.G. Attridge, and N.R. Axford, The Manual of Photography: Photographic and Digital Imaging, 9th Ed., Focal Press, 2000, pp. 39-60.

[72] N. Ahmad, N. Lawal, M. O'Nils, B. Oelmann, M. Imran, K. Khursheed, "Model and placement optimization of a sky surveillance visual sensor network," Broadband wireless communication, computing and applications, UPC, Barcelona, Spain, 2011.

[73] N. Ahmad, K. Khursheed, M. Imran, N. Lawal, M. O'Nils, "Cost optimization of a sky surveillance visual sensor network," Proceedings of SPIE 8437, Real-Time image and video processing, Brussels, Belgium, 2012.

[74] Smallwood and K. Thelander, "Developing methods to reduce bird mortality in the Altamont Pass Wind Resource Area", pp. 73, August 2004.